EMISSIONS FROM A GAS-BURNING PULSE COMBUSTOR

JIRI DAVID

A thesis submitted to Middlesex University in partial fulfilment of the requirements for the degree of Master of Philosophy.

December 1993

The work was carried out at the Energy Technology Centre,
Middlesex University, School of Mechanical Engineering,
Bounds Green Road, London N11 2NQ.

ABSTRACT

The pulse combustor has a number of attractive features for heating applications. These include simplicity of construction, compactness for a given heat input rate, enhanced exhaust gas heat transfer and most importantly low CO and NO_x emissions. With more stringent air quality and emissions standards soon to be in force in many countries, the latter has received much attention among the producers of gas appliances.

This study investigates the performance of and emissions from a Helmholtz-type pulse combustor with varying parameters such as gas input rate, tailpipe length, combustion chamber volume and composition of the natural gas being used as a fuel. The experimental work was primarily focused on the measurements of O_2, CO_2, CO and NO_x concentrations in the pulse combustor exhaust gas; such data are difficult to find in the general literature. Measurements of the aspirated combustion air flow rate and operating frequency were also made.

Initially some modifications to the natural-gas-fired pulse burner of 5kW output constructed by A. Suthenthiran were made and new gas sampling ports and probes were designed and constructed. An orifice plate flow meter and air-box were also designed and constructed in an attempt to measure the pulsating air flow of the combustor. It was found, however, that the combustor would not operate with the air-box fitted. The air/fuel ratios of the combustor were therefore calculated from the measured exhaust gas analysis by means of a specially written computer program. Much attention was also given to the selection of reliable gas analysis equipment and as a result five different gas analyzers were tested.

It was found that the investigated pulse combustor was capable of operation only under fuel-lean conditions since the stoichiometric air/fuel ratio was never reached. Percentage excess air levels when using the mains gas (NGA) as a fuel were typically found in the range of 5 - 40 %.

The variation of carbon monoxide exhaust levels with gas flow rate displayed, in most cases, a characteristic 'U' shaped curve gently sloping down and reaching minimum CO concentration (typically below 300 ppm), before rising steeply as stoichiometry was approached. It was also found that in the lower and middle operating range CO levels were notably reduced with increase in combustion chamber volume and slightly reduced with increase in tailpipe length. Furthermore, the CO/CO_2 ratio did not exceed the maximum permissible limit of 0.02 set by appliance safety standards for any of the conducted trials.

Test results for all investigated variables indicated that production of nitrogen oxides was strongly temperature dependent; a finding which is consistent with the literature. In addition, NO_x emissions were observed to rise with increase in gas flow rate, tailpipe length and combustion chamber volume respectively. With measured NO_x levels below 60 ppm our results agree with the values reported elsewhere. Furthermore, oxides of nitrogen monitored in this study consisted mainly of thermal NO formed by the Zeldovich mechanism.

The pulse combustor was operated on family 2H test gases ie. NGA (mains), NGB, NGC (high in H_2) and NGD (high in N_2) in order to evaluate the effect of changes in fuel composition on its performance. A conventional method based on the modified Harris & Lovelace diagram was used to define an acceptable area within which all family 2H gases would be interchangeable. Propane was found not to be interchangeable with the reference gas NGA.

ACKNOWLEDGMENTS

I wish to express my sincere gratitude to my director of studies Mr.P.Barham for his guidance during my study and for correcting the manuscript of this thesis.

My special thanks also go to my supervisors, Prof.J.Kubie and Dr.W.C.Maskell, who have been a great help to me by assessing my progress along the way.

I wish to acknowledge the Committee of Directors of Polytechnics, British Council and Middlesex University for the financial support of my study. My appreciation and thanks are due to Prof.J.Kubie for organising my funding.

I would also like to extend my thanks to all my colleagues at the Energy Centre for their help and support. In particular Dr.M.Benammar, Dr.A.Ioannou, Mr.J.Valha, Mr.D.J.Gopaul, Mr.J.Jones and Mr.L.Egbe.

Finally, thanks are due to the technical staff of the Energy Centre, Machine Tool and Fluid Laboratories.

LIST OF CONTENTS

LIST OF TABLES

LIST OF FIGURES

LIST OF MAJOR SYMBOLS

Latin alphabet

A cross-sectional area of tailpipe

c speed of sound

c_p specific heat at constant pressure

c_v specific heat at constant volume

C coefficient of discharge

CCV combustion chamber volume

d diameter of orifice

D diameter

E velocity of approach factor

f frequency

F Weaver coefficient

GCV gross calorific value

GFR gas flow rate

h enthalpy

H heat content

L length of tailpipe

Nu Nusselt number

NCV net calorific value

p_a atmospheric pressure

p'' pressure of saturated water vapour

PEA percentage excess air

Pr Prandtl number

Δp differential static pressure

q_v volume flow rate of air

Q_h heat input

r gas constant

R electrical resistance

Re Reynolds number

RD relative density

S Weaver flame speed factor

t temperature

t_{Ad} adiabatic flame temperature

t_{Exh1} exhaust gas temperature at combustion chamber exit

t_{Exh2} exhaust gas temperature at tailpipe exit

t_{Mean} mean temperature

t_{Water} water bath temperature

T absolute temperature

TE thermal efficiency

TAR theoretical air requirement

TPL tailpipe length

v_{Max} maximum velocity

v_{Mean} mean velocity

V volume, voltage

W Wobbe number

x mole fraction

Greek alphabet

α excess air coefficient (actual A/F ratio divided by stoichiometric A/F ratio)

γ ratio of specific heats

ε expansibility factor

ρ mass density of fluid

ρ_1 upstream density

φ relative air humidity

χ moist air coefficient

CHAPTER 1 : INTRODUCTION

1.1. BACKGROUND

1.1.1. Foreword

The energy policies of many countries have changed over the last two decades as the result of "energy crises" in the 1970's. Some governments promoted nuclear approaches as the most promising means of power production. However, since the Chernobyl catastrophe, public opinion in a number of countries halted, or at least slowed down, ongoing nuclear programs. The production of cheap and clean energy based on thermonuclear fusion does not seem to be likely in the near future and renewable sources of energy cannot cover the never ending increase in energy consumption.

The above implies that we will have to rely on conventional methods of power production using crude oil, natural gas, and coal for the foreseeable future. But we can and must utilise fossil fuels much more efficiently, thus postponing their depletion and protecting our environment. With the awareness of a potential energy shortage and effects of global warming, ozone layer depletion, smog, and acidic rain on the earth, it is necessary more than ever before to think in terms of energy conservation.

Dwindling reserves, instability of supplies, and rising prices of fossil fuels have sparked the development of combustion systems with higher efficiencies and lower emissions of carbon monoxide, nitrogen and sulphur oxides into the atmosphere. Pulse combustion has emerged as one of the most promising techniques which satisfy the above requirements.

1.1.2. Pulse combustion

Combustion with self-sustained oscillations is known as "pulse combustion", and the related burners are referred to as "pulse-combustion burners" or "pulse combustors". In the internal combustion engine, the timing of the intermittent combustion is

governed by electric discharges of the spark plug. In pulse combustors, on the other hand, the processes follow spontaneously after ignition.

The major advantages of pulse combustion over conventional combustion methods lie in higher system thermal efficiency and lower pollutant (NO_x and CO) emissions. Fuel savings, increased combustion intensity and convective heat and mass transfer rates are also among the attractive features of pulse combustors that can reduce operating and capital costs of many processes. Another apparent benefit is that the pulse burner is relatively simple in construction and it is self-powered, demanding no external power (except for starting) for either combustion or exhaust extraction. The whole system is compact and does not require any expensive exhaust duct work. The main drawbacks are noise emission, vibration, and limited turndown ratios.

Pulse combustion is not a new technology. Combustion-driven oscillations were reported in the late 1700's [1]. Since that time, most effort has been put into their elimination. However, in the middle of this century an interest in the useful application of the oscillatory phenomenon developed in the field of aircraft propulsion and gas turbines. One of the better known examples of a pulse combustor is the German V-1 rocket motor of the Second World War [2]. As superior jet engines became available, pulse combustors disappeared from aeronautics. In the last three decades, a renewed attention to pulse combustion, mainly for heating applications, has arisen leading toward the successful marketing in the early 1980's of the Lenox Pulse warm-air furnace [3] and the Hydro-Pulse heating unit for residential heating [4].

The design and development of pulse combustors has proceeded largely by trial and error, a method that is time-consuming, expensive, and that does not insure an ideal design. Even though the first statement on the conditions required for sustained combustion-driven oscillations was made by Lord Rayleigh in 1878 [5], there is not available a fully comprehensive mathematical model of pulse combustion because of the degree of complexity of the processes that occur within a combustor. They are highly coupled and involve a multidimensional, transient flow which is

strongly turbulent, with variable transport properties.

1.1.3. Principle of operation

Pulse combustion is achieved when the heat released by the combustion process spontaneously excites pressure waves within the system. The combination of the combustion processes with the flow oscillations results in a periodic heat release rate. Rayleigh [5], in describing the phenomenon, states :

> "If heat be periodically communicated to, and abstracted from, a mass of air vibrating (for example) in a cylinder bounded by a piston, the effect produced will depend upon the phase of the variation at which the transfer of heat takes place. If heat be given to the air at the moment of greatest condensation, or be taken from it at the moment of greatest rarefaction, the vibration is encouraged. On the other hand, if heat be given at the moment of greatest rarefaction, or abstracted at the moment of greatest condensation, the vibration is discouraged."

This means that the phase relationship between the resonant pressure wave and the release of energy from chemical reactions will control the operation of the pulse combustor. Therefore, in order to maintain the pulsation within the burner, the point of maximum pressure oscillation should be close to the point of maximum heat release. Furthermore, the fresh charges of combustibles should be admitted into the combustor when its pressure is close to or at a minimum.

We can classify pulse combustors as Helmholtz, Schmidt, Reynst and Rijke types depending on their design. A typical gas-fired mechanically-valved pulse combustor of the Helmholtz-type consists of a closed cylinder, which forms the combustion chamber, with an open exhaust tube (tailpipe) at one end and air and gas valves at the other (see Figure 1). The tailpipe, of much smaller diameter than that of the combustion chamber, is usually shaped into, or contains, a suitably formed heat exchanger. A spark plug is most commonly used to ignite the combustible mixture drawn into the chamber.

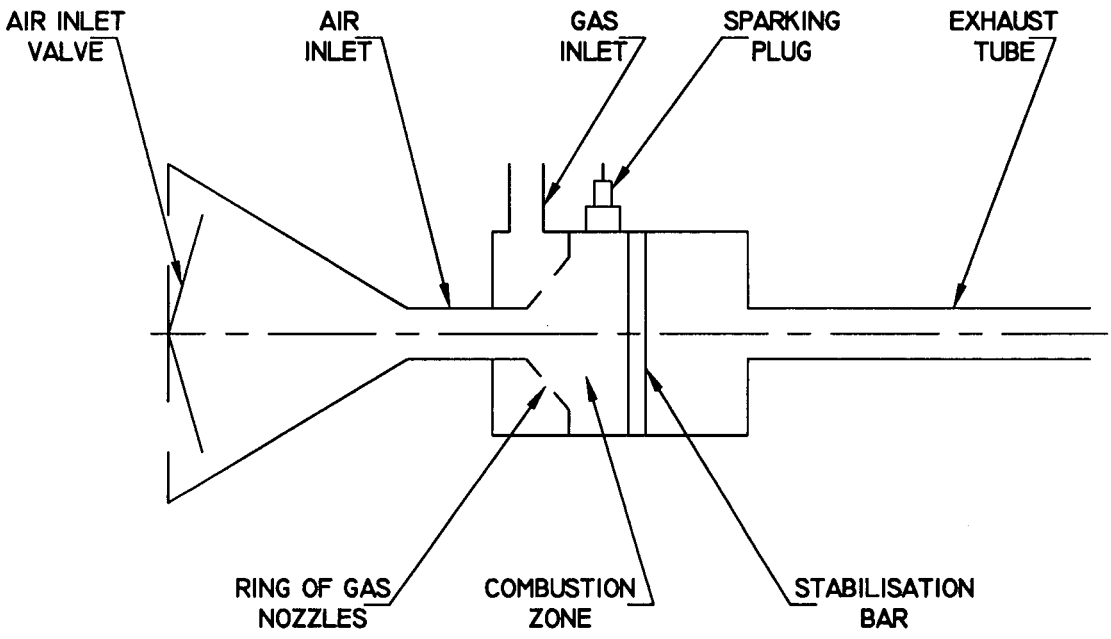

Figure 1 Typical Helmholtz burner, after Reay [6].

Figure 2 shows schematically the pulse combustion operating cycle of the investigated Helmholtz-type burner. It can be divided into a starting phase, which is depicted in Figure 2.a, and two subsequent working phases (see Figure 2.b, and 2.c). In this burner there are not separate flapper valves delivering the gas and air supply but, as Figure 2 illustrates, only one flapper valve that admits a combustible mixture into the chamber.

During the initial start-up (see Figure 2.a), gaseous fuel and air (from a fan) are forced into the mixing head and enter the combustion chamber via the flapper valve. Once the chamber is charged, a spark is used to ignite the gas/air mixture. The ensuing combustion increases the combustor pressure which, in turn, causes the flapper valve to close and the hot exhaust gas to move towards the open end of the tailpipe (see Figure 2.b). The momentum of the gases leaving the combustor decreases the pressure within the chamber to a level below that of the incoming mixture. Consequently, the flapper valve reopens and admits a new charge of fuel and air into the combustor (see Figure 2.c). Meanwhile the pressure wave from the initial explosion, reflected off the open end of the exhaust pipe, returns some hot

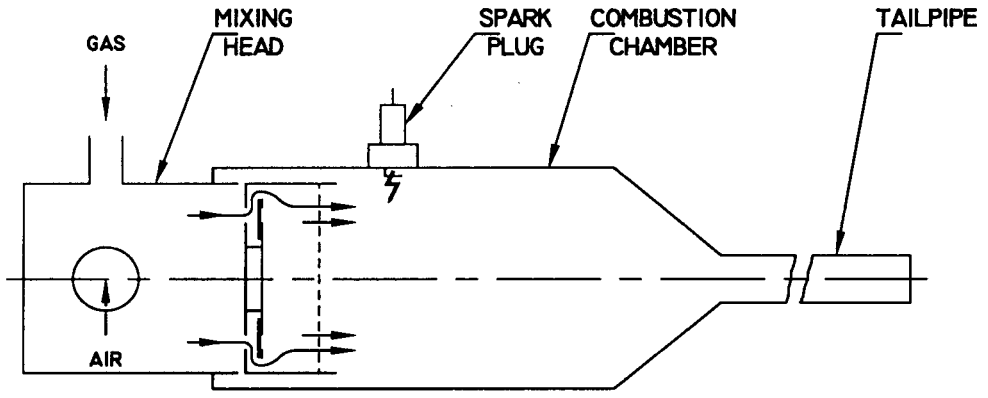

2.a. Starting phase; gas and air mixture introduced into combustion chamber.

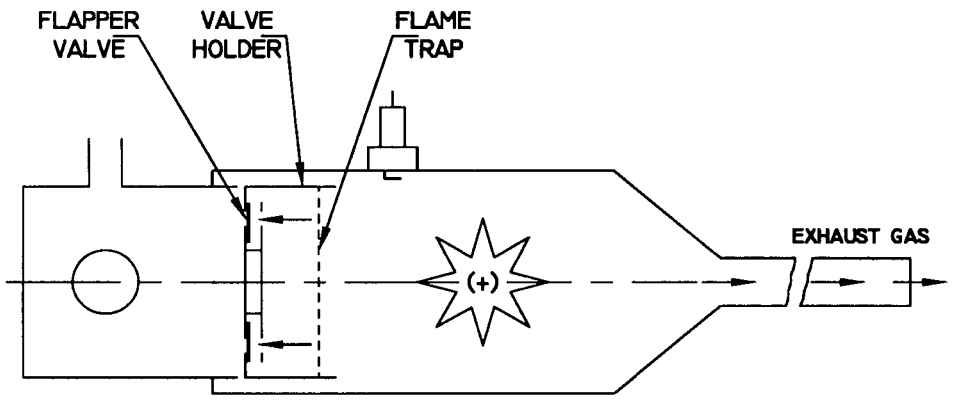

2.b. Exhaust phase; inlet valve closed.

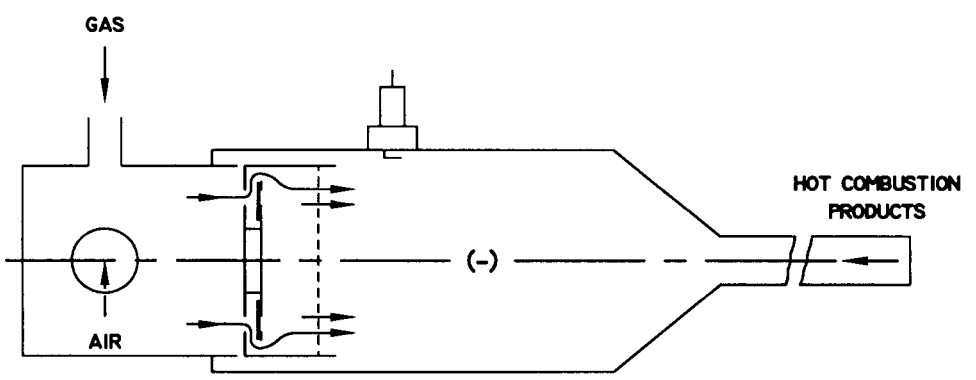

2.c. Intake phase; inlet valve open.

Figure 2 Operating cycle of the investigated pulse combustor.

combustion products to the chamber and closes the flapper valve so that the cycle is repeated from 2.b. It is thought that these hot exhaust gases initiate combustion of the new gas/air mixture without the need for a spark. When resonance is established, the pressure gradient between the inlet and the combustion chamber is sufficient to induce a new charge and the starting fan and spark generator are no longer required.

1.2. HISTORY : DEVELOPMENT AND APPLICATIONS

1.2.1. Foreword

In recent years, there have been several thorough reviews of the broad literature related to this concept, as well as four major conferences devoted to pulse combustion technology, the proceedings of which document ongoing research projects. There is no obvious best approach to classifying the uses of pulse combustion. In this review, after looking at some early designs, the various important applications of pulse combustors will be considered. The research and development carried out by British Gas and the collaboration with Middlesex University is discussed in the last section of this literature survey.

1.2.2. Early designs

The "musical" or "singing" flame is probably the first known example of pulsating combustion. It was first reported in 1777 [1, 7] by Byron Higgins when a gas flame placed in a round, vertical tube caused the spontaneous excitation of one of the natural acoustic modes of the tube. His observations indicate that there are conditions which control the resulting oscillation such as the location of the flame within the tube, the dimensions of the tube, the characteristics of the fuel supply tube, etc. Subsequent studies by Professor Le Conte [8] in the middle of the nineteenth century proved that external sound excitation can drastically change the properties of open

flames. Furthermore, these studies revealed that the response of such flames depends upon the amplitude and frequency of the sound wave and the part of the flame on which the sound impinges.

In 1859, Rijke [1, 5] reported a thermally-driven oscillation. He observed that the placement of a heated metal gauze at a distance of L/4 from the bottom of an open ended vertical tube of length L results in the excitation of the basic acoustic mode of the tube. It is important to note that the heat addition process initiates a steady upward flow in the tube which is the key to the occurrence of the oscillations. This design became later known as the Rijke tube.

The first attempts to utilise the positive and useful aspects of pulsating combustion were made in air breathing propulsion systems and gas turbines in the early years of the twentieth century [9, 10, 11]. These pioneering efforts were probably inspired by the internal combustion engine whose repetitive combustion process is, in fact, a forced, pulsating combustion process. This influence was clearly seen in Lorin's jet engine of 1908 in which combustion occurred periodically inside a cylinder with a reciprocating piston and thrust was achieved as the combustion products left the engine via the exhaust nozzle.

At the beginning of the century it was not yet clear whether the pressure energy of the exploding mixture should be used directly or indirectly (with the help of a propeller). Esnault-Pelterie, a French inventor, favoured the indirect solution and in 1906 designed a mechanically-valved unit as a gas generator for a power turbine [10]. The combustor consisted of a tube having flapper valves at both ends and an exhaust nozzle in the centre which guided the hot gases needed for driving a turbine wheel. Combustible mixtures were prepared in carburettors upstream of the flapper valves. Marconnet, Esnault-Pelterie's successor, proposed the direct use of a single aerodynamically-valved pulse combustor for propulsion in 1909 [11] which resembles many of today's units (see Figure 3). Principles similar to those employed by Marconnet were also used in Karavodine's work on a pulse combustion gas turbine in 1908 [9]. However, Holzwarth was the first to develop a practical gas turbine which utilized a pulse combustion process in the same year [12]. Finally, in

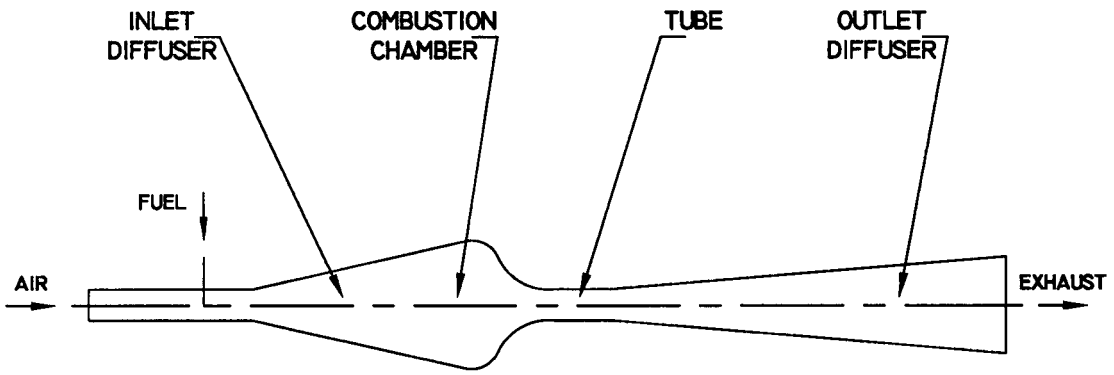

Figure 3 The Marconnet pulse jet [11].

1910, Esnault-Pelterie designed a pulse jet which consisted essentially of two quarter-wave combustors operating out of phase with each other [10].

This early work was recorded in a number of French, German and Swiss patents, dating from about 1900 to 1910, and linked with the above mentioned inventors as well as the names of Gobbe, Reidel, Armengaud and others [10].

1.2.2. Propulsion

After a gap of many years, interest in the pulse jet was renewed around 1931 in Germany when Schmidt [10] took out a patent on a pulse combustor which was similar in its operating principles to that of Marconnet. Figure 4 shows that Schmidt's design has a uniform cross section along the combustion chamber and exhaust tube. This is known as the Schmidt design or quarter-wave combustor (compare Figure 4 and Figure 1 to see the difference between the Schmidt-type burner and Helmholtz-type burner). Because of problems with his pulse jet, Schmidt was forced by the Luftwaffe in 1941 to cooperate with Deitrich, who worked for Argus. Supported by the German government, the team's research led in 1941 to the successful Argus-Schmidt tube for propelling the V-1 "Buzz Bomb" which was used in the bombing of London [14].

The high expectations by the Nazi regime of reversing the course of World

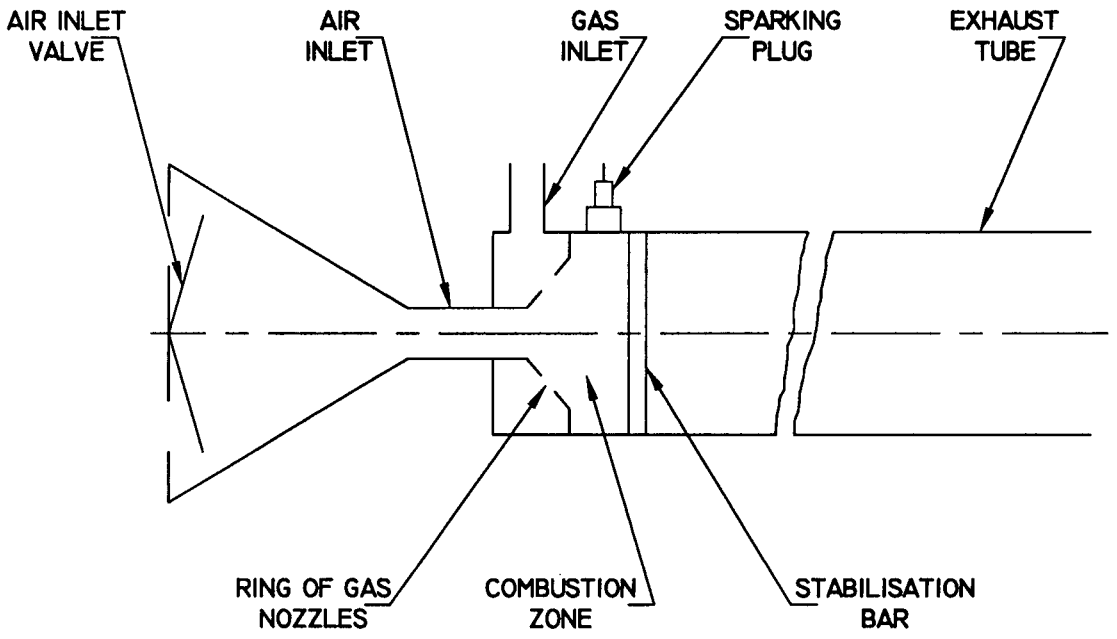

Figure 4 *Schmidt burner, after Ray [6].*

War II by using this destructive bomb were not fulfilled. Tests conducted in 1943 clearly proved that the originally specified speed of 700 km/h and other parameters were not to be met due to the ram effect on the flapper valves at high speeds which severely reduced jet thrust. This allowed the Allies to develop an effective defence system against the V-1, now flying at speeds not exceeding 500 km/h [2].

Some work on pulse jets was also done in the United States during the Second World War. The U.S. efforts led to the development of an aerovalved unit in 1944 [2]. However, the capture of a complete V-1 by the Allies resulted in the abandonment of the valveless jet program. French engineers became involved shortly after the War when a miniature unit (Dyna-Jet) [15], based on the V-1 design, was used as a model aeroplane engine.

The relatively poor performance of pulse jets (largely due to a lack of significant precombustion charge compression) compared with more modern thrust producers such as turbojets or turbofan engines caused a loss of interest in the pulse jet in the late 1940's. However, in 1950, the French national aero-engine manufacturer SNECMA developed the aerodynamically-valved "Escopette"

(Blunderbuss) [16] pulse jet for the propulsion of a target drone aircraft. Subsequently, in 1953, the "Ecrevisse" (Cray-fish) [17] design became available from the same company. It contained a 180° turn in the primary pulse combustor so that the inlet was facing the same direction as the exhaust. This solution increased the thrust since the jet utilised not only the main exhaust thrust but also that developed by reverse flow through the aerodynamic valve. The Foa's rectifier [11] was another contribution to obtaining a better ratio of forward-to-back flow.

In 1955, Porter and Persechino (USA) [16] were working on the use of valved pulse units for helicopter blade tips. Reynst [10] also suggested a variety of applications of pulse combustors to wing surfaces for propulsion and drag decrease. There are direct links between SNECMA and work conducted by Lockwood (started about 1958 in America) [15] whose vertical-lift device incorporated a set of one or more "Ecrevisse" units pointing vertically downward and firing through augmenters.

One of the last works on pulse combustion thrust devices reported in the literature came from the Thermo-Jet company [15]. In 1970, they produced an aerodynamically-valved unit with four symmetric air inlet tubes which reduced combustor length and increased frequency.

1.2.4. Gas turbines

The idea of the replacement of conventional constant-pressure combustion systems by systems based on a constant-volume pressure-gain cycle of a pulse combustor dates back at least to 1906, as discussed in section 1.2.2.

The best-known advocate in this field was F.H. Reynst whose entire career was devoted to the study of pulsating combustion. He filed his first patent application for the "combustion pot" in Switzerland in 1938 [10]. Figure 5 shows the Reynst design which became another distinct concept in the field of pulse combustion along with the Schmidt, Helmholtz and Rijke types of combustors. There is a fundamental difference between the "combustion pot" and the Schmidt burner. In the Schmidt tube, the air and exhaust gas enter and leave through different

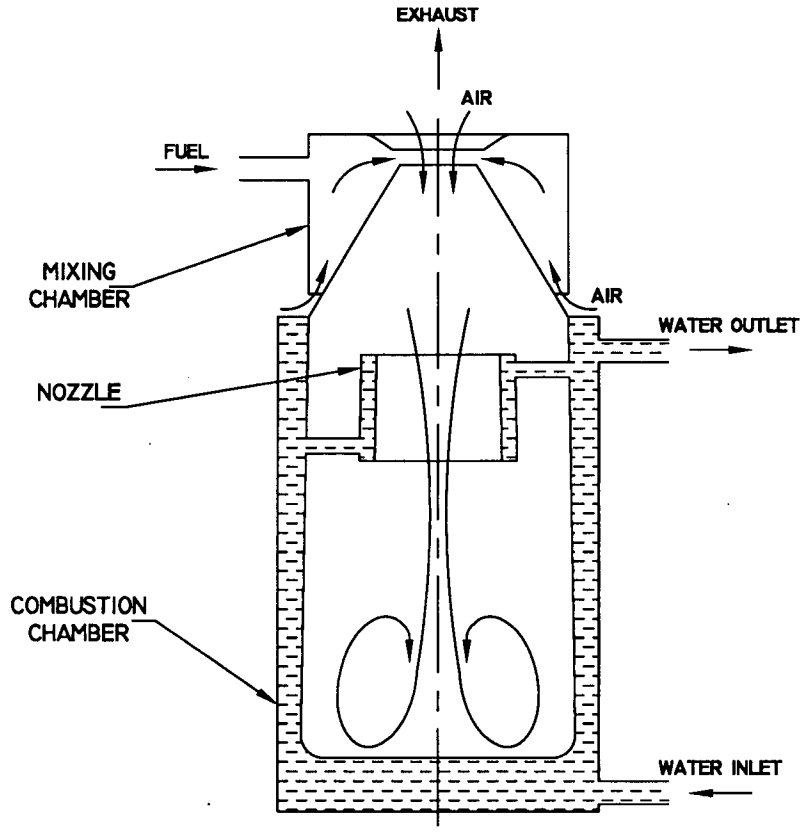

Figure 5 *Reynst's "combustion pot" [10].*

openings. In the Reynst design, on the other hand, the air and combustion products enter and leave the "combustion pot" through the same opening. While this design was not pursued after his death in 1958, possibly because of the severe noise problem, his other work encompassed fire-tube and water-tube boilers, aircraft propulsion and pulverized coal combustion.

In 1958, Porter developed a single-tube liquid fuel burner for pressure boosting a gas turbine [18]. This design features the use of the back flow to pump cooling air which mixes with the hot pulse combustion products at the burner exit so as to produce the desired exit gas temperature.

SNECMA designed, made and tested several thousand different configurations of harmonic burners without moving parts and obtained more than 40 patents covering many industrial applications of pulsating combustion [19]. Nine of these patents, taken out from 1948 to 1971, dealt with the application of pulse combustion

techniques to low power gas turbines. The pressure rise reported by the SNECMA workers was very low. They used the "Escopette" and "Ecrevise" pulse jets arranged in groups of 2,3,6,9 and 30, firing successively, and never two at once, in order to obtain continuous flow of exhaust gas. However, the precise timing of the ignition of a number of burners would always present some difficulties.

In the late 1960's, Muller carried out studies on a rotary valved pulse combustor for gas turbine pressure boost [20]. In his work, a conical rotary valve was used to control the periodic inflow of air into Helmholtz-type combustors which were found to be preferable to quarter-wave type combustors because they could be operated over a wider frequency range. The specific fuel consumption and combustion efficiency of this design were disappointing and work on his approach was carried no further.

Finally, another important contribution to this field can be attributed to Kentfield, whose work, directed at improving fundamental and practical knowledge of the valveless pulse combustor concept, commenced in 1966 at Imperial College, London, and has continued since 1970 at the University of Calgary [21]. His first combustor for gas turbine pressure boosting was somewhat similar to the SNECMA "Escopette" design but employing a different form of fluidic device for redirecting the inlet back-flow. Kentfield's subsequent studies also involved the evaluation of geometrical characteristics of burners, multiple inlets and outlets, and acoustic coupling of pairs of pulse combustors at the inlet and/or exit.

1.2.5. Steam raising

The first work on the investigation of the oscillatory combustion of coal particles was probably conducted by Audibert [13] in 1924. The flow oscillations were introduced by use of a rotary valve that periodically interrupted the flow of primary air and coal particles in a vertical tube burner.

F.H. Reynst [10] consistently advocated the use of pulsating combustion for increasing the combustion intensity in pulverized-fuel fired equipment and published

several papers which dealt with the pulsating combustion of pulverized coal. As a practical test of these ideas, a brown coal-fired pulsating combustor was constructed in Germany in the middle 50's by Sommers [22] who was probably the first to utilize a coal burning pulsating combustor for steam raising. He attached a valveless, quarter-wave type combustor to an existing boiler with steam superheaters. Coal dust was pneumatically metered into the downward pointing combustor, where it mixed and burnt with the preheated air supplied by a fan. Secondary air was added at the exit of the pulse combustor. This plant was operated for several months and performance data showed extremely high combustion and heat transfer rates inside the combustor. However, the crown of the boiler and other components vibrated as consequence of the gas oscillations.

In 1967, Babkin [23] reported work on a heavy fuel oil fired system using two coupled pulse combustors working under counterphase conditions. Again a conventional boiler was converted to incorporate the combustors which were equipped with aerovalves because of problems with mechanical valves when burning heavy fuel oil. Babkin was able to operate his burners under both pulsating and non-pulsating conditions and observed that the luminosity of the flame decreased when transition from steady to pulsating operation occurred. It should be noted that his design was not self-pumping.

Katsnel'son *et al.* [24] carried out empirical studies aimed at optimizing the geometry of quarter-wave type pulse combustors for steam generation systems. The optimum combustion chamber design found from his work was a pear-like shaped chamber attached to a constant diameter tail pipe. In Katsnel'son's burners, combustion was completed before leaving the tail pipe with only 5% excess air and again, as in almost all Russian work on pulse combustion, the self-pumping feature of pulse burners was not utilized.

In 1968, Hanby and Brown of the University of Sheffield [25] published a paper on a small pulsating combustor burning pulverized bituminous coal. They used a quarter-wave type combustor that had a mechanical flapper valve at its air inlet. Almost complete (95%) combustion of the coal was obtained in the combustor in a

mean residence time of 0.08 seconds. This is considerably shorter than the burning times in industrial burners which are of the order of 1 second. In another work, Hanby [26] investigated theoretically the oscillatory combustion of coal particles which is believed to enhance the combustion process. The most frequently used explanation is that the formation of an envelope of combustion products around the particle of coal blocks diffusion of oxygen to the particle surface. It is thought that flow pulsations periodically remove the envelope from the particle and improve the access of oxygen to its surface, thus enhancing its burning rate.

Severianin, another Russian research worker, took out patents on several pulse combustion devices and published papers on them about 1970 [27]. Emphasis was put on a dipole combustor consisting, in fact, of two in-line Schmidt-type pulverized coal-fired pulse burners. Severianin's review [28] was presented at the Atlanta Symposium on Pulse Combustion Applications in 1982 and summarised various systems for boilers, acoustic cleaning of heated surfaces, water and space heating, drying, ash particle coagulation, cleaning of liquid wastes and bitumen liquefaction. He concludes that the noise produced by the burning zone is a major problem which obstructs implementing of the method in industry.

Coal and wood burning pulsating combustors, whose design is based upon the principles of the Rijke tube (see section 1.2.2), are described in References 28, 29 and 30. In these burners, the heated gauze of the classical Rijke tube is replaced by a metal grid which supports a fuel bed. The combustion process provides the energy for driving flow oscillations which, in turn, produce a periodic and highly intense combustion process (feedback loop), thus maintaining the pulsations. Tests conducted at the Georgia Institute of Technology [29, 30] demonstrated that the Rijke combustor (see Figure 6) can burn unpulverized bituminous and sub-bituminous coals over wide ranges of coal feed rates and air/fuel ratios. A combustion efficiency from 97 to 99 percent was achieved with ten percent excess air compared to conventional stokers that require 60 percent excess air for similar performance. Such high combustion efficiencies, together with small quantities of excess air, lead to high thermal efficiencies by reducing exhaust flow losses.

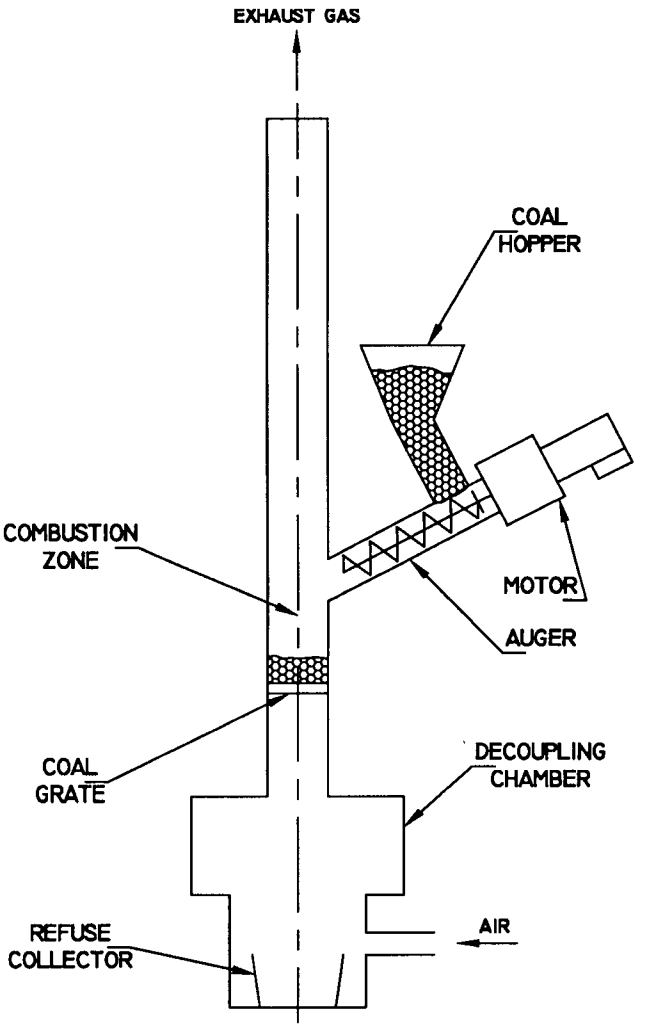

Figure 6 *Coal-burning Rijke tube pulsating combustor [29].*

1.2.6. Water heating

The German engineer Huber [31] was probably the first to apply pulse combustion for water heating. In 1948 he designed and built a pulse combustion unit for heating the circulating water in cold engines. This small, gasoline-fired, mechanically-valved combustor of about 6 kW output and over 90% efficiency was, in 1950, modified to burn natural gas. Subsequently, Huber produced a gasoline-burning unit with a small combustion chamber and spiral resonance tube lacking exit and entrance symmetry which was devised for residential heating and became known as the

"Swingfire".

Reynst suggested a wide variety of hot water heaters based on the improved "combustion pot" in his papers dating from 1943 to 1959 [10]. The pot still had the form of the original fuel can but the exhaust pipe took the shape of a diffuser of about twice the length of the pot. The air inflow during the low pressure part of the cycle aspirated and atomized the fuel. The ensuing mixture was admitted through an annular gap into the can and ignited by the hot gases of the previous cycle. This unit was said to have been heard for several miles, making it extremely unsuccessful from this standpoint.

The most successful application of pulse combustion to gas-fired water-heating has been the Lucas-Rotax Pulsmatic boiler and its upgraded version, the Hydro-Pulse heating unit of Hydrotherm, Inc. Both were developed by J.A. Kitchen [4] in Canada; the first in the period 1956-61 and its successor in 1976. Inspired by the high performance of the Swingfire pulse heater, Kitchen started a series of experiments at the Lucas-Rotax plant in Toronto with the intention of building a small water-heating boiler burning natural gas and propane. His most important innovations included a cushion chamber in the gas line upstream of the gas valve and a single resonance tube branching into smaller-diameter heat-exchanger tubes. After replacing all iron castings of the original design exposed to the condensate with sheet copper and stainless steel, inserting a condensate drain into the exhaust line and suppressing the noise level to about 57 dBA, the 29.3 kW model went into production in 1960. Its pulsating combustion system consisted of gas and air cushion chambers, one gas and one air inlet valve, mixing head assembly, flame trap, combustion chamber and jet-pipe assembly. Automatic controls took care of the purging and start up operation, as well as safety features. The Pulsmatic furnace was much smaller than a comparable furnace of standard construction and was capable of burning either natural gas or propane. Another favourable feature was that the combustion products could be simply exhausted by means of a 50 mm plastic pipe through a suitable outside wall and fresh air supplied in a similar manner. During its laboratory tests, overall efficiencies ranging from about 87 to 93% and

frequencies varying from 58 to 84 Hz were recorded [32]. Greensteal Ltd. of Winnipeg took over all manufacturing and distribution of the Pulsmatic in 1961 and continued production until 1966. A total of 546 units were built, in addition to about 150 that were manufactured by Lucas-Rotax. After a ten year gap the American company Hydrotherm renewed production of the improved Pulsmatic under the name Hydro-Pulse.

Francis *et al.* [33] developed in the early 1960's a small, gas-fired immersion heater which was operated with fully automatic ignition and control, including pulse-failure protection by means of a pressure switch. With inlet and exhaust mufflers, plus a mechanical air valve, this unit was similar in many respects to the Lucas-Rotax design. However, the fuel line had no mechanical valve.

Finally, a report on the development of a pulse combustion instantaneous water heater was presented in 1982 at the Symposium on Pulse Combustion Applications in Atlanta [34]. This unit, resembling the Hydro-Pulse design, had a gas input of about 58.6 kW and operated at thermal efficiency of 89-92% without the use of a secondary heat exchanger. The concentric gas and air flapper valves were located at the top of a 140 litre tank and the gases were mixed in a neck before entering a spherical combustion chamber.

1.2.7. Comfort air heating

In 1958, Kamm suggested a mechanically-valved pulse jet unit for residential heating [16]. In his design, fresh air for heating was drawn into an acoustically-coupled chamber surrounding the combustor and exhaust pipe during the positive pressure half of each pulse. The warmed air was discharged to the area of use during the negative pressure halves without the need for an air blower. Kamm concludes that use would also have to be made of the hot exhaust gases which escape to the chimney in order to improve the overall efficiency of his unit.

In the 1960's, Huber worked with Eberspacher in developing a successful line of gasoline-fired pulse combustors for heating commercial vehicles [15]. Fuel was

supplied from a gasoline tank by means of a carburettor into the mixing head connected to a pear-shaped combustion chamber and air entered the combustor via a diaphragm valve.

A vertical, propane fuelled pulse combustor unit having a maximum thermal output of approximately 80 kW was constructed at the University of Calgary in the early 1970's as a construction-site heater [21]. The device incorporated an aerovalved combustor of Kentfield's design and proved to be very reliable, compared with conventional equipment, because of the absence of cyclically-moving components. However, the noise levels were reported to be too high (about 100 dBA) for workers close to the heater.

In the early 1960's, the American Gas Association Laboratories (AGAL) in Cleveland began development of a high efficiency warm-air residential heating unit [3]. It is quite certain that the incentive was the certification of the Pulsmatic for residential sale by the same laboratories in 1958 [4]. Lenox Industries, a leading warm air furnace manufacturer, took over the project and after intensive research began production of the Lenox Pulse warm-air home-heating unit in 1981. The currently available units in the 11.3 to 27.5 kW output range are marketed in the U.K. in three modifications for up-flow, down-flow and horizontal installation. The higher efficiency of the upgraded heaters (up to 96%) is achieved through a new heat exchanger design which features a finned cast iron combustion chamber, temperature resistant steel tailpipe, aluminized steel exhaust decoupler section and a finned stainless steel tube condenser [35]. The furnace is equipped with a gas expansion tank, gas intake flapper valve, air intake flapper valve, spark plug igniter, flame sensor, purge blower and can be changed over from natural gas to propane.

A prototype model of a low-cost, high efficiency pulse combustion space heater was developed at AGAL in Cleveland between 1982 to 1983 [36]. The mechanically-valved unit operated at a firing rate of about 5.3 kW with a thermal efficiency approaching 92 % and heat transfer occurred from an oval-shaped combustion chamber, exhaust pipe and a secondary heat exchanger. After noise suppression to 60 dBA, a field test of ten units was performed in the 1983-1984

heating season.

1.2.8. Miscellaneous applications

One of the areas for the use of aerovalved pulse combustors is that of drying. Muller [37] reported in 1967 a study of corn drying and conveying using the SNECMA pulse jets in South Africa. In the U.S., a pulse combustor, originally developed for helicopter propulsion, was converted by the Bureau of Mines to a lignite dryer [38].

The development of a pulse combustion fired deep fat fryer at AGAL in the early 1980's is discussed in References 39, 40 and 41. The work attempted to improve the thermal efficiency of commercial cooking equipment by using pulse combustion techniques and recovering exhaust heat in other types of appliances.

Finally, it remains to mention some of the other suggested uses of pulse combustion which have not been covered in this review such as ice-melting, insecticide fogging, gasification, hot gas recirculation, fan or blower replacement, griddles, refuse incineration, heat pumps, etc.

1.2.9. Summary of main components in pulse combustors

A large number of components make up an operating pulse combustor. The major components from the standpoint of the classification of pulse combustors are the air-inlet valves and resonance tubes.

Three different general types of air-inlet valves have been described in the literature : the mechanical valve, the aerodynamical valve (aerovalve) and the rotary valve. Mechanical valves may be freely moving (flapper valves) or designed to have a restoring force which makes them normally closed (reed valves). The presence of a valve at the inlet results in high pressure boost from the outflow and a reduction of inlet noise. Aerodynamically valved systems are simple in construction and do not suffer from fatigue problems because of the absence of moving parts. Rotary-valved units work at fixed frequency which may lead to a reduction in performance.

One of the most important factors affecting the acoustic behaviour of a pulse combustor is the ratio of the resonance-tube diameter to the combustion-chamber diameter. Where the two are about equal, the term "Schmidt-type pulse combustors" (based on the operating principle of the acoustic quarter-wave tube) has been used. For the case where the ratio is small, the term "Helmholtz-type pulse combustors" (similar to the acoustic Helmholtz resonators) has been adopted.

1.2.10. Conclusion

In each of the applications considered, one or more of the special features of pulse combustors are utilized, such as high rates of heat transfer, high combustion intensity, ability to pump against small back pressure, low exhaust emission levels, fuel savings, etc. In addition, pulse combustors appear to be flexible in terms of fuel type and as a result, solid, liquid and gaseous fuels have been tried in various applications. The combination of the above attributes of pulse combustion systems can result in a favourable economic comparison with conventional combustors. The main drawback of systems based on pulse combustion lies in the high noise levels which are the key obstacle to putting pulse combustors into production.

Despite a history of about 80 years of work, there have been only two commercially successful applications of pulse combustion : Pulsmatic (Hydro-Pulse) heating unit and Lenox Pulse warm-air furnace for residential heating. It can be concluded that these pulse combustion devices not only reduce heating costs by virtue of their high thermal efficiency but their compact size and easy installation and maintenance are also attractive. It is also important to note that by use of proper application of acoustic fundamentals, the noise emitted by these devices can be reduced and controlled so as to produce a sound spectrum acceptable to the human ear.

Considering the potential benefits of the pulse combustion in a number of applications, it is hoped that this technique will receive more attention by sponsoring agencies and play a more prominent role in the field of combustion technology in

the near future.

1.3. BRITISH GAS AND MIDDLESEX UNIVERSITY WORK ON PULSE COMBUSTION

Along with other industrialised countries, Great Britain's research establishments took an interest in pulse combustion. In the U.K. the majority of the research and development work on pulse combustors has been confined to the British Gas laboratories at Watson House and the Midlands Research Station.

An experimental unit converted from town to natural gas and using an aerovalve was investigated at Watson House in the early 70's [42]. Problems were encountered with silencing, since the use of long intake ducts caused substantial back flow of exhaust gas. A small Helmholtz-type pulse combustor produced at British Gas by J.R. Watson [42] in 1982 clearly showed the potential advantages of pulse burners for applications in high efficiency gas appliances. Two years later, a larger variable geometry combustor was developed as a storage water heater and tested by S.A. Windmill to determine the factors affecting its performance [42].

The links between British Gas and Middlesex University (Polytechnic) were established in 1986 and in 1988 an experimental mechanically valved unit of a Helmholtz-type was supplied to Middlesex. From 1988 to 1989, A. Suthenthiran, a Research Fellow at Middlesex Energy Technology Centre, thoroughly investigated and improved the design of the original 15 kW "Mark 1" combustor [43, 44, 45, 46, 47, 48]. This work included the measurements of combustor pressure variations, frequency and emissions (CO_2, CO and NO_x) at the tailpipe outlet as well as the investigation of emitted noise levels. His efforts led in 1990 to the development of a smaller, more compact 5 kW "Mark 2" burner for use as a kitchen water heater [49]. In the same year, an MSc project report on pulsating combustion was submitted by D. Kassehchi [50].

Presently, there are two research students working at Middlesex University on pulse combustors. The present study, dealing with the emissions and interchangeability of gaseous fuels, and a second study which is concerned with

scaling factors in the design of pulse combustors. The latter, reflects the interest of British Gas in the possibilities of employing large pulse combustor units for residential heating applications.

1.4. OBJECTIVES OF THIS WORK

The present experimental work was conducted as an extension to Suthenthiran's investigations on the 5 kW Helmholtz-type burner. Some modifications were made to the gas-supply system, air-supply system and flapper valve assembly. The overall objective was to quantify the performance of and emissions from a pulse combustor running on a range of test gases which comprised NGA (mains), NGB, NGC (high in H_2) and NGD (high in N_2). These are the standard family 2H gases used for fuel flexibility tests of gas appliances. The operation of the combustor on propane was also examined. Investigated variables included load (gas flow rate), air/fuel ratio, combustion chamber volume and exhaust pipe length and diameter.

The achievement of this involved :

1. Modifying and setting up the existing 5 kW pulse combustor.
2. Selection and checking of reliable gas analysis equipment.
3. Preliminary tests in order to determine the operational range of tailpipe lengths and diameters. Gas was supplied from the mains.
4. Flow measurements of the aspirated combustion air and gas and comparison of the measured air/fuel ratios to the values obtained from an exhaust gas analysis.
5. Measurements of the exhaust gas emissions from burning NGA (mains) for different gas flow rates, optimum tailpipe length range and different combustion chamber volumes respectively.
6. Measurements of the exhaust gas emissions from burning NGB, NGC, NGD and propane (gas cylinders) for the optimum tailpipe length and combustion chamber volume.

CHAPTER 2 : PULSE COMBUSTOR PERFORMANCE

2.1. OPERATING CHARACTERISTICS

2.1.1. Foreword

Since the pulse combustor under investigation was of the Helmholtz type, this section is aimed at the examination of the operating characteristics of this class of pulse combustor. A literature survey of past research work was made and this established the main factors which influence the performance of this type of pulse combustor. Since this study is concerned with emissions and the gas interchangeability aspects of pulse combustors, the background work on these aspects is reviewed.

2.1.2. Frequency

The frequency of the combustion cycle (typically in the 35 to 200 Hz range) is one of the most important features of pulse combustors because of its effect on the heat transfer rate from the hot gases in the tailpipe.

The equation predicting the operating frequency of a Helmholtz-type pulse combustor [16, 45, 51] is usually expressed as that of the Helmholtz acoustic resonator:

$$f = (c/2\pi)(A/LV)^{0.5} \quad . \tag{2.1}$$

This equation relates the resonant frequency, f, with the speed of sound, c, cross-sectional area of the tailpipe, A, the combustion chamber volume, V, and the length of the tailpipe, L.

Since the speed of sound is proportional to the square root of the absolute temperature, it follows that it is impossible to compare directly the measured frequencies of operating burners with those predicted by the acoustic formula because the gas temperature is not known. The assumption usually made is that the resonant frequency must lie somewhere between that for the adiabatic flame

temperature and that for the exhaust outlet temperature.

Using an average temperature can lead to considerable differences in the predicted frequency compared with the measured value as shown by Keel and Shin [51]. Having investigated the operating mechanism and the characteristics of the flame motion in a Helmholtz-type pulse combustor, they found that the change of fuel flow-rate had a direct influence on the operating frequency and concluded that equation 2.1 does not represent the exact resonant frequency.

Keller *et al.* [52] used characteristic times to describe the mechanism that controls the relative timing between the resonant pressure wave and the instantaneous energy release. They varied the total ignition delay time, while maintaining the geometry and mean temperature constant within the combustor for a given mass flux, thus keeping the right side of the equation 2.1 fixed. It was shown that the resulting out-of phase (with pressure) component of the heat input caused a shift in operating frequency as predicted by Rayleigh. This fact reveals another source of frequency uncertainty in the case of combustion-driven oscillations. However, it should be noted that the experiment was carried out in conditions of a forced air and fuel supply and the constant mass flux was maintained by the addition of nitrogen diluent to the reactants.

The results published by Hargrave *et al.* [53] display similar trends to those reported for a Helmholtz design of pulse combustor by Francis *et al.* [33], Keller *et al.* [52] and Griffiths *et al.* [54] with operating frequency decreasing as the exhaust tube length increased. Unlike the work in References 33 and 45, Hargraves's study shows little variations in frequency with increasing combustion chamber volume.

2.1.3. Pressure

Large pressure waves produced in the combustion chamber and consequent flow oscillations in the tailpipe are believed to be responsible for high rates of heat transfer, thus enhancing the thermal efficiency of pulse combustor heating systems. The pressure variations control the operation of the pulse combustor by affecting the

difference between the internal burner pressure and that of the air and/or fuel supply. There is no need for external fan work since the pressure generated in the combustor is sufficient to drive the exhaust gases through more restrictive heat exchangers than are used with conventional burners.

According to Griffiths *et al.* [55], the pressure within a combustor, for a given firing rate, is dependent on combustion chamber size and tailpipe diameter in such a manner that with decrease of these two parameters the generated pressure increases. A systematic study conducted by Keller *et al.* [52] confirmed experimentally the validity of Rayleigh's criterion for combustion-driven oscillations. Because the mechanisms of energy release in the pulse combustor involve many complex processes the authors introduce the concept of "total ignition delay time". It is defined as a function of the characteristic time required to mix the fuel with the air and the reactants with the hot gases as well as the characteristic time for the chemical reaction to occur. These were used to describe the timing between the release of energy and the resonant pressure wave. It was concluded that the magnitude of the pressure oscillations was dependent more on this phase relationship than it was on the magnitude of the energy release rate.

Hargrave *et al.* [53] report experiments with a methane-fired Helmholtz-type pulse combustor and present typical pressure traces for the combustion chamber, exhaust exit and mixing chamber. The results obtained from pressure measurements for 1.8 m , 2.2 m and 2.6 m long tailpipes and fixed heat input of 5 kW show that there is a slight increase in peak pressures with increasing tailpipe length.

Keel and Shin [51] recorded pressure signals within the combustion chamber of a Helmholtz burner and reported the formation of double peaks. The first peak was created during the main reaction period and the second was caused by the re-inflow of air (compressibility effect). Another observed phenomenon was the phase lag between the air inlet pipe pressure and the combustion chamber pressure. The velocity obtained by dividing the distance between pressure transducers by the time delay calculated from the phase lag corresponded to the speed of sound (340 m s^{-1}), which was regarded as the propagating velocity of the acoustic wave. This paper also

discussed the relative timing between the fluctuating pressure and the heat release which determines the stability of the resonant oscillations. The amplitude of this pressure was shown to be proportional to the square of the actual fuel consumption rate.

2.1.4. Heat transfer

One of the most cited advantages of pulse combustors is the high rate of convective heat transfer in the tailpipe which is thought to be due to the scrubbing action of the oscillatory flow. The fundamental pulsation mechanism of the combustor strongly influences the heat transfer. However, the heat transfer affects the exhaust gas temperature which in turn modifies the operating frequency.

Theoretical studies examining the influence of the flow pulsation in fluids on heat transfer [56, 57, 58] concluded that there is a significant increase in heat flux under pulsating conditions which is a function of the amplitude, wave form and frequency of flow variations. The enhancement of convective heat transfer in pulse combustors received much attention in studies published by Reay [6], Francis *et al.* [33] and Hanby [59]. Hanby [60] also demonstrated that the presence of combustion-driven oscillations causes substantially increased heat transfer coefficients. According to the literature these were reported to vary from 250% greater [61] to 70% less [62] than those for steady flow. There is some uncertainty in the literature about the degree of augmentation because in some works the pulsating heat transfer is compared to that of steady, but not always fully turbulent flow, while in others it is compared with heat transfer rates predicted by correlations for turbulent flow.

The only available concept for modelling the behaviour of heat transfer under oscillatory-flow conditions is the quasi-steady state theory. Even though the amplitude and frequency range of the pulsations in the resonance tube of the pulse combustor are beyond limits of this theory, it is frequently used in the literature [53, 59, 60, 63]. This method allows modification of the Dittus-Boelter equation for turbulent heat transfer [64] :

$$Nu = 0.023 Re^{0.8} Pr^{0.4} \quad (2.2)$$

to pulsating flow conditions.

Hargrave *et al.* [53] measured the tailpipe heat flux for a Helmholtz-type gas-fired pulse combustor over a range of fuel inputs. This paper revealed that the values of the pulsating heat transfer were higher, both at the exhaust tube inlet and exit, than those calculated for steady flow. It was also shown that the highest heat transfer coefficients (about 45 to 70% above the steady case) occurred at the inlet to the tailpipe. Furthermore, they observed some higher coefficients towards the exit of the tailpipe and explained that this was caused by the condensation of water vapour which intensified the convective heat transfer. However, more than 80% of the heat was said to be transferred within the first 1 meter of the tailpipe where the enhancement of the heat transfer stemmed only from the flow oscillations. The report concluded that the experimental heat transfer rates were in reasonable agreement with predictions derived from a quasi-steady state theory.

The most comprehensive work on the effects of various flow parameters on heat transfer augmentation was published by Dec and Keller [61]. The tested Helmholtz burner was operated from 54 to 101 Hz with a broad range of pulsation amplitudes and mean tailpipe Reynolds numbers. In this paper, the convective heat transfer was characterised by the Nusselt number. Systematic control of the operating frequency, amplitude and mean flow rate enabled the authors to determine trends of Nusselt numbers for each parameter over a sufficient range. The maximum enhancement of Nusselt number was reported to be 2.5 compared with steady flow and it was found to have a linear relationship with both pulsation frequency and amplitude. The data were compared with quasi-steady state theory, which was concluded not to be adequate for describing experimental results from this study because it does not consider the frequency effect on heat transfer.

2.1.5. Thermal efficiency

Heat transfer coefficients in the case of oscillatory flow, as shown in the previous section, were found to be much greater than for steady flow. As a result, pulse combustors can extract more heat from combustion products without the need for large heat exchangers, thus achieving a high thermal efficiency with a more compact design than appliances based on conventional methods of combustion. However, the cooling of the exhaust flow, in order to recover as much heat as possible, results in the formation of a condensate which may cause corrosion as well as disturb the pulsating flow.

Thermal efficiency (TE) of a heating system is defined as a ratio of useful energy obtained from a unit of fuel to the energy initially contained in that unit [65]. Thermal efficiency can be determined by a direct method which expresses TE as a percentage of the ratio of the useful heat output to the heat input or by an indirect method which presents TE as the difference between 100% and the total percentage losses based on either the gross or net calorific value of fuel. In most instances, the latter is used for assessing thermal performance of heating systems. However, now that exhaust gas condensation is commonly practised eg. condensing boilers, the thermal efficiency should be based on the gross calorific value of the fuel. The procedure of the indirect method is described in BS 845 [66] and the considered losses in the case of gaseous fuels are : loss due to sensible heat in the dry flue gases, loss due to enthalpy in the water vapour in the flue gases, loss due to unburned gases in the flue gases and radiation, convection and conduction losses.

Reference 32 demonstrates the thermal efficiency calculation for the Pulsmatic boiler using both techniques. Results obtained by the direct method varied between 89 and 94 % and were only slightly higher than those from the indirect method. The thermal efficiency of another commercially successful design, Lenox Pulse air heater, is claimed to be as high as 96 % [35].

2.1.6. Noise and methods of its suppression

The main disadvantage of pulse combustion which is mentioned throughout the literature is the high noise levels (usually above 100 dBA) which has prevented more frequent use of pulse combustors in commercially successful applications despite their many advantages. From the standpoint of high thermal efficiency, large pressure amplitudes are desirable because they enhance heat transfer [61] but from the viewpoint of noise emission these are unwanted because they increase sound radiation from the device [59]. Therefore there must be some operational compromises in order to reach the optimum design of a pulse combustor.

Noise-control methods usually fall into three categories. These are : limitation of noise at the source, protection of the receiver and use of suppressors in the noise path. The first method cannot be applied in the case of pulse combustion because the emitted noise is an inherent problem of resonance which has to be established in order to successfully operate a pulse burner. The second method is not applicable, either, since many intended applications of pulse combustion fall into the field of domestic appliances. Therefore, only the third approach offers a solution to the noise problem and will be discussed.

The simplest way of noise suppression is to enclose the combustor with sound-absorbing material. There are three other approaches which could reduce noise emission to a level acceptable to the human ear (below 80 dBA) [32]. These are : acoustic mufflers that reflect sound energy back to the source, acoustic decouplers that reduce sound above a critical frequency and transmit sound below that frequency and reactive silencers (quarter-wave tube, Helmholtz resonator, etc.) that generate a wave pattern which cancels out the original acoustic signal [7, 65, 67]. Application of decoupling chambers to the inlet and/or outlet of pulse combustors is the most commonly reported method of noise control in the literature [3, 6, 35, 36, 39, 42, 48, 53].

2.1.7. Pulse combustor modelling

In general, the development of new pulse combustors has been based on costly trial and error methods, empirical design procedures and qualitative understanding of the processes that govern their operation such as Rayleigh's criterion. Combustor modelling provides a means to obtain a quantitative understanding of combustion phenomenon and can be used in design and to facilitate interpretation of data obtained from pulse combustion systems.

Guidelines and basic considerations for pulse combustion modelling were discussed by Edelman *et al.* [68]. Chiu and Croke [69] developed a quasi-one-dimensional pulse combustion model to assess pressure and velocity oscillations and to establish scaling laws linking the burning rate and overall heat transfer. Barr *et al.* [70] combined a one-dimensional wave model with submodels to describe both the air/fuel injection and the energy release processes. However, these models used some empirical relationships determined from experimental data because of the degree of complexity of pulse combustion processes.

2.2. EMISSIONS FROM PULSE COMBUSTION

2.2.1. General

The stringent regulations to curb emission levels of pollutants recently imposed by many industrialised countries have forced manufacturers of combustion systems to look for new techniques for burning fossil fuels. Pulse combustion with its claimed low carbon monoxide and nitrogen oxide emissions undoubtedly belongs among these methods. The minimising of pollutants and maximising combustion efficiency is contradictory, since combustion efficiency reaches its maximum theoretically at stoichiometric conditions which are associated with high temperatures [71]. These temperatures lead to high levels of NO_x.

This section will focus on emissions from pulse combustors running on

gaseous fuels. These fuels generally consist of combustible species : hydrogen (H_2), carbon monoxide (CO), hydrocarbons (C_xH_y) and inert species such as carbon dioxide (CO_2), nitrogen (N_2), etc. The basic stoichiometric equations for the combustion of gaseous fuels can be expressed as follows [72] :

$$2\ H_2 + O_2 \rightarrow 2\ H_2O \qquad (2.3)$$

$$2\ CO + O_2 \rightarrow 2\ CO_2 \qquad (2.4)$$

$$C_xH_y + (x+y/4)\ O_2 \rightarrow x\ CO_2 + y/2\ H_2O\ . \qquad (2.5)$$

These equations relate the number of moles of the reactants and the products. Stoichiometric conditions are achieved when a fuel and oxidant are mixed such that the theoretical amount of oxygen, which can be calculated from the above equations, is present to completely oxidise all the combustibles of the fuel. The corresponding amount of air required is known as the stoichiometric or theoretical air. For gaseous hydrocarbon fuels this means that exactly enough oxygen is available for all carbon to form carbon dioxide and all hydrogen to form water vapour with no unused oxygen found in the products. In practice, however, fuels are rarely burned at stoichiometric conditions; the air/fuel mixture is either lean, indicating an excess of air, or rich indicating a lack of air.

2.2.2. Carbon monoxide

Carbon monoxide is one of the most important components of combustion gases since it represents the first product of carbon oxidation. Its presence in exhaust gases indicates incomplete combustion due to lack of oxygen (under fuel-rich conditions) and low flame temperatures, thus affecting the thermal efficiency of a combustion system (see section 2.1.5).

Transformation of carbon to carbon dioxide is a very complex process which consists of many intermediate reactions. The degree of this change depends on the

amount of oxygen [67], the temperature and residence time in the flame front [73] and cooling rate of the post combustion gases [75]. Measured levels of carbon monoxide in the flame zone are higher than the values predicted by equilibrium for adiabatic combustion and the most probable mechanism through which this abundant carbon monoxide is consumed is [74] :

$$CO + OH \leftrightarrows CO_2 + H \ . \qquad (2.6)$$

It is assumed that all the carbon initially present in the fuel will be first oxidised to CO and then converted to CO_2 by the above mechanism whose rate is slower in comparison with that of CO formation [75]. While the elementary steps for oxidation of carbon monoxide are known, the detailed mechanisms which determine exhaust CO levels are not fully understood.

In pulse combustion, low emissions of carbon monoxide may be related to high mixing rates and rapid oxidation under oscillatory conditions [76] as well as to high pressures in the combustion chamber [50, 68]. Whilst there are no theoretical studies of carbon monoxide formation in pulse combustors in the literature, there are a number of papers presenting measured CO concentrations [34, 36, 39, 42, 46]. The reported levels of CO in pulse combustor exhaust gases do not generally exceed 400 ppm for optimum operating conditions and in some cases are as low as 40 ppm [77]. For example, the CO/CO_2 ratio achieved by Lenox Pulse units when properly installed is below 0.004 [35] which is five times lower than current limit for domestic gas appliances [78].

2.2.3. Nitrogen oxides

The two major oxides of nitrogen (NO_x) which are formed as a result of burning gaseous fuels in combustion systems are nitric oxide (NO) and nitrogen dioxide (NO_2). Concentrations of the latter are generally small compared to the former [75] and nitric oxide can be present at high levels in the exhaust gases of

traditional combustors. Thermal NO is formed during combustion by the reaction of atmospheric nitrogen with oxygen at high temperatures and fuel NO by converting nitrogen compounds in the fuel to NO at comparatively low temperatures. Thermal NO is the dominant source of oxides of nitrogen unless the fuel being burned has high content of chemically bound nitrogen.

Under fuel-lean and stoichiometric conditions the formation of thermal NO takes place mainly in the post-flame region [73] after completion of combustion by the well-known Zeldovich mechanism [79] :

$$N_2 + O \rightleftharpoons NO + N \qquad (2.7)$$

$$N + O_2 \rightleftharpoons NO + O \qquad (2.8)$$

The thermal NO formation rate is strongly dependent on temperature and relatively slow compared to the combustion rate.

Under fuel-rich conditions NO formation is less well understood. Fenimore [80] found that there was another source of NO near the reaction zone which could not be explained by the Zeldovich route. This is known as Prompt NO. There has been some controversy in the literature as to what is the cause of this rapid formation of NO in the flame. Thompson *et al.* [81] and Sarofim *et al.* [82] proposed that the excessive levels of NO could be related to the super equilibrium concentration of atomic oxygen present early in the flame, whereas Iverach *et al.* [83] explained the phenomena through direct reaction of hydrocarbon radicals with molecular nitrogen.

The most important factor governing formation of nitric oxide (and hence total NO_x) is the flame temperature following by residence time and excess oxygen levels [67, 73, 84]. With decrease of the three parameters the production of nitrogen oxides decreases. Reducing the excess air causes a rise in the flame temperature which in turn increases thermal NO. Under fuel-lean conditions the NO formation is more temperature than excess oxygen dependent and thus NO_x levels decrease with increase in excess air. Conventional combustor design allows for high

temperatures and long residence times in order to complete oxidation of carbon monoxide. These conditions, however, lead to high NO_x concentrations which may be reduced only by costly methods such as the exhaust gas recirculation, secondary combustion, indirect injection, etc.

Systems based on pulse combustion do not require such NO_x reducing techniques because of the very nature of this type of combustion which produces inherently low levels of NO_x. The reported values are usually below 60 ppm [16, 36, 46, 77], which are less than half of those for conventional heating units [77], and often even in the range of 10-20 ppm [85]. Reference 77 also shows that nitrogen dioxide accounts for less than 20% of the total measured oxides of nitrogen for a pulse furnace and Reference 36 suggests an even lower percentage (10%) for a pulse combustion space heater.

Pulse combustors are normally operated under fuel-lean conditions which eliminates formation of prompt NO. Hence the production of NO can be described by the Zeldovich formation mechanism. There are at least two possible ways to explain the reduced concentration of thermal NO in pulse combustor exhaust products. Intermittent combustion does not allow the system to acquire high overall temperatures as in the case of continuous combustion and the residence time of hot gases in the combustion zone is rapidly shortened thus quenching the formation of thermal NO.

The latter mechanism, investigated by Keller and Hongo [86], was proved to be responsible for the lower NO values. It was concluded that a short residence time is due to a rapid mixing of residual gases from the previous cycle, cooled by an increased heat flux in the combustion chamber, with hot combustion products. Furthermore, the measured velocities showed virtually no back flow from the tail pipe to the combustion region (45 mm streamwise from the entrance to the combustion chamber) thus ruling out exhaust gas recirculation as a possible mechanism controlling the production of NO in this study.

In general, the NO_x emissions from pulse combustors increase with firing rate and fall to a low level as the excess air levels rise [46, 85]. Reference 86 indicates

that there is no significant effect of pressure on the production of nitric oxide.

2.3. FUEL FLEXIBILITY

2.3.1. General

The availability of natural gases from various gas fields has generated renewed interest in burner flexibility and gas interchangeability prediction. The likelihood of gases having different compositions will increase as more natural gas discoveries are made. Furthermore, in the future, when natural gas reserves become depleted, fuel producers might manufacture gases from coal and other alternative energy sources. Therefore existing and advanced combustion systems must be tolerant to variations in fuel characteristics. However, a compromise has to be made because to produce appliances working over a wide range of gases may be too costly.

Natural gas is a mixture of hydrocarbons (mainly methane) and other gases and can vary broadly in its properties. The properties which determine its combustion performance in an appliance are : flammability limits, minimum spark ignition energy, calorific value, relative density and most importantly burning velocity and Wobbe number. The latter is defined as [65] :

$$W = \frac{Gas\ calorific\ value}{\sqrt{Gas\ relative\ density}} . \qquad (2.9)$$

Wobbe number is especially useful in comparing gaseous fuel mixtures because it indicates the effect of changes in gas composition on appliance heat output under a constant pressure supply.

Burning velocity is defined as the velocity of a flame propagating through the unburnt gas mixture in a direction normal to the flame front [67]. The flame appears to be stable if the burning velocity equals the component of the mixture stream velocity normal to the flame front. High flow rate and a low burning velocity may cause flame lift. On the other hand, low flow rate and a high burning velocity may

lead to lightback. There is no standardized method of its measurement and the literature reveals considerable differences between the values obtained by various techniques [65, 87]. As a result, Great Britain's gas industry uses the Weaver flame speed factor for gas mixtures rather than burning velocity. It is derived from tabulated flame-speed coefficients and expresses the burning velocity of the mixture as a percentage of the maximum burning velocity of a hydrogen/air mixture which is assigned the value of 100 [67].

2.3.2. Classification of gases

The International Gas Union (IGU) established a classification scheme [88], based on Wobbe number, which is now adopted in European Standards. Three families of gases are identified :

Family 1 - gases (various types of town gas) having a Wobbe number in the range 22.6 - 29.8 MJ m^{-3},

Family 2 - gases (natural gases) having a Wobbe number in the range 39.3 - 54.8 MJ m^{-3},

Family 3 - gases (propane, butane) having a Wobbe number in the range 73.4 - 87.6 MJ m^{-3}.

Family 2 was subdivided into two groups because of the wide variation of possible compositions of natural gases. These are Group H and L with a Wobbe number spanning 45.7 - 54.8 MJ m^{-3} and 39.3 - 45.0 MJ m^{-3} respectively. In the U.K. only gases within Group H are distributed.

2.3.3. Testing of appliances

It is necessary to operate gas appliances safely under conditions when variations in gas composition occur. This can be ensured by testing all appliances with a range of gases. This procedure involves the use of a reference gas of the average composition which is expected to be normally supplied to the appliance and limit

gases. The latter are of the extreme compositions that could be distributed for short periods in case of emergency. The limit gases are chosen to simulate the worst conditions with respect to completeness of combustion, lifting or lightback of the flames. Table 1 shows the compositions of the current family 2H test gases used in Great Britain [89].

Test gas	Designation		Composition / vol %				Wobbe number / MJ m^{-3}
	GB	IGU	CH_4	C_3H_8	H_2	N_2	
Reference	NGA	G20	100	0	0	0	50.68
Incomplete combustion	NGB	G21	87	13	0	0	54.61
Lightback	NGC	G22	65	0	35	0	46.37
Lift	NGD	G23	92.5	0	0	7.5	45.62
Burn-back sooting	NGC2	G24	68	12	20	0	51.96

Table 1 *Family 2H test gases [89].*

2.3.4. Interchangeability of natural gases

The principal qualities that gases of family 2H should posses in order to be acceptable for distribution are : similar Wobbe number to that of a reference gas, good flame stability, reliable ignition and complete combustion. Natural gases satisfying these criteria without the need for any adjustment to appliances are said to be "interchangeable" with existing supplies. The best way to assess interchangeability of a gas is to conduct large field measurements. However, this would be very expensive and time consuming. Therefore, a number of techniques are used to predict gas interchangeability.

The method for family 2H gases which is best known in the U.K. is based on the Harris & Lovelace diagram [87], but now utilizes an improved version [88,

89]. Here, Wobbe number is plotted against Weaver flame speed factor in order to define an acceptable and an emergency area within which all gases are interchangeable. The limit gases are used to determine the boundaries of these areas. This concept, however, has a disadvantage caused by slight variation of Weaver flame speed factor for distributed natural gases.

The approach currently followed [90, 91] is based on gas composition rather than on empirically derived characteristics. It expresses all gases in terms of a 4-component mixture of methane, other hydrocarbons, hydrogen and inerts. A volume of interchangeability can be defined in a 3D coordinate system consisting of a Wobbe number axis, hydrogen axis and propane+inerts axis.

2.3.5. Pulse combustor fuel flexibility

Existing procedures for interchangeability prediction are designed for conventional combustion systems. For advanced systems other factors should be also included such as NO_x emissions, noise, etc. in addition to traditional combustion criteria.

Even though that it was proved [92] that changes in fuel composition affect phase relationship between the heat release and the resonant pressure waves which control the pulse combustion process, there are no known published interchangeability prediction techniques designed for pulse combustors. The only relevant study was conducted for the Gas Research Institute (USA) by Griffiths *et al.* [77] who determined the effect of fuel gas composition on furnace and boiler performance for a large number of residential units. They used reference and limit gases, the composition of which was considerably different from those used in the U.K. Two of the tested systems were pulse combustion units which operated successfully on all four test gases and showed lower levels of NO_x than the other units.

CHAPTER 3 : EXPERIMENTAL APPARATUS

3.1. DESCRIPTION OF EXISTING COMBUSTOR RIG

3.1.1. General

The present study used, as its starting point, a pulse combustor of the Helmholtz type which was constructed by A. Suthenthiran [49] at Middlesex Polytechnic in 1990. This gas-fired unit, of 5 kW output, was based on the design of the 15 kW combustor originally supplied by British Gas.

Figure 7 shows a schematic diagram of the existing combustor, the main parts of which are a mixing head, flapper valve assembly, combustion chamber and exhaust tube. The burner was mounted in a 38 l capacity water tank with the combustion chamber fully immersed. The tank was equipped with a circulation pump which kept the water thoroughly mixed so that it had a uniform temperature. The pulse combustor and tailpipe, combined with gas-supply, air-supply and ignition systems, formed a unit capable of operating as a pulse combustion water heater.

3.1.2. Mixing head

The mixing head, of about 30 cm^3 volume, was used to premix the reactants upstream of the flapper valve. The air port and gas port were arranged radially to the centre line of the combustor and 90 degrees apart. Air entered the head through a 15 mm diameter copper pipe and gas was injected via a 3 mm diameter orifice. The mixing head was made of brass and its position could be adjusted relative to the combustion chamber.

3.1.3. Flapper valve assembly

An exploded view of the flapper valve assembly is given in Figure 8. A flapper valve admitting the gas/air mixture into the combustion chamber was located inside the valve holder (brass). This Teflon coated fibre glass valve of 0.13 mm thickness

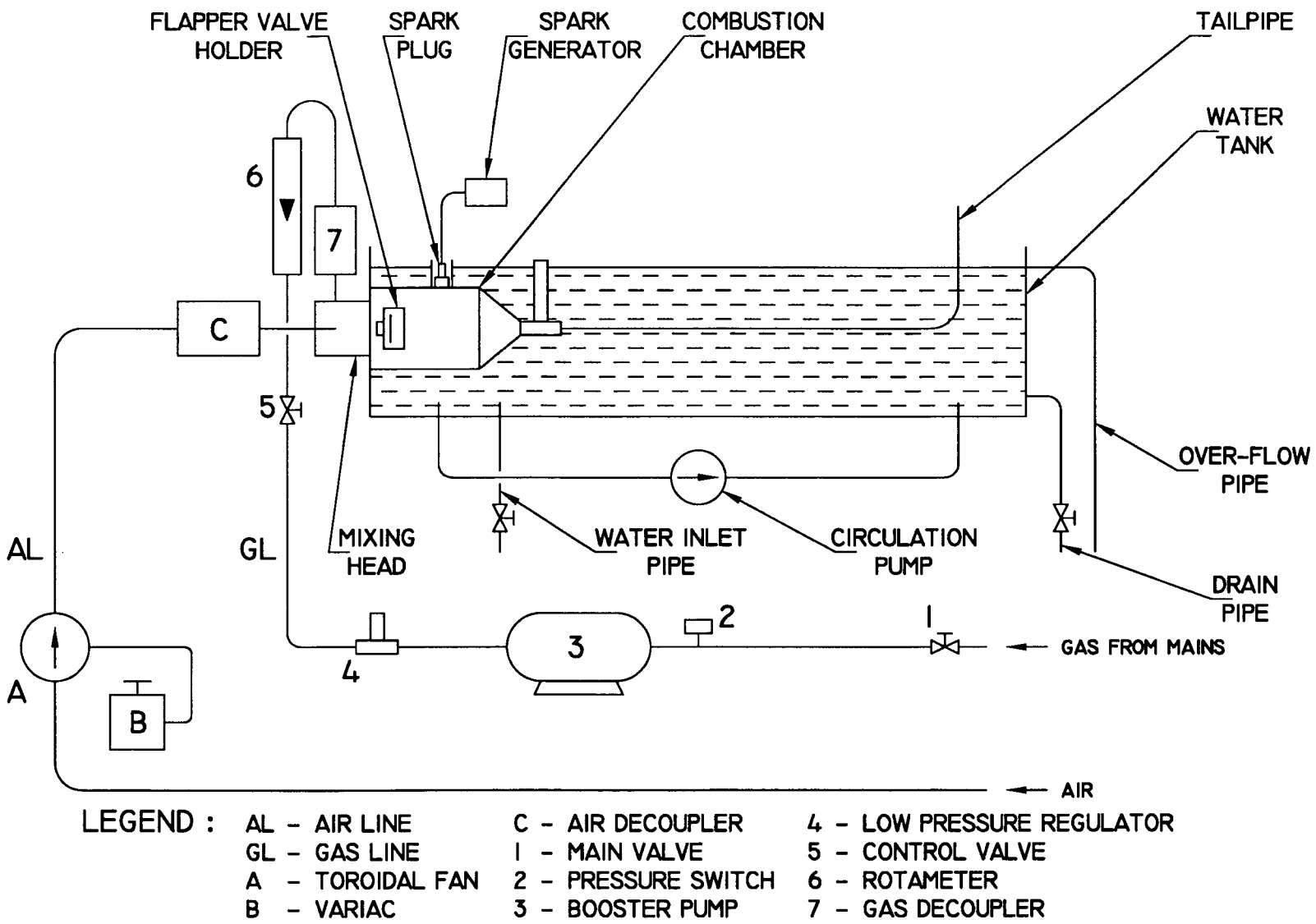

Figure 7 Schematic diagram of the existing combustor rig.

moved freely back and forth over the spacer (mild steel) depending on the pressure difference between the supply lines and the combustion chamber. It opened and closed against the backing plate (mild steel) and valve holder respectively. The operation of the valve is illustrated in Figure 2. A flame trap made of mild steel mesh prevented any damage to the valve which might have been caused by the temperature exceeding the Teflon limit (260 °C).

3.1.4. Combustion chamber and exhaust tube

The pulse combustor comprised a brass-walled cylindrical combustion chamber having a volume of about 111 cm^3 which was adjustable by moving the flapper valve assembly within the combustion chamber. The combustible mixture drawn into the chamber was ignited by means of a spark plug located at the top of the chamber in a copper-tube protector. It was powered by a spark generator operating at approximately 200 discharges per minute.

A cast-iron fitting, incorporating a thermocouple port, connected the tapered end of the combustion chamber with a copper tailpipe of inner diameter 8 mm and 1.2 m length. Only a small section of the tailpipe protruded into the air; the main part was surrounded by water.

3.1.5. Gas-supply system

Gas from the mains (20 mbar static pressure) entered the system via the main valve (1) and then passed through a gas pressure switch (2) which was set up for 10 mbar minimum pressure. The gas was boosted by a compressor (3) to a pressure of 25 mbar in order to eliminate the effect of the fluctuations in the laboratory gas line on the combustor performance. A pressure regulator (4), incorporated in the line downstream of the compressor, allowed the gas to exit at around 16 mbar. Gas rate to the burner was controlled by the valve (5) and metered using a variable-area rotameter (6) calibrated for standard mains gas (relative density 0.6). A 180 cm^3 gas

decoupler was fitted between the rotameter and mixing head in order to smooth the flow through the rotameter, thus enabling a reasonably steady reading of the gas flow rates.

3.1.6. Air-supply system

Starting air was supplied by a toroidal fan (A), the speed of which could be controlled by a variac (B). The air entered and left the fan via a 2.5 m and 1.4 m long plastic tube (25 mm internal diameter) respectively. The noise levels of the unit were reduced at the inlet by inclusion of a 200 cm^3 air decoupler (C).

3.2. MODIFICATIONS AND ADDITIONS TO THE EXISTING RIG

3.2.1. General

A schematic diagram of the modified combustor rig is given in Figure 17 (p. 82).

Due to the unsatisfactory performance of the existing combustor the original exhaust tube was replaced with a longer 2.00 m tailpipe. This was connected to a motor car silencer in order to lower the noise levels of the operating unit.

Modifications were made to the flapper valve assembly (see Figure 8). It was observed that the original flapper valve had lost some of its rigidity due to the high temperatures occurring in the combustion chamber. Consequently, the valve had become partially deformed by being pressed against the gas/air mixture inlet ports. As a result, a new 35% thicker valve was introduced.

Due to cyclic forces acting on the valve holder screw, the nut became loose after a period of operation resulting in the deterioration of the combustor performance. A spring washer insertion eliminated this problem (see Figure 8).

In view of the intended investigation of the combustion chamber volume effect on the combustor operation, the possibility of flapper valve assembly adjustment within the chamber was checked. The longitudinal movement of the valve

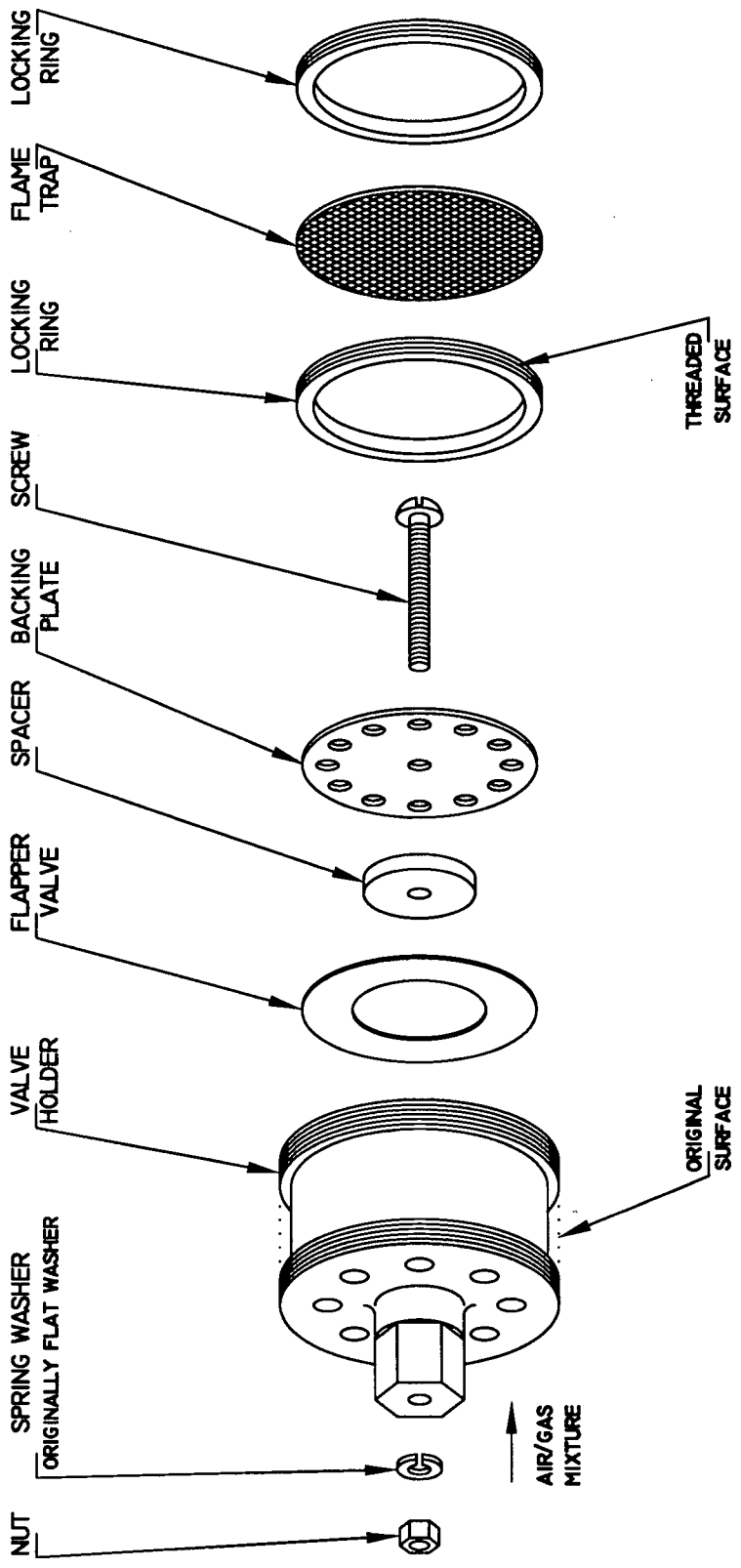

Figure 8 *Flapper valve assembly.*

holder was found to be restricted by friction between external thread of the holder and internal thread of the combustion chamber. The latter was exposed to the hot combustion products and therefore became covered with a layer of deposited oxides. The threads were cleaned, oiled and the middle section of the valve holder thread cut off leaving only a narrow threaded strip at each end (see Figure 8), thus enabling the movement of the flapper valve assembly 20 mm deeper into the chamber than before.

Finally, a two-way valve (8) was added to the gas line between the low pressure regulator (4) and booster pump (3) in order to be able to operate the combustor on a gas supplied from a nearby cylinder (10). The gas leaving this cylinder was at a pressure close to 150 bar and this was reduced by a high pressure regulator (9) before entering the low pressure regulator.

It should be noted that the 2.00 m long tailpipe of 8 mm internal diameter and combustion chamber volume adjusted to 110 cm^3 will be referred to as "optimum configuration" of the pulse combustor in the later chapters.

3.2.2. Air-flow measurement

One of the variables to be investigated in this study was the flow rate of combustion air into the burner. Suthenthiran [43] employed a variable-area rotameter to determine the air flow rate in his work. However, this was not successful because of the inertia of the flowmeter float under pulsating conditions. The float fell during part of the initial cycle and closed the air inlet of the flowmeter, thus preventing the operation of the unit. It was thought that the introduction of an orifice plate flow meter in series with air-box to the air line before the air decoupler would be a feasible way for air flow measurement in the present study.

According to ISO Technical Report 3313 [93] it is possible to measure pulsating fluid flow in a pipe by means of an orifice plate, which is designed for steady flow, under certain conditions. Generally, it is necessary to insert a rigid receiver eg. air-box, which provides sufficient damping of the flow rate fluctuation,

between the pulsating flow source and the pressure-difference device eg. orifice plate. A Hodgson number can be applied to calculate the minimum required damping volume of an air-box. However, in order to use the Hodgson number criterion several data must be known such as waveform of the pulsations, mean flow rate in the measuring orifice, pulsating frequency etc. These could be neither measured nor estimated for the pulsating flow in this study. Therefore, a decision was taken to manufacture two air-boxes; a small box of 5 litre volume, whose size was based on the usual ratio of air-box volume/flow rate for reciprocating engines, and a second, large enough to satisfy the Hodgson number criterion (50 litre volume).

An orifice plate flow meter, the main components of which are shown in Figure 9, was designed and machined according to BS 1042 [94]. A differential pressure was measured between the wall tappings, one of which was on the upstream side and the other on the downstream side of the plate. The volume rate of flow through an orifice, q_v, can be calculated using the following equation :

$$q_v = CE\varepsilon\frac{\pi d^2}{4\rho}\sqrt{2\Delta p \rho_1} \ , \qquad (3.1)$$

where C is coefficient of discharge,
E velocity of approach factor,
ε expansibility factor,
d diameter of orifice,
ρ mass density of the fluid,
Δp differential static pressure
and ρ_1 upstream density.

Using BS 1042 and by substituting 0.6238 for C, 1.03 for E, 0.013 m for d, 1 for ε, and 1.183 kg m^{-3} for ρ and ρ_1 in equation 3.1 we get :

$$q_v = 20.83\sqrt{\Delta p} \ , \qquad (3.2)$$

where q_v represents the volume flow rate of air in 1 min^{-1} for the manufactured orifice if Δp is in mm H_2O.

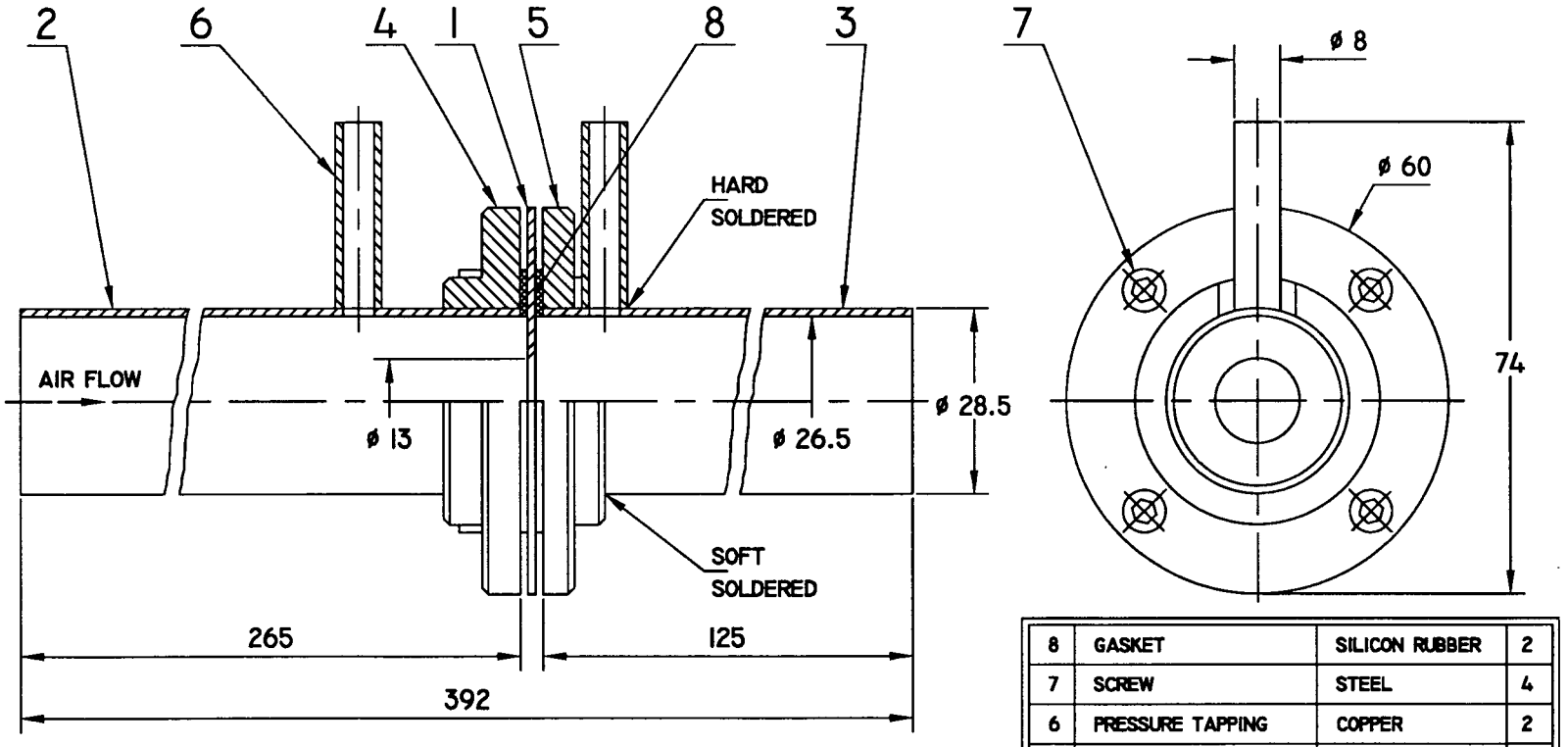

No.	Description	Material	Qua.
8	GASKET	SILICON RUBBER	2
7	SCREW	STEEL	4
6	PRESSURE TAPPING	COPPER	2
5	DOWNSTREAM FLANGE	BRASS	1
4	UPSTREAM FLANGE	BRASS	1
3	DOWNSTREAM TUBE	COPPER	1
2	UPSTREAM TUBE	COPPER	1
1	ORIFICE PLATE	MILD STEEL	1

Drawn by Jiri David

Figure 9 Orifice assembly.

3.2.3. Temperature measurement

Temperature readings of combustion products were taken at two measuring ports (see Figure 17, p. 82). These were placed 45 mm downstream from the combustion chamber exit (port 1) and from the tailpipe exit (port 2) respectively. Mineral-insulated metal sheathed thermocouples of type "K" (+ leg Ni-Cr, - leg Ni-Al) were connected to a digital thermometer of Comark 2501 type, the accuracy of which was verified by comparing a few readings with tabulated values of microvoltage for the given thermocouple type. The thermocouples were of 3 mm diameter with a maximum operating temperature 1100 °C continuous and output tolerances ± 1.5 °C or 0.004 t, which ever is greater. The temperature of the bath in the water tank was measured by means of a mercury in glass thermometer.

3.2.4. Exhaust gas sampling ports

A modified cast-iron fitting incorporating two exhaust sampling ports as well as the temperature port 2 (see Figure 10) was attached between the downstream end of the tailpipe and the silencer (see Figure 17). It was mounted with two stainless steel sampling probes (3.5 mm internal diameter), one of which was facing the stream of the outcoming exhaust gas directly and the other entered the fitting at an angle of 35° as illustrated in Figure 10.

3.2.5. Available gas analysis equipment

Five different gas analyzers were available at Middlesex University during the experimental part of this study. Their features are summarised in Table 2 on the following page.

Type / Analyzed gases / vol % or ppm		LANCOM 3200	KM 9004	SONOX	ADC WA558-2*	MEXA-324GE
O_2	Range	0 - 20 %	0 - 25 %	-	0 - 10 %	-
	Resolution	0.1 % O_2	0.1 % O_2	-	0.01 % O_2	-
	Sensor Type	Electro-chemical cell	Electro-chemical cell	-	Paramagnetic cell	-
	Accuracy	±0.4 % O_2	-0.1 +0.2 % O_2	-	±0.05 % O_2	-
CO	Range	0 - 1999 ppm	0 - 4000 ppm	-	0 - 500 ppm	0 - 10 %
	Resolution	1 ppm CO	1 ppm CO	-	1 ppm CO	0.01 % CO
	Sensor Type	Electro-chemical cell	Electro-chemical cell	-	Infrared absorption	Infrared absorption
	Accuracy	±4 % r†	±10ppm/±5%r†	-	±1 % r†	±0.04%/±2%r†
CO_2	Range	0 - 99.9 %	0 - 20 %	-	3 - 20 %	-
	Resolution	0.1 % CO_2	0.1 % CO_2	-	0.1 % CO_2	-
	Sensor Type	Calculated	Calculated	-	Infrared absorption	-
	Accuracy			-	±1 % r†	-
NO_x	Range	0 - 1999 ppm	-	0 - 4000 ppm	-	-
	Resolution	1 ppm NO_x	-	1 ppm NO_x	-	-
	Sensor Type	Electro-chemical cell	-	Electro-chemical cell	-	-
	Accuracy	±4 % r†	-	±5 % r†	-	-
NO	Range	-	-	0 - 2000 ppm	-	-
	Resolution	-	-	1 ppm NO	-	-
	Sensor Type	-	-	Electro-chemical cell	-	-
	Accuracy	-	-	± 5 % r†	-	-
NO_2	Range	-	-	0 - 2000 ppm	-	-
	Resolution	-	-	1 ppm NO_2	-	-
	Sensor Type	-	-	Electro-chemical cell	-	-
	Accuracy	-	-	± 5 % r†	-	-
SO_2	Range	0 - 1999 ppm	-	0 - 2000 ppm	-	-
	Resolution	1 ppm SO_2	-	1 ppm SO_2	-	-
	Sensor Type	Electro-chemical cell	-	Electro-chemical cell	-	-
	Accuracy	±4 % r†	-	± 5 % r†	-	-
HC	Range	-	-	-	-	0 - 10000 ppm
	Resolution	-	-	-	-	10 ppm HC
	Sensor Type	-	-	-	-	Infrared absorption
	Accuracy	-	-	-	-	±20ppm/±2%r†

* O_2, CO and CO_2 ranges are much wider; only those applicable to this study are shown.

† Accuracy in percentage of readings; when two figures are given, the first represents error limits in vol % or ppm of analyzed gas and the second in percentage of readings. The greater of the two applies.

Table 2 *Specifications of available gas analyzers.*

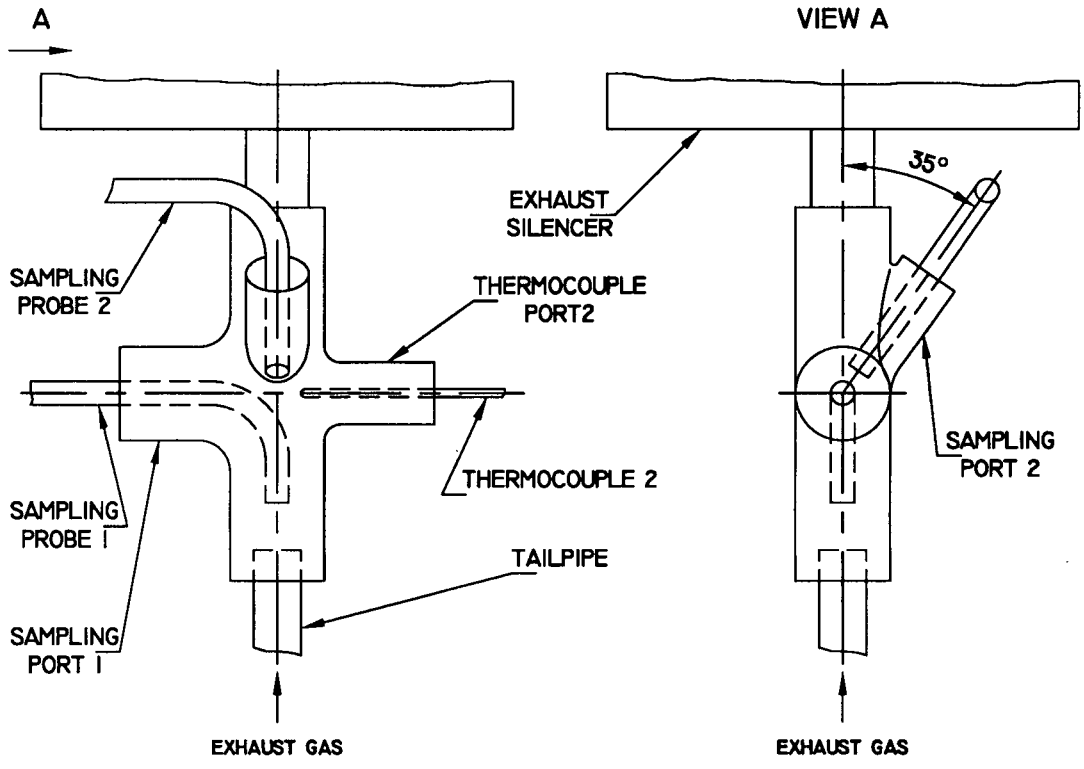

Figure 10 Exhaust gas sampling fitting.

CHAPTER 4 : RESULTS AND DISCUSSION

4.1. FOREWORD

This chapter firstly describes all the preliminary work which was necessary in order to establish the performance of the test rig and the reliability of the test instrumentation and measuring techniques. Secondly the results of five major investigations, ie. exhaust gas analysis for varying gas flow rate, tailpipe lengths, combustion chamber volumes, different fuel gases and operating frequency measurement, are discussed and details of the experimental techniques used are given.

4.2. PRELIMINARY WORK

4.2.1. Time dependent temperature behaviour

At the very beginning of the experimental work it was decided to investigate briefly the exhaust gas and water bath temperature changes with time in order to became more familiar with the time taken to establish steady state conditions. Temperatures at the combustion chamber exit (t_{Exh1}), temperatures at the tailpipe exit (t_{Exh2}) and water bath temperatures (t_{Water}) were recorded using the equipment described in section 3.2.3. NGA from the mains was supplied to the unit working with optimum configuration* of the tailpipe and combustion chamber. Gas input was maintained constant at 10 l min^{-1} during the test.

Figure 11 shows t_{Exh1} rising sharply immediately after the first ignition followed by levelling at approximately 844 °C for the remaining time. The recorded temperature was about 250 °C below the maximum operating limit of the thermocouple used. t_{Exh2} increased almost linearly with time during a 50 minute period (apart from two initial readings) and t_{Water} demonstrated an exponential-like trend with the slope declining as time increased.

The amount of the condensate coming out of the exhaust tube was observed

* See the end of section 3.2.1.

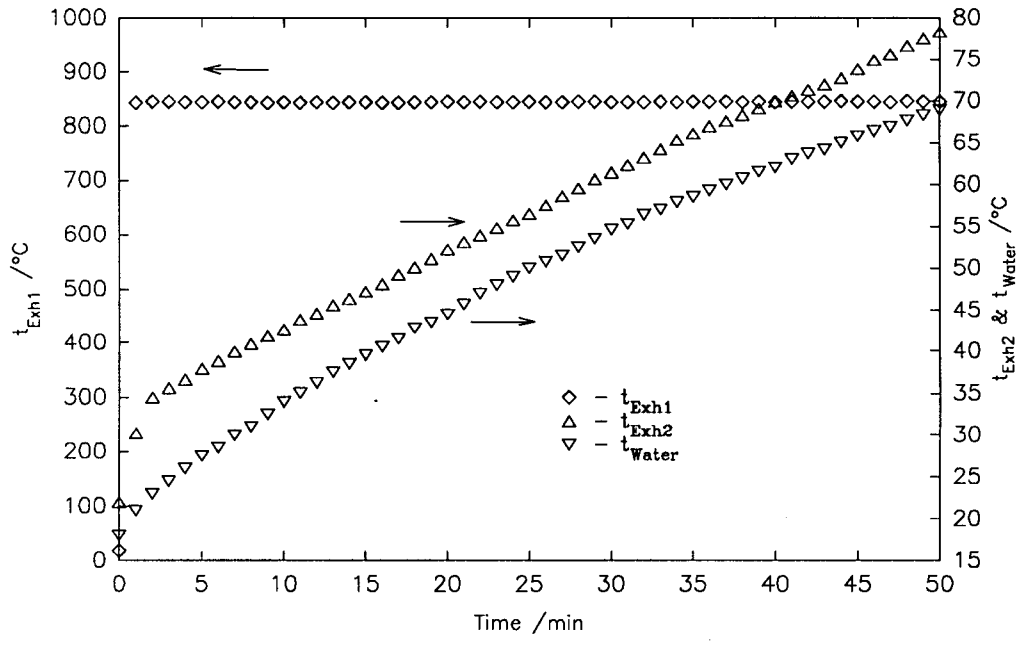

Figure 11 Dependence of exhaust gas temperatures (t_{Exh1}, t_{Exh2}) and water bath temperature (t_{Water}) on time.

throughout the test so as to determine the water bath temperature which was high enough to prevent water droplet formation. Water droplets may disturb the operation of the combustor and cause corrosion in the silencer. It was found that the condensate production was substantially reduced above t_{Water} = 60 °C when the water content of the exhaust gas took the form of a vapour. This is in agreement with calculated dew point of water of 59.3 °C assuming stoichiometric combustion of NGA. Consequently, it was decided to maintain the water temperature in the tank at 65 °C in further investigations.

4.2.2. Selection of gas analyzer

Confidence in the reliability of the gas analysis equipment used in this work was essential for comparison of measured exhaust gas emissions with literature data. A considerable effort was put into checking the available gas analyzers (see Table 2) in order to ensure correct and consistent readings. Exhaust products emitted by gas-

fired pulse combustors comprise oxygen, nitrogen, carbon monoxide, carbon dioxide, nitrogen oxides, and water vapour. The present project required the selection of equipment capable of measuring oxygen, carbon monoxide and nitrogen oxides exhaust gas concentrations which are the factors indicating combustion quality (O_2, CO) and appliance safety (CO, NO_x).

The oxygen sensors of the available analyzers were checked against the output from a gas mixing apparatus, incorporating low-rate solenoid flow meters of high accuracy, which allowed the production of an air/nitrogen mixture containing set oxygen concentrations. The mixture was first collected in a sealed plastic bag equipped with a tap and then examined using three different analyzers. The obtained data is displayed in Table 3 and shows close agreement among the three tested oxygen sensors. The difference between the adjusted values (left column of the table)

Gas mixing apparatus O_2 / vol %	LANCOM 3200 O_2 / vol %	KM 9004 O_2 / vol %	ADC WA558-2 O_2 / vol %
1.0	1.6	1.5	1.53
2.0	2.5	2.5	2.51
3.0	3.5	3.5	3.47
4.0	4.5	4.4	4.45
5.0	5.4	5.4	5.37
6.0	6.4	6.3	6.35
7.0	7.3	7.3	7.31
8.0	8.3	8.3	8.29

Table 3 *Oxygen levels recorded by available gas analyzers; O_2/N_2 mixture of known composition was provided by gas mixing apparatus.*

and measured values was most probably caused by intrusion of ambient air into the bag which increased oxygen concentrations of the samples. It was concluded that all three gas analyzers satisfied the requirements of this study as far as the measurement of O_2 was concerned.

The carbon monoxide sensors of the analyzers were tested against a span gas

of known composition as follows : 420 ppm of CO, 2.5428 % CO_2 and nitrogen.

CO concentrations measured by LANCOM, KM, ADC and MEXA analyzers were 581 ppm, 417 ppm, 408 ppm and 0.04 % respectively. The KM analysis was the closest to the known concentration and was within the limits of its quoted accuracy. The LANCOM CO sensor appears to have been faulty which may be due to cell deterioration. The composition of the span gas also allowed the ADC carbon dioxide sensor to be checked and a value of 2.45 % of CO_2 was recorded. It should be also noted that many problems were encountered during the calibration of ADC carbon monoxide and carbon dioxide sensors. A professional adjustment would have been needed to guarantee reliability of the readings.

In view of the above findings it was decided to use the KM 9004 gas analyzer for the investigation of O_2 and CO exhaust gas concentrations in the present work. However, it was felt that the combustion products of the investigated burner should also be measured using different analyzers in order to confirm the selection of the KM analyzer, and also to choose a suitable NO_x analyzer and to evaluate the effect of the sampling probe position on the exhaust gas analysis. The data obtained during additional six tests are presented in Figures 12, 13 and 14. The combustor ran on NGA (mains) with the 2.00 m tailpipe, 110 cm^3 combustion chamber volume and connected exhaust silencer. The temperature of the water bath was maintained at 65 ±1 °C throughout the tests. Several sampling lines of 3.5 mm internal diameter having a plastic connector at either end of the PTFE tube were fabricated and used to pass the exhaust products to the examined sensors. Exhaust gas concentrations of O_2, CO and NO_x on a dry basis were recorded for gas flow rates ranging from 8 to 11 l min^{-1} in 0.5 l min^{-1} intervals.

Figure 12 shows reasonable agreement among the oxygen levels detected by the analyzers, thus supporting the results given in Table 3. Confirmation of the high CO error of LANCOM measurements can be seen in Figure 13. The same graph displays, in general, somewhat lower ADC carbon monoxide concentrations than those recorded using the KM; this is in accordance with the span gas result. Test D was carried out using the MEXA gas analyzer whose CO resolution (0.01%) was not

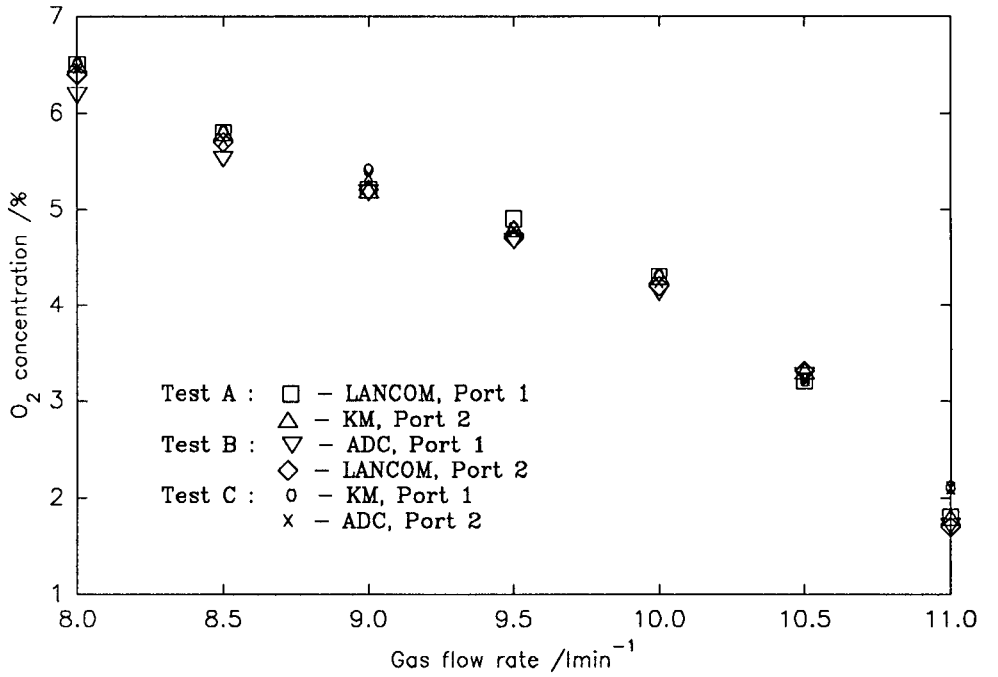

Figure 12 Comparison of O_2 concentrations in exhaust gas measured by different analyzers.

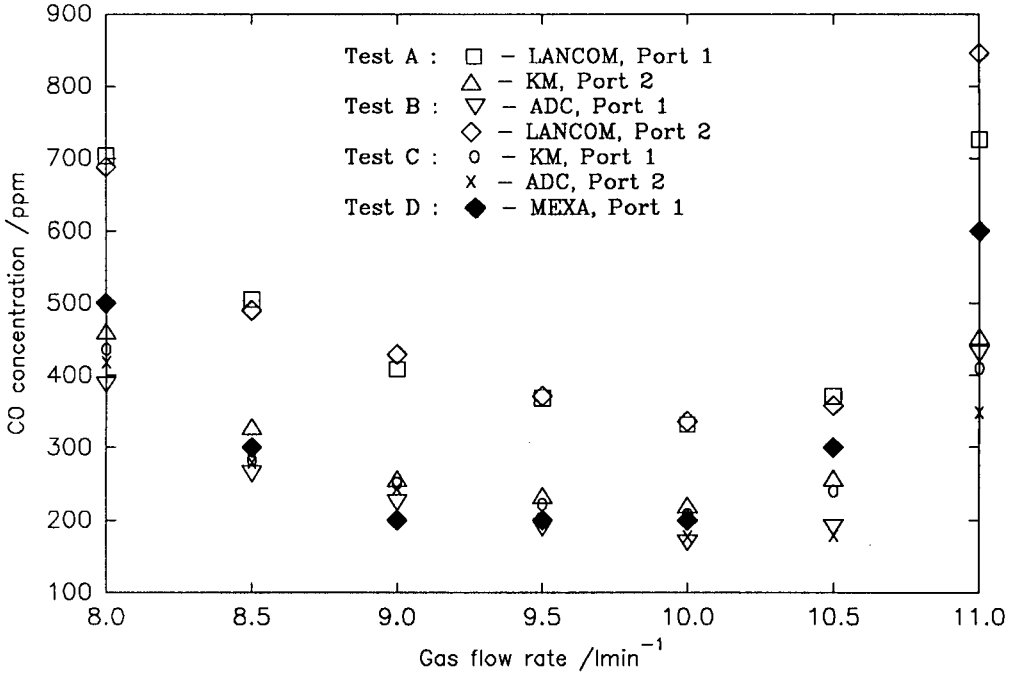

Figure 13 Comparison of CO concentrations in exhaust gas measured by different analyzers.

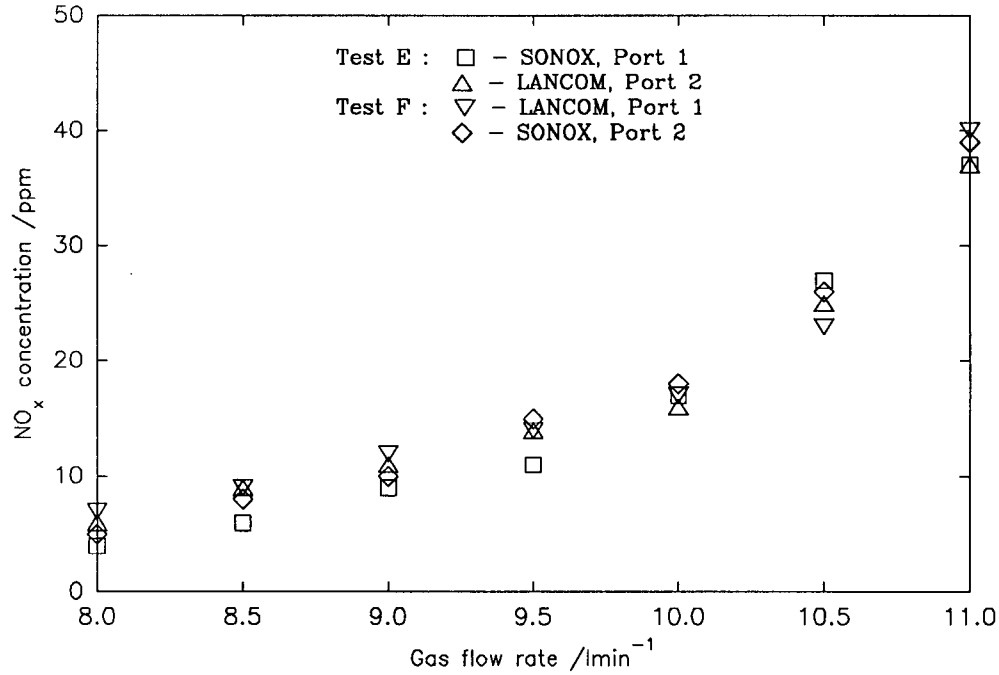

Figure 14 *Comparison of NO_x concentrations in exhaust gas measured by different analyzers.*

sufficient to analyze accurately the carbon monoxide content of the combustion products. The degree of scatter in Figure 13 increases as the minimum and maximum gas flow rates are approached, since only a small change of gas input in these regions caused significant variation in CO formation. Finally, test E and F (see Figure 14) show similar nitrogen oxides data taken by the available NO_x analyzers ie. LANCOM and SONOX. The latter gave slightly lower figures in the first half of the firing range. Difficulties were experienced with SONOX water filter which became soaked after 30 minutes of exhaust gas sampling. It was feared that water being drawn into the analyzer could eventually lead to malfunctioning of the NO_x sensor.

The investigation conducted justified the selection of the KM 9004 analyzer for the O_2 and CO measurements and resulted in a decision to evaluate the NO_x exhaust gas production by the LANCOM 3200 analyzer in this work. Taking into account the results of all six tests, it was concluded that the position of the sampling probe did not have any apparent influence on the exhaust gas analysis. Small

disagreement existed between data obtained using the same gas analyzer and different sampling port. This was due to gas flow fluctuations resulting in difficulties in setting up identical gas flow rates for different tests.

4.2.3. Pulse combustor performance for varying tailpipe length and diameter

Prior to the main test program, it was necessary to define the range of tailpipe geometries ie. lengths and diameters, which would guarantee satisfactory operation of the pulse combustor. Advantage was taken of the large number of copper exhaust tubes manufactured by A. Suthenthiran during his work [45, 46, 47]. Some of these tailpipes were used without modification but the majority of them required changes in shape. Some design refinement was carried out to enable the fitting of the exhaust silencer to the tailpipes.

As in all preliminary tests, the combustion chamber volume of the unit was 110 cm^3 and natural gas from the mains was used as fuel. Table 4 presents 16 different tailpipe geometries and gives brief comments on their performance. It can be seen that the combustor was able to start with all but one configuration. However, the criteria of at least 5 minutes running time with reasonably smooth operation was satisfied only by 7 exhaust tubes. These are gathered into two groups in Table 4. The first includes tailpipes of 8 mm internal diameter and lengths ranging from 1.85 to 2.40 m and the second includes tailpipes 1.25, 1.00 and 0.90 m long of 6 mm internal diameter. Use of the latter group was not pursued because the pulse unit exhibited starting difficulties and was not capable of running without forced air supply except for the 1.25 m exhaust pipe. Thus only the first group of the tailpipes was selected for further investigation.

4.2.4. Orifice plate calibration

The orifice described in section 3.2.2 was tested against a variable area rotameter and thermo anemometer in order to verify the accuracy of the design. A steady air

Tailpipe length / m	Tailpipe internal diameter / mm	Starting	Performance	Gas input range / l min^{-1}	Toroidal fan
2.75	8	Not difficult	Cannot run continuously	-	-
2.40	8	Not difficult	Runs continuously	9 - 10.5	Off
2.20	8	Not difficult	Runs continuously	7.5 - 11	Off
2.00	8	Not difficult	Runs continuously	7.5 - 11.5	Off
1.85	8	Not difficult	Runs continuously	9 - 12	Off
1.65	8	Not difficult	Cannot run continuously	-	-
1.50	8	Difficult	Cannot run continuously	-	-
1.40	8	Not difficult	Cannot run continuously	-	-
1.30	8	Not difficult	Cannot run continuously	-	-
1.20	8	Not difficult	Cannot run continuously	-	-
1.00	8	Difficult	Cannot run continuously	-	-
1.50	6	Cannot start	-	-	-
1.25	6	Very difficult	Runs continuously	3.5 - 6	Off
1.00	6	Very difficult	Runs continuously	3.5 - 7	On
0.90	6	Difficult	Runs continuously	4.5 - 7	On
1.70	10	Not difficult	Cannot run continuously	-	-

Shaded cells contain preselected tailpipes.

Table 4 *Preliminary tests of various tailpipes.*

supply was provided by the toroidal fan of the combustor rig and regulated by a variac connected to the fan. The air was passed through the rotameter to the orifice followed by the anemometer whose tip was placed radially in the centre of the air line cross section. Readings of rotameter volume flow rate of air, q_v (l min^{-1}), orifice pressure difference, Δp (mm H_2O) and maximum thermo-anemometer air velocity, v_{Max} (m s^{-1}) were recorded for different air flow rates. The measured pressure differences were converted to volume flow rates using equation 3.2, section 3.2.2.

The volume rate of flow in a pipe of circular cross section can be calculated according to equation 4.1.

$$q_v = (\pi D^2/4) v_{Mean} \quad (4.1)$$

Since the Reynolds numbers for all adjusted flows exceeded the limit for turbulent flow (value of 2300) it was assumed that the mean velocity equals approximately 0.8 of the maximum velocity [95]. Therefore the following equation was derived to correlate the volume flow rate with the maximum air velocity in this investigation :

$$q_v = 26.47 v_{Max} . \quad (4.2)$$

The coefficient 26.47 includes the cross-sectional area of the pipe, ratio of v_{Mean}/v_{Max} and a conversion factor so as to obtain results in l min^{-1}.

Figure 15 plots the flow rates measured by means of the orifice plate and thermo anemometer against variable area rotameter readings. The graph shows slightly lower flow rate values for both the orifice and anemometer than those indicated by the rotameter. This discrepancy, probably due to some error in readings taken from a fluctuating rotameter, did not exceed 2 % and 4.8 % in case of the orifice plate and thermo anemometer respectively. These findings showed that the orifice was designed properly and could measure air flow rates with a reasonable accuracy.

4.2.5. Calculation of air/fuel ratios from the exhaust gas analysis

Although it is possible to obtain the air/fuel ratio used during testing by direct measurement of the gas and air flow rates, a flexible computer program (see Appendices A, B and C) was prepared to facilitate calculation of air/fuel ratios for different fuel gases from a knowledge of the volumetric analysis of the products of combustion. This acts as a check on the measured air/fuel ratio which may be suspect due to the difficulty of measuring a pulsating flow. A worked example given in Appendix A demonstrates the calculation procedures used in the program "Gas" for one of the conducted tests. Presentation of the computer results for the same test

is shown in Appendix D.

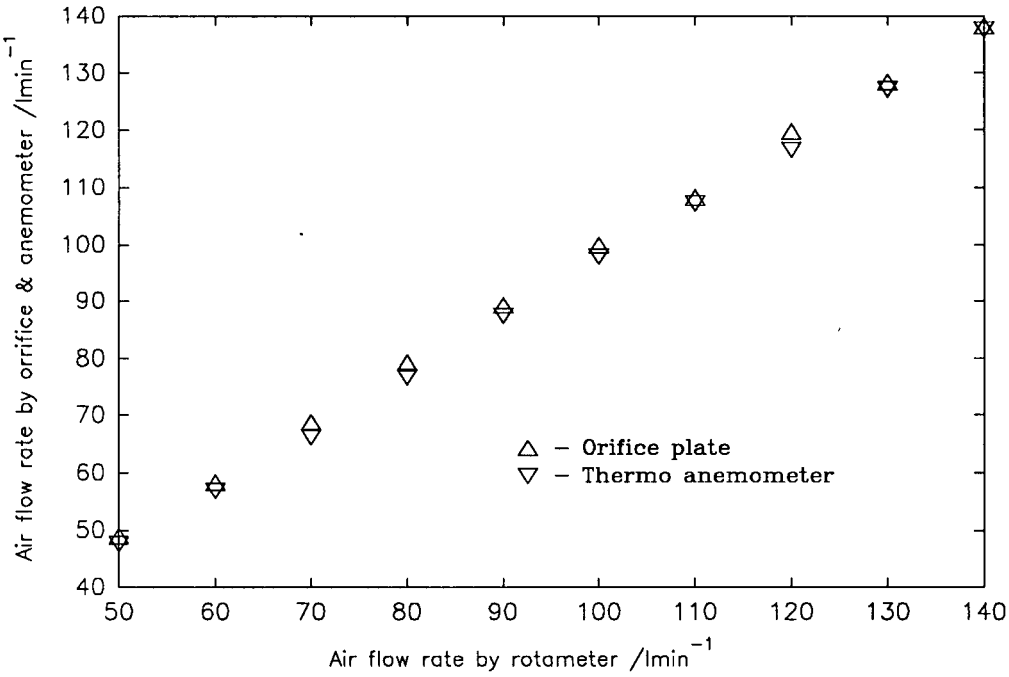

Figure 15 *Testing of the orifice plate in steady turbulent flow.*

4.2.6. Air-box employment

As mentioned in section 3.2.2, two air-boxes of 5 litre and 50 litre volume respectively were designed and constructed. Consequently, preliminary tests were carried out to determine the size and location of the air-box in the air line which would ensure both reasonable steady operation of the pulse combustor and reliable measurement of the pulsating air flow using the designed orifice plate. The configurations investigated are illustrated in Figure 16. The two air-boxes were fitted immediately before the air decoupler (A, B) and immediately after and before the toroidal fan (C, D) and (E,F) respectively. The position of the orifice is also depicted in the diagram. Unfortunately, it was discovered that the combustor was extremely sensitive to insertion of any large volume vessel in the air line and it did not run longer than a few cycles with any of the configurations. One possible explanation is that the negative pressure during the intake period was not sufficient to overcome

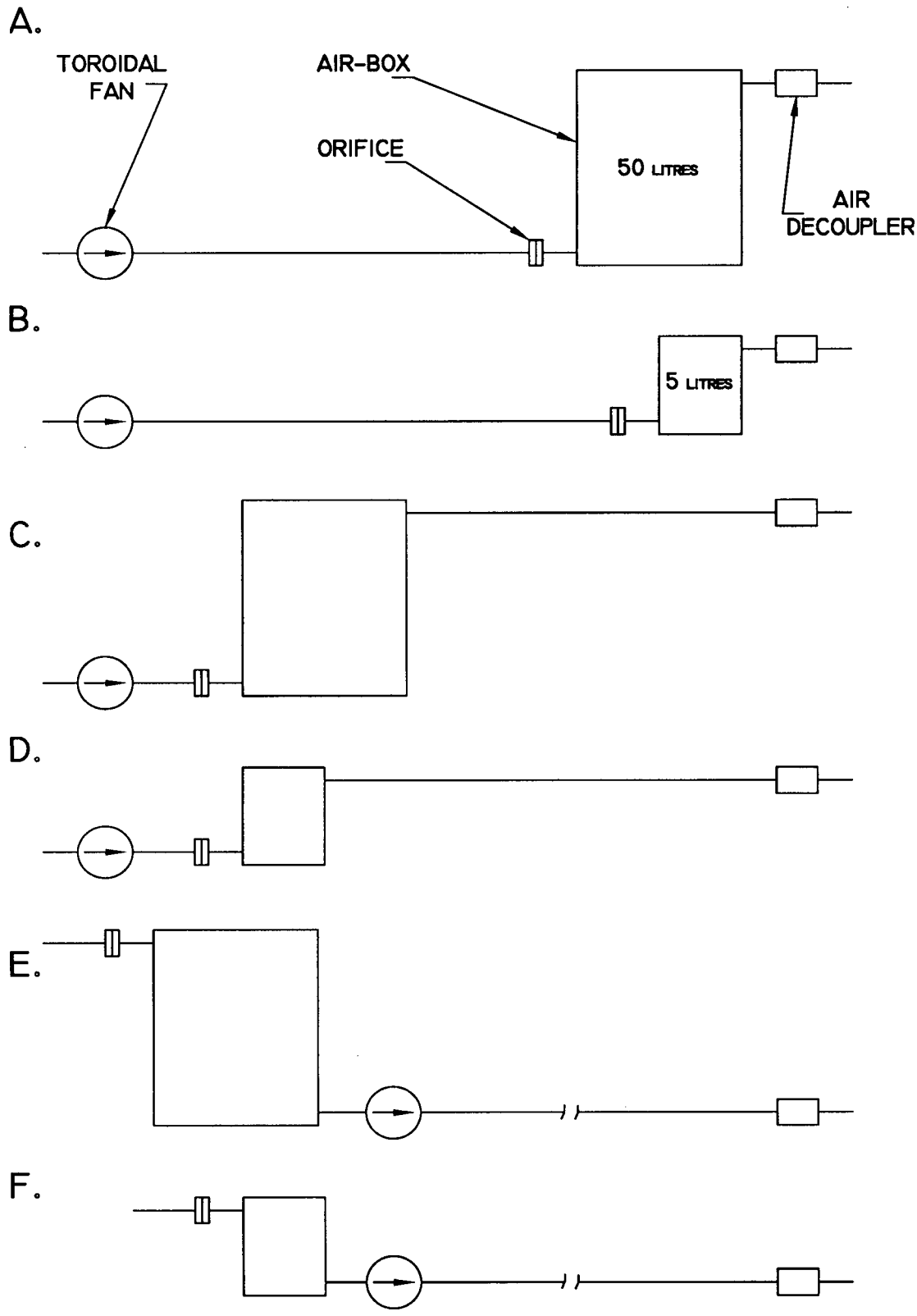

Figure 16 Location of air-boxes along the air line.

the additional pressure loss due to the air-box insertion. As a result the induced combustible mixture became too fuel rich and the combustor ceased to work.

Because there was not any alternative method available for the measurement of the pulsating air flow to the combustor it was decided to employ the orifice plate flow meter without the air-box in this study.

4.2.7. Final experimental set-up of combustor rig

Figure 17 shows the set-up of the combustor test rig which was used during the main experimental work. The recorded quantities are shown as symbols next to the corresponding equipment. The KM 9004 analyzer was connected to the sampling port 1 and the LANCOM 3200 analyzer extracted exhaust gas via sampling port 2 (see Figure 10, p. 68). It is also important to note that the measured exhaust gas concentrations were based on dry samples and the combustor was running with a connected exhaust silencer throughout the tests.

4.3. EXHAUST GAS ANALYSIS FOR VARYING GAS FLOW RATE

4.3.1. General

The objective of this investigation was to measure and to represent graphically the variation of the exhaust gas concentrations of O_2, CO, CO_2 and NO_x with changes in the gas flow rate and to relate these to some other important combustion characteristics such as the exhaust gas temperature, air/fuel ratio and percentage excess air. The pulse combustor was operated with a 2.00 m long tailpipe of 8 mm internal diameter, a combustion chamber volume of 110 cm^3 and using natural gas from the mains as a fuel. The aforementioned tailpipe length and combustion chamber volume were chosen because of giving the best combustor performance throughout the preliminary work.

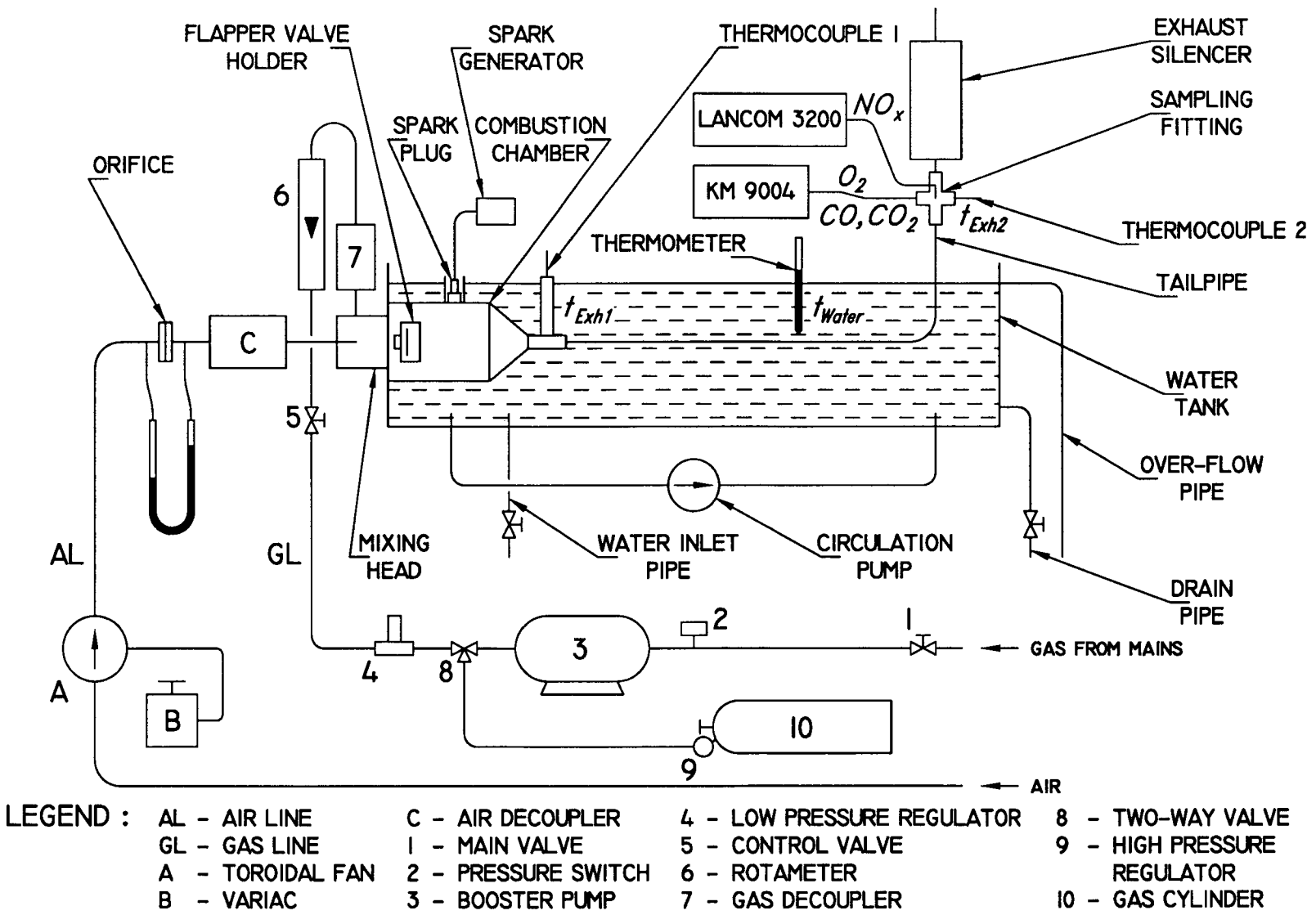

Figure 17 Schematic diagram of the final set-up of the investigated combustor rig.

4.3.2. Experimental technique

Having filled the tank with water up to the overflow level, the circulating pump was turned on. A supply of starting air into the mixing head was provided by the toroidal fan. At the same time the spark generator was switched on. Subsequently, the gas main valve was opened prior to starting the booster pump. After opening the control valve, fuel gas was delivered into the mixing head and the ensuing air/fuel mixture was ignited by means of a spark plug. Once the resonance was established, the spark generator and starting fan were switched off and this was followed by the adjustment of the gas flow to maintain stable pulse combustion. About 45 minutes running time was needed to reach the required water bath temperature of 65 °C. During this period the gas analyzers were set up and connected to the sampling probes. Measurements of the ambient air temperature and relative humidity were also taken.

Readings were first recorded at the minimum working gas flow rate for satisfactory operation of the combustor. The gas input was then increased in 0.5 l min^{-1} intervals. Steady state conditions for the combustor and analyzers were achieved after approximately a 5 minute running period. Single readings of the following quantities were recorded for each gas flow rate : pressure difference across the orifice plate (Δp), exhaust gas temperature at the combustion chamber exit (t_{Exhl}) and oxygen (O_2), carbon monoxide (CO), carbon dioxide (CO_2) and nitrogen oxides (NO_x) concentrations in the exhaust gas. The temperature at the tailpipe exit was also monitored during the tests but only upper and lower limits were recorded. Reasonably constant water bath temperatures (65 ± 1 °C) were obtained throughout the investigations by adjusting the flow of cooling water to the tank. The procedure outlined in this section was repeated three times so as to guarantee the reliability of results. A specimen of a table containing the measured data as well as calculated averages for Test 1 is given in Appendix E.

4.3.3. Results and discussion

From the averages and results presented in Appendix D, a series of graphs was plotted (Figures 18, 19, 20, 21 and 22) for the optimum configuration examined in Test 1. The top horizontal axis of each graph indicates heat inputs in kW for the corresponding gas flow range. Satisfactory operation of the combustor was accomplished between the gas flow rates of 8 l min^{-1} and 11 l min^{-1} which corresponds to a turndown ratio of 1.38.

Figure 18 shows the exhaust gas variation of oxygen and carbon dioxide concentration with gas flow rate for the optimum configuration. It can be seen that oxygen levels decrease and carbon dioxide levels increase as stoichiometric conditions are approached, which is in agreement with Griffiths *et al.* [54, 55]. However, running at stoichiometric conditions, at which the oxygen concentration in the exhaust gas should drop to zero, could not be achieved since the operating frequency rapidly increased at a gas flow rate above 11 l min^{-1} and this caused stalling of the combustor. Carbon dioxide dependence on the gas flow rate shows a mirror image of oxygen values as a result of the indirect measurement of CO_2 levels which were calculated by the analyzer used from the oxygen concentrations.

The variation of carbon monoxide and nitrogen oxide concentration with gas flow rate for TPL = 2.00 m and CCV = 110 cm^3 is presented in Figure 19. This shows a characteristic 'U' shaped curve for CO (reported in References 42, 46 and 50) and a NO_x curve rising sharply in the upper half of the operating range which agrees with other reported variations [46]. At the lower end of the gas flow range, the carbon monoxide concentration was high due to incomplete combustion resulting from lower flame temperature at weaker mixtures. The temperature within the combustion chamber rose with increase in heat input (see Figure 20) which in turn caused lower CO levels. At a certain gas flow rate, however, the CO decline with heat input increase ended and from this point onwards there was a sharp rise in CO emissions despite a higher combustion temperature. As indicated in section 2.2.2, carbon monoxide production is not only controlled by flame temperature but also by

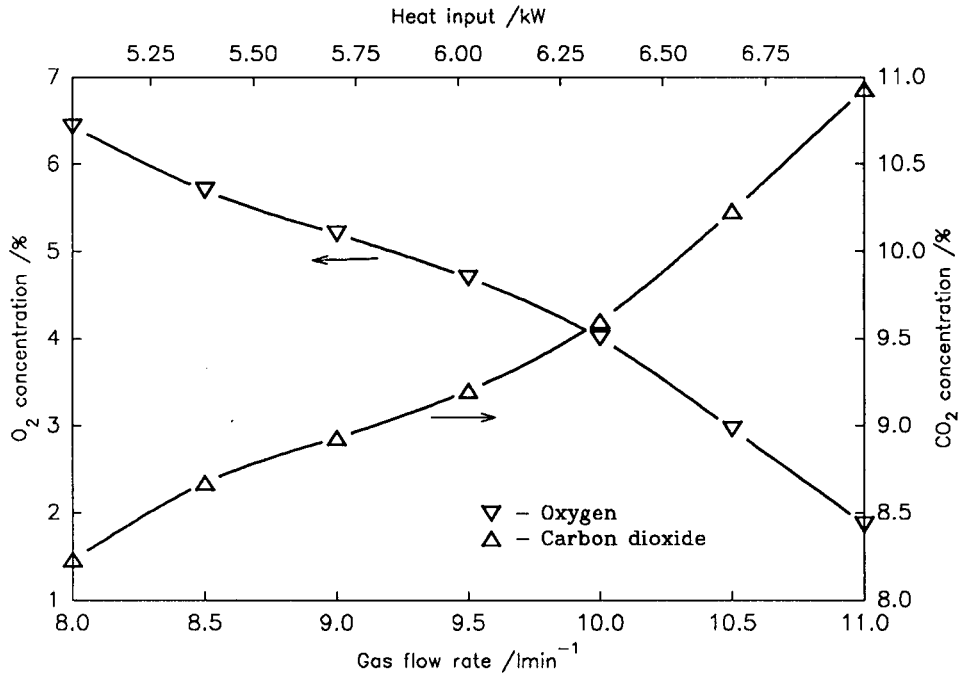

Figure 18 *Variation of oxygen and carbon dioxide concentration with gas flow rate for 2.00 m long tailpipe and 110 cm^3 combustion chamber volume (Test 1).*

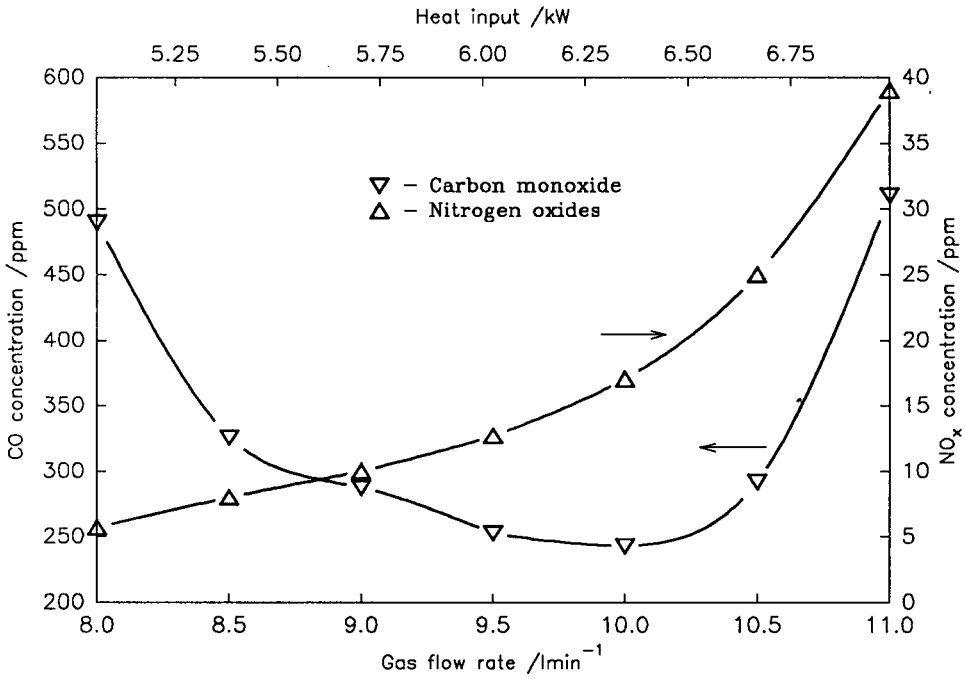

Figure 19 *Variation of carbon monoxide and nitrogen oxide concentration with gas flow rate for 2.00 m long tailpipe and 110 cm^3 combustion chamber volume.*

the amount of oxygen available for carbon oxidation, residence time in the flame front and cooling rate of post combustion products. The increase of the operating frequency with heat input (see Figure 50, p. 118) possibly shortens the residence time and enhances the tailpipe heat flux (cooling rate) thus increasing CO emissions. However, general lack of oxygen or poor mixing in the air/gas stream, leading to a local oxygen deficiency, is probably the dominant factor contributing to significant levels of CO at the higher end of the gas flow range since the exhaust O_2 level is fairly low at a gas flow rate of 11 l min^{-1} (see Figure 18).

Figure 20 displays a rise in exhaust gas temperature at the combustion chamber exit, t_{Exh1}, as the air/gas mixture became richer towards the upper end of the heat input range. From the comparison between Figure 19 and 20 one can see that NO_x emissions were strongly dependent on temperature which agrees with theoretical and experimental evidence in the literature (see section 2.2.3). Furthermore, NO_x concentrations fell to a low level as the excess air increased (compare Figures 19 and 22), which is in agreement with references 46 and 85.

The comparison of measured and computed air/fuel ratios for the optimum configuration is depicted in Figure 21 and shows a high discrepancy between the two at the lower part of the gas input range. This confirms the necessity of air-box employment for accurate measurement of pulsating air flow by means of an orifice plate. Since it was impossible to run the combustor with an air-box (see section 4.2.6) and therefore not satisfying the provisions of ISO Technical Report 3313 (refer to section 3.2.2), it was decided to rely in the following tests on the air/fuel ratios calculated from the exhaust gas analysis by program "Gas" (viz. section 4.2.5). However, since neither of the two curves reached the NGA stoichiometric air/fuel ratio of 9.76 (see Appendix D) we can assume that the combustor was capable of operation only under fuel-lean conditions.

Finally, Figure 22 displays the variation of percentage excess air and CO/CO_2 ratio with gas flow rate for a 2.00 m long tailpipe and combustion chamber volume of 110 cm^3. Percentage excess air levels dropped over the investigated gas flow range from 39.2 % to 7.78 %, which corresponds to exhaust gas oxygen

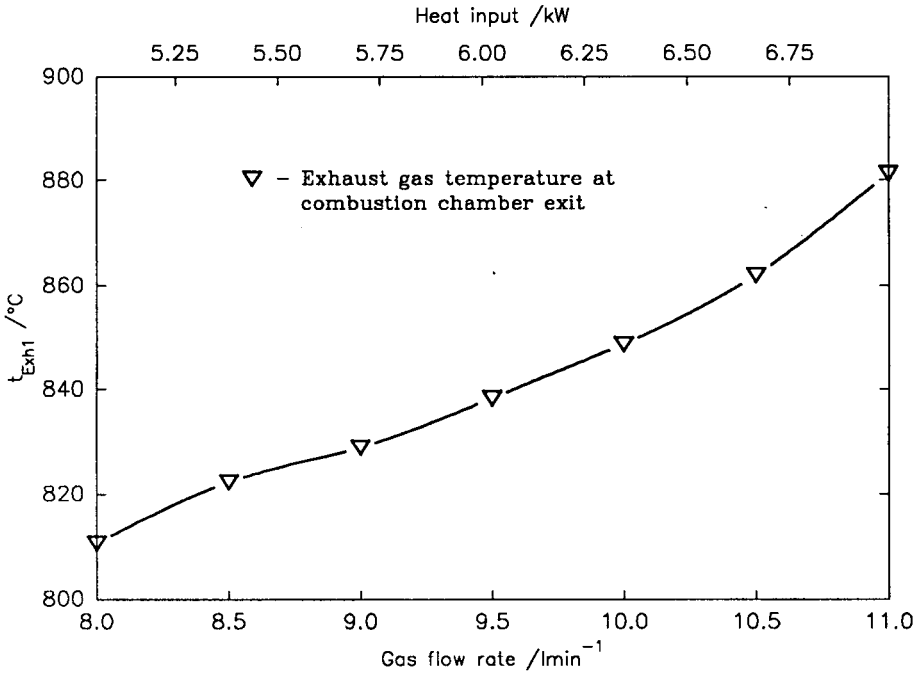

Figure 20 *Variation of exhaust gas temperature (t_{Exh1}) with gas flow rate for 2.00 m long tailpipe and 110 cm^3 combustion chamber volume (Test 1).*

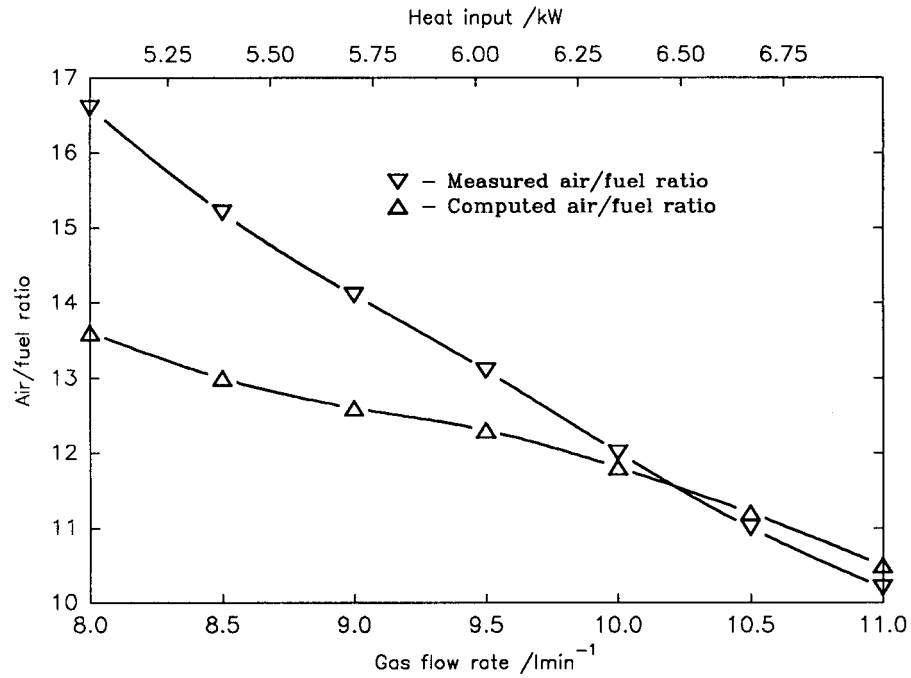

Figure 21 *Comparison of measured and computed air/fuel ratios for 2.00 m long tailpipe and 110 cm^3 combustion chamber volume.*

concentrations of 6.43 % and 1.87 % respectively (see Figure 18). CO/CO_2 ratio shows similar 'U' shaped curve as CO in Figure 19 with the top ratio of about 0.006, which is more than three times lower than the maximum permissible CO/CO_2 limit set by appliance safety standards [78].

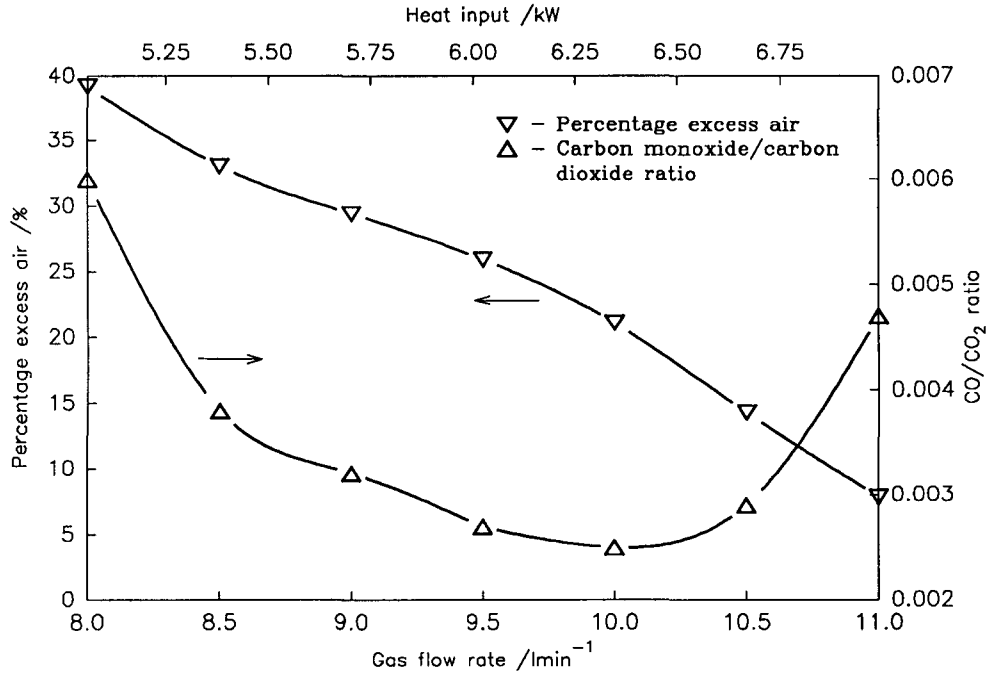

Figure 22 Variation of percentage excess air and CO/CO_2 ratios with gas flow rate for 2.00 m long tailpipe and 110 cm^3 combustion chamber volume (Test 1).

4.4. EXHAUST GAS ANALYSIS FOR VARYING TAILPIPE LENGTH

4.4.1. General

Two basic tailpipes, having lengths of 2.00 and 1.65 m and of 8 mm internal diameter, were investigated in conjunction with four extension pieces 0.10, 0.20, 0.25 and 0.30 m long in order to assess the effect of exhaust tube length on the combustion products analysis and pulse combustor performance for different gas inputs. Combination of the aforementioned lengths allowed coverage of tailpipes ranging from 1.90 m to 2.30 m, increasing in 0.10 m steps (see Figure 23). These five exhaust tubes were selected taking into consideration the tailpipe length range

predetermined in section 4.2.3. The exhaust tubes and extension pieces were joined together by a connector which facilitated a smooth passage for the exhaust flow between the two components. Natural gas from the mains was used as a fuel.

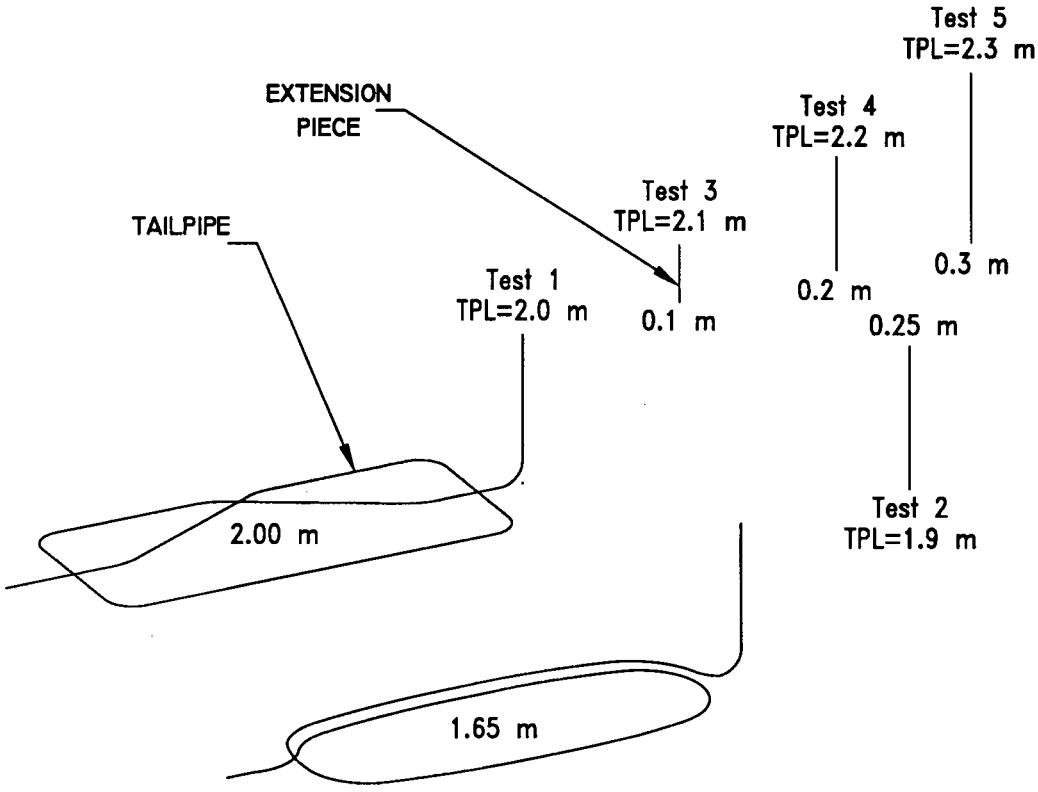

Figure 23 Different lengths and shapes of investigated tailpipes.

4.4.2. Experimental technique

Firstly, the investigated tailpipe was mounted between the combustion chamber and exhaust gas sampling fitting. The next experimental steps were very much the same as those outlined in section 4.3.2. One slight modification was made due to the findings of section 4.3.3 on air flow measurement ie. the pressure drop across the orifice was not recorded.

4.4.3. Results and discussion

From the data obtained eight graphs, each showing five curves representing different tailpipe lengths (TPL), were plotted (see Figures 24 - 31). Gas flow rate limits within which the combustor ran satisfactorily were determined for each tailpipe as follows: 9 - 12.5 l min^{-1} for TPL of 1.90 m, 8 - 11 l min^{-1} for TPL of 2.00 m, 8 - 10.5 l min^{-1} for TPL of 2.10 m, 8 - 10.5 l min^{-1} for TPL of 2.20 m and 8 - 10 l min^{-1} for TPL of 2.30 m. These gas input ranges give us a maximum and minimum turndown ratio of 1.39 and 1.25 for the 1.90 m and 2.30 m long tailpipe respectively. It should be noted that with tailpipe length increase the operating range becomes narrower.

Figure 24 presents the variation of O_2 concentration with gas flow rate for different tailpipe lengths. We can observe that the 2.00 m, 2.10, 2.20 m, and 2.30 m long tailpipes, which were formed from the 2.00 m long basic tailpipe and corresponding extension pieces (see Figure 23), show oxygen concentrations diminishing with increase in tailpipe length. This trend is even more evident if we compare oxygen levels of the 2.00 m tailpipe with those of the shortest exhaust tube for corresponding gas inputs. We can speculate that such a behaviour is probably dependent on the operating frequency of the combustor. The 1.90 m curve is somewhat further apart from the four longer tubes possibly as a result of the different shape of the tailpipe (see Figure 23).

Figure 25 shows the variation of carbon dioxide concentration with gas flow rate for the five investigated tailpipes. It should be noted that CO_2 levels were computed by the KM 9004 gas analyzer from O_2 values. It is seen that as the tailpipe gets longer the CO_2 concentrations rise. Furthermore, the CO_2 concentration in the combustion products of the pulse burner decreased as the gas rate was turned down and the burner operated at higher air/fuel ratios (refer to Figure 30). Eventually the air/fuel mixture became too lean and the pulse combustion process could not be sustained below gas input rates of 9 l min^{-1} and 8 l min^{-1} for the 1.90 m long tailpipe and the rest of the examined exhaust tubes respectively.

The variation of carbon monoxide concentration with gas flow rate for

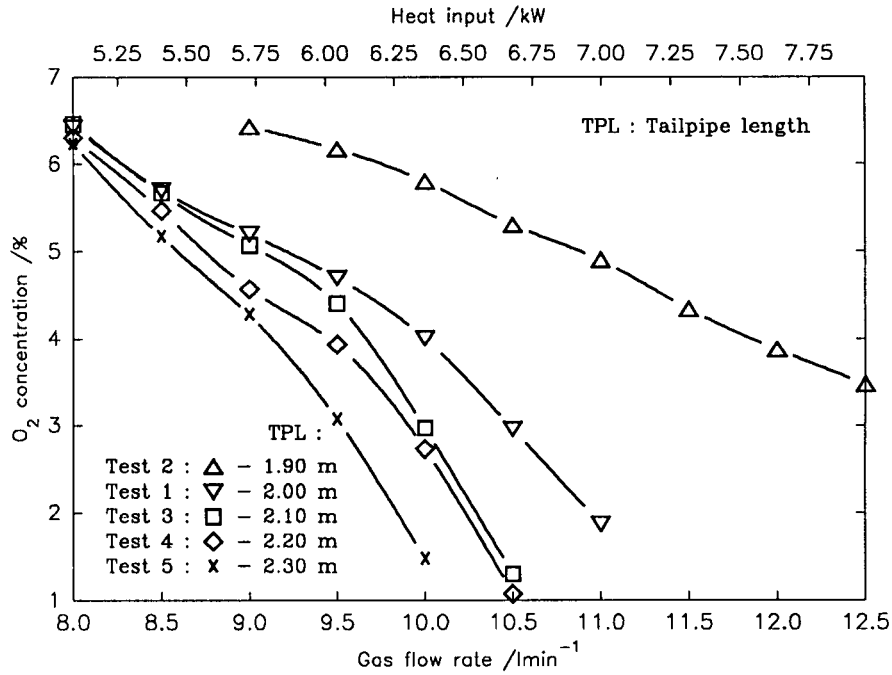

Figure 24 Variation of oxygen concentration with gas flow rate for different tailpipe lengths.

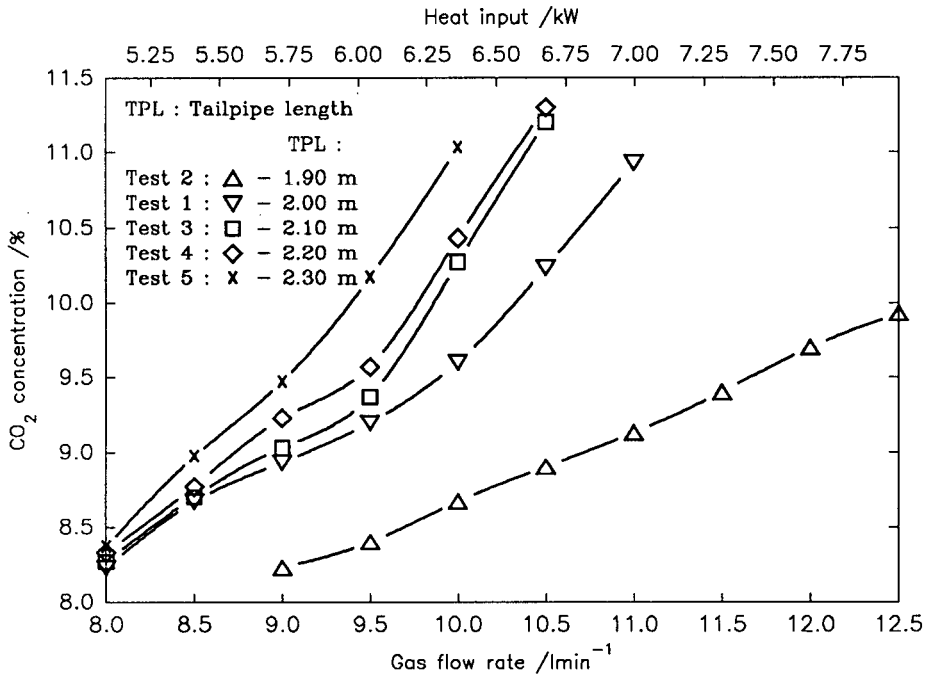

Figure 25 Variation of carbon dioxide concentration with gas flow rate for different tailpipe lengths.

different tailpipe lengths is presented in Figure 26. The four longer exhaust tubes gave characteristic 'U' shapes with gently sloping curves coming down and reaching minimum CO values, before rising steeply as the stoichiometry condition was approached. The curve obtained in Test 2 for the 1.90 m long tailpipe could also be interpreted as a very shallow 'U' form. The shape of the 'U' curves and the CO minimum locations along the gas flow rate axes depended on the operating range for the particular tailpipe in such a manner that the former got wider and the latter moved towards the upper operating limit of each pipe as the tailpipe length decreased. If we consider the lower and middle operating range of each pipe and compare CO production at, say, gas input of 9 l min^{-1}, we can observe CO levels slightly decreasing with increase in tailpipe length. This phenomenon appears to be contrary to Kassehchi's findings [50]. As discussed in section 2.2.2, CO formation is a function of the flame temperature, residence time and cooling rate. Since CO emissions decline with flame temperature rise we should observe lower t_{Exhl} for, say, the 2.00 m exhaust tube than for the 2.30 m exhaust tube, which was the case (see Figure 28). It follows that our results show consistency with theory. In addition, the residence time and cooling rate are most probably dependent on frequency, which was found to decrease with tailpipe length increase [33, 45, 52, 53, 54]. Assuming an increase in CO levels with higher operating frequency due to reduction of the residence time and enhancement of the heat transfer (cooling rate) one can anticipate higher CO concentration for the 2.00 m tailpipe than for 2.30 m tailpipe at a 9 $lmin^{-1}$ gas rate as shown in Figure 26, thus supporting the above conclusion.

Figure 27 shows the variation of nitrogen oxide levels with gas flow rate for different tailpipe lengths and indicates a reduction in NO_x emissions (more apparent in the upper half of the operating ranges) with decreasing exhaust tube length. Figure 28 shows a similar trend for the exhaust temperature at the combustion chamber exit and so supporting evidence of the well-known temperature dependency of NO_x production is manifested. The increase of NO_x for longer tailpipes, which was found to be in agreement with Reference 50 may also stem, to some extent, from longer residence times caused by possible reduction in operating frequency as the exhaust

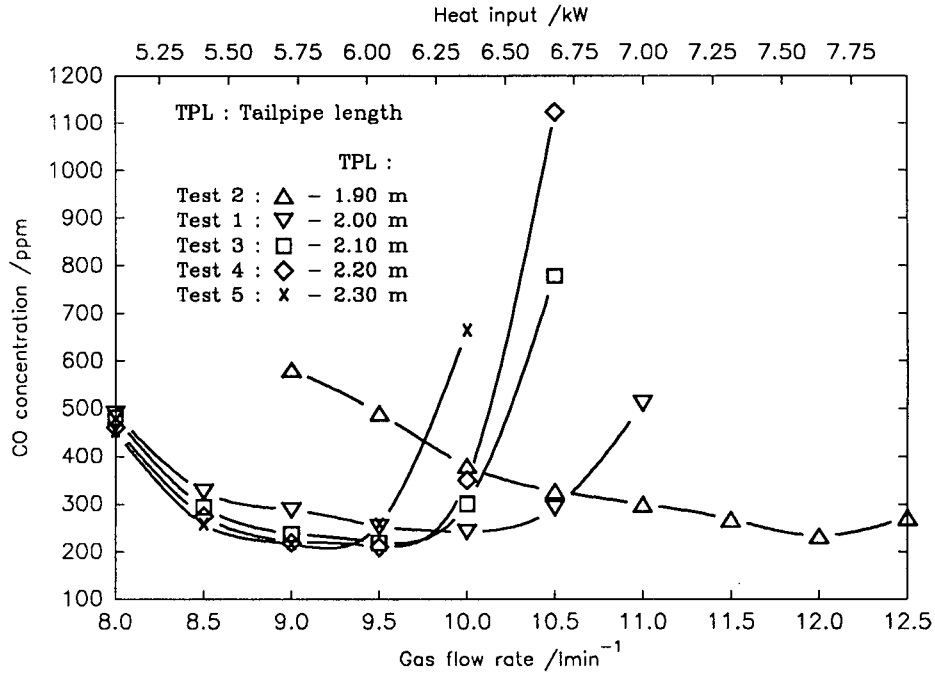

Figure 26 *Variation of carbon monoxide concentration with gas flow rate for different tailpipe lengths.*

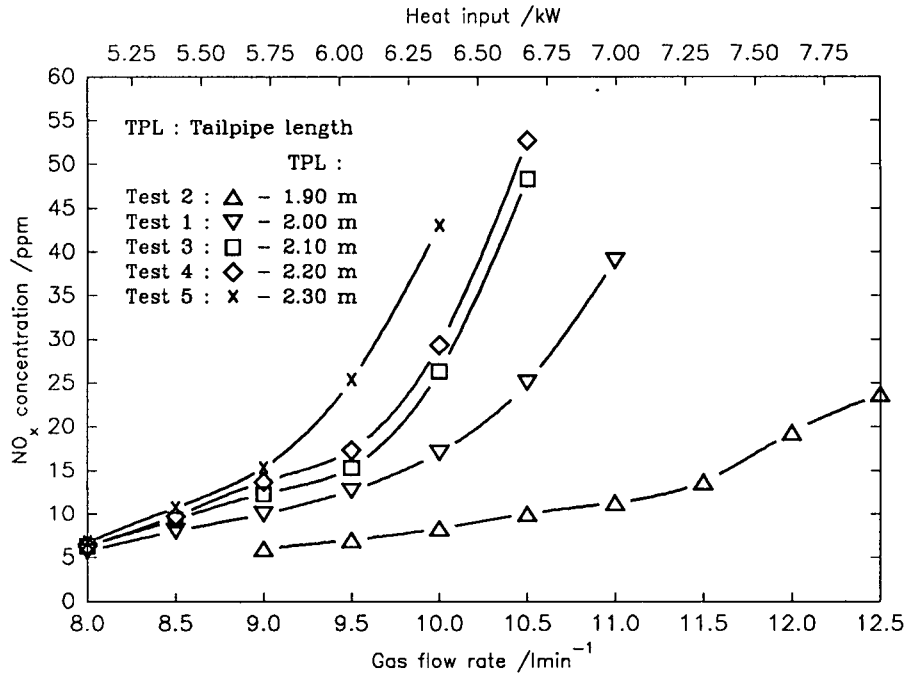

Figure 27 *Variation of nitrogen oxide concentration with gas flow rate for different tailpipe lengths.*

tube length increases (see section 2.1.2, p. 41). The measured levels of nitrogen oxides did not exceed 60 ppm, thus supporting what was said in the literature survey regarding NO_x formation (see section 2.2.3).

A comparison between Figure 28, which depicts the variation of exhaust gas temperature, t_{Exh1}, with gas flow rate for different tailpipes, and Figure 30 reveals that t_{Exh1} rises as the mixture becomes less lean and approaches stoichiometric conditions. In order to confirm the tendency of t_{Exh1} to rise as the TPL gets longer the adiabatic flame temperatures were determined from the exhaust gas analysis for the 2.00 m and 2.30 m long tailpipe as outlined in Appendix F (see Figure 53). It is shown that the flame should acquire a higher temperature for the longer pipe than for the shorter pipe due to the lower air/fuel ratio in the case of the 2.30 m pipe (see Figure 30). This finding corresponds with the t_{Exh1} measurements for the two tailpipes.

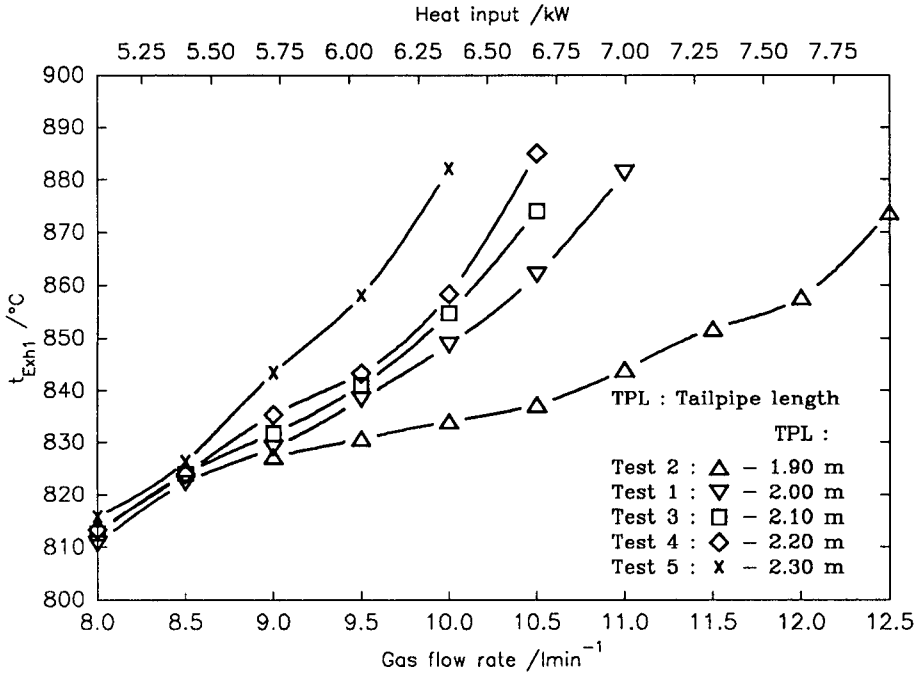

Figure 28 *Variation of exhaust gas temperature at combustion chamber exit (t_{Exh1}) with gas flow rate for different tailpipe lengths.*

Figure 29 demonstrates one of the most important advantages of pulse combustion systems over conventional designs ie. low CO/CO_2 ratios. Even the highest ratio obtained (TPL = 2.20 m, GFR = 10.5 l min^{-1}) is still almost half of the

British standard regulated value of 0.02 [78]. All the tubes showed the best performance in the middle of their operating range where CO/CO_2 ratios were very low with a lowest achieved ratio of 0.0022 in the case of the longest, 2.30 m tailpipe.

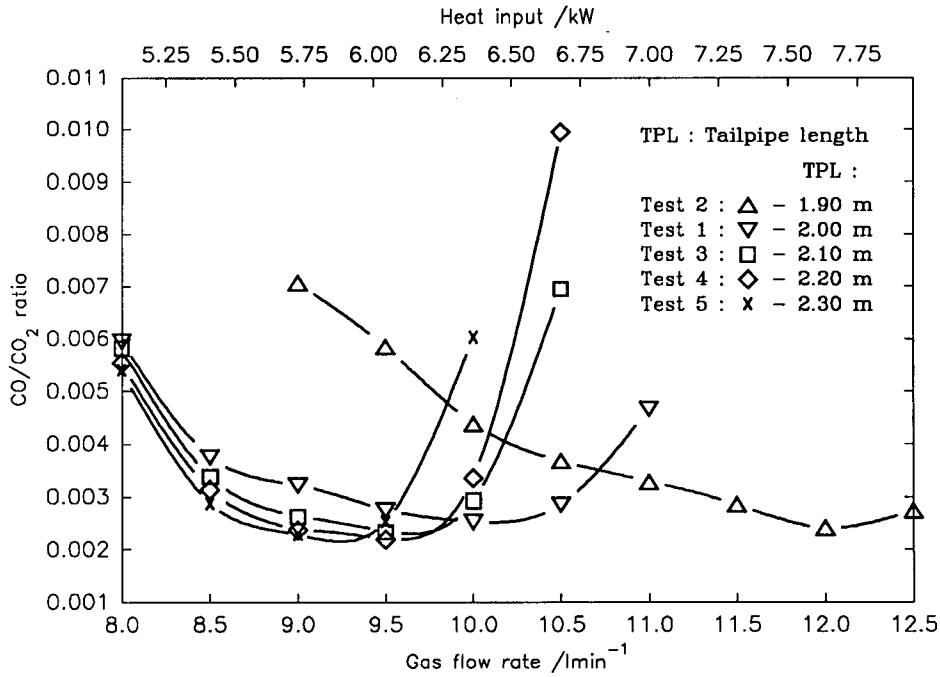

Figure 29 *Variation of CO/CO_2 ratio with gas flow rate for different tailpipe lengths.*

Figures 30 and 31 are based on results summarised in Appendix D and G where the air/fuel ratio and percentage excess air are computed from the exhaust gas analysis. Figure 30 shows the relationship between the air/fuel ratio and the gas flow rate for the tested tailpipes and it can be seen that the air/fuel ratio diminished as tailpipe lengths increased. Furthermore, as the gas input rate was increased the air/fuel ratio was reduced and the mixture became richer. The lowest A/F ratio of 10.16 was determined for the 2.20 m tailpipe which is higher than the stoichiometric ratio for NGA (9.76) by about 0.4.

Figure 31 shows another combustion characteristic ie. percentage excess air (PEA) as a function of gas input for different tailpipe lengths. PEA was found to decrease with the increase in tailpipe length as well as gas flow rate. It can also be

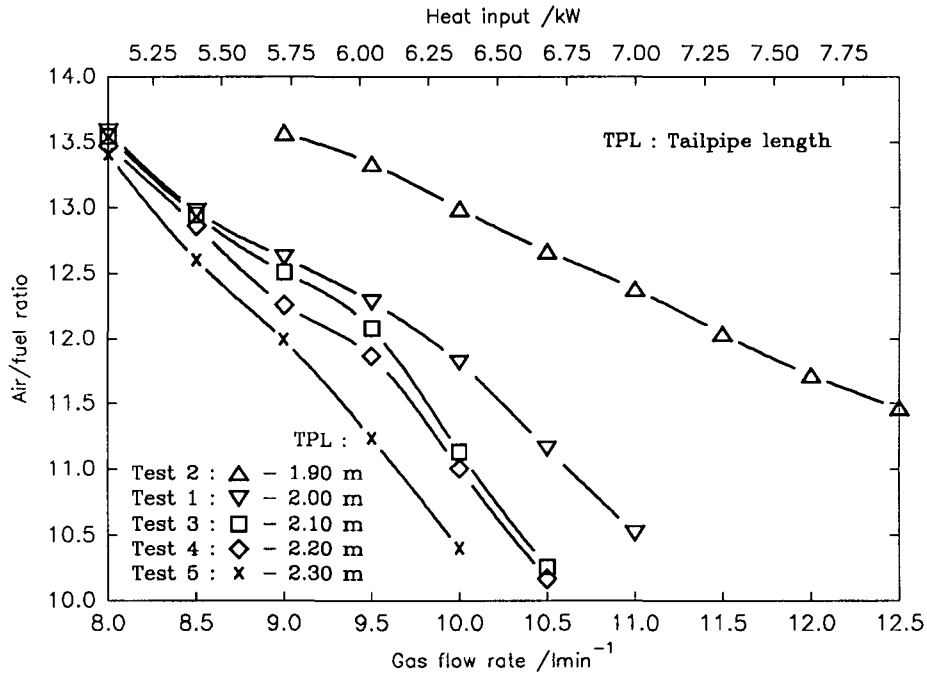

Figure 30 *Variation of air/fuel ratio with gas flow rate for different tailpipe lengths.*

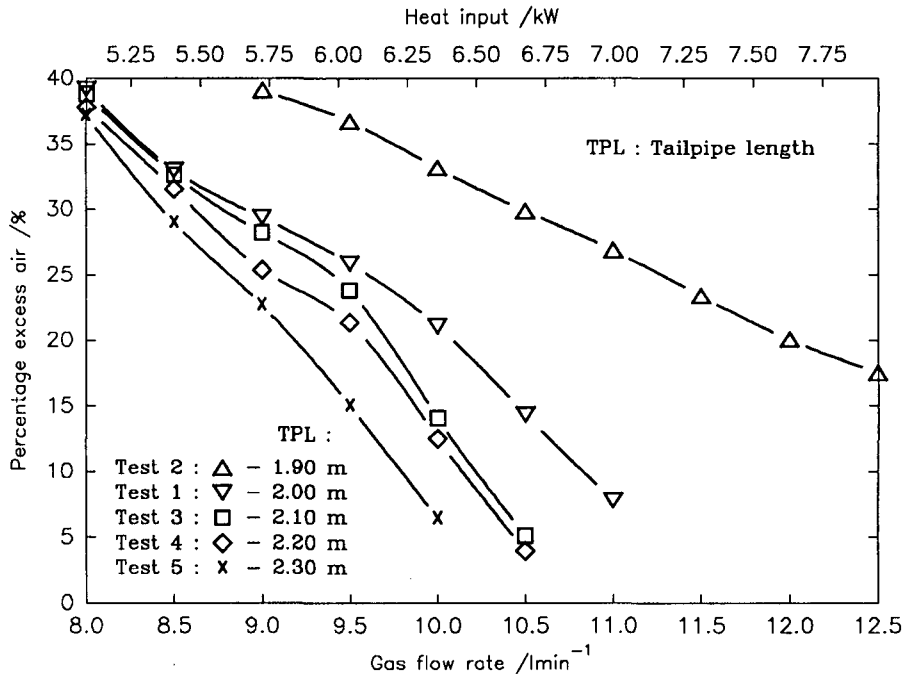

Figure 31 *Variation of percentage excess air with gas flow rate for different tailpipe lengths.*

seen that the pulse combustor was not able to operate with PEA above 40 % or below 3 % for any of the investigated exhaust tubes.

4.5. EXHAUST GAS ANALYSIS FOR VARYING COMBUSTION CHAMBER VOLUME

4.5.1. General

This investigation was carried out to observe the effect of combustion chamber size on the operation and exhaust gas emissions of the pulse combustor when burning natural gas supplied from the mains. The combustion chamber length was varied by moving the valve holder within the chamber thus changing the effective volume (see section 3.1.4 and 3.2.1). The tailpipe length was maintained at 2.00 m in this study.

4.5.2. Experimental technique

Prior to the commencement of this work, the rear of the burner was dismantled to enable the adjustment of the required combustion chamber volume. This was done by rotating the valve holder clockwise or anticlockwise within the combustion chamber. The combustor was reassembled and the experimental procedure used was identical to that described in section 4.3.2 (except that Δp values were not recorded).

4.5.3. Results and discussion

Results were obtained for combustion chamber volumes (CCV) of 90 cm^3, 100 cm^3, 110 cm^3 and 120 cm^3. The operating range of the two limit volumes over which the combustor ran satisfactorily was 8.0 - 10.5 l min^{-1} thus providing a turndown ratio of 1.31. The two middle volumes gave a slightly higher upper gas input rate of 11 l min^{-1}.

Variation of the exhaust gas oxygen and carbon dioxide concentrations with gas flow rates for the four combustion chamber volumes is shown in Figures 32 and

33 respectively. A reduction in the O_2 exhaust gas levels is noted as the combustion chamber volume increased and gas rate was turned up. CO_2 curves, which were derived from the oxygen data, show an antithetical behaviour. A rise in carbon dioxide concentrations with increase in combustion chamber volume corresponds with Windmill's observations [42]. The maximum and minimum CO_2 concentrations stated in this study were very similar to our results of 11.1 % for $CO_{2,Max}$ (GFR = 10.5 l min^{-1}, CCV = 120 cm^3) and 7.93 % for $CO_{2,Min}$ (GFR = 8.0 l min^{-1}, CCV = 90 cm^3).

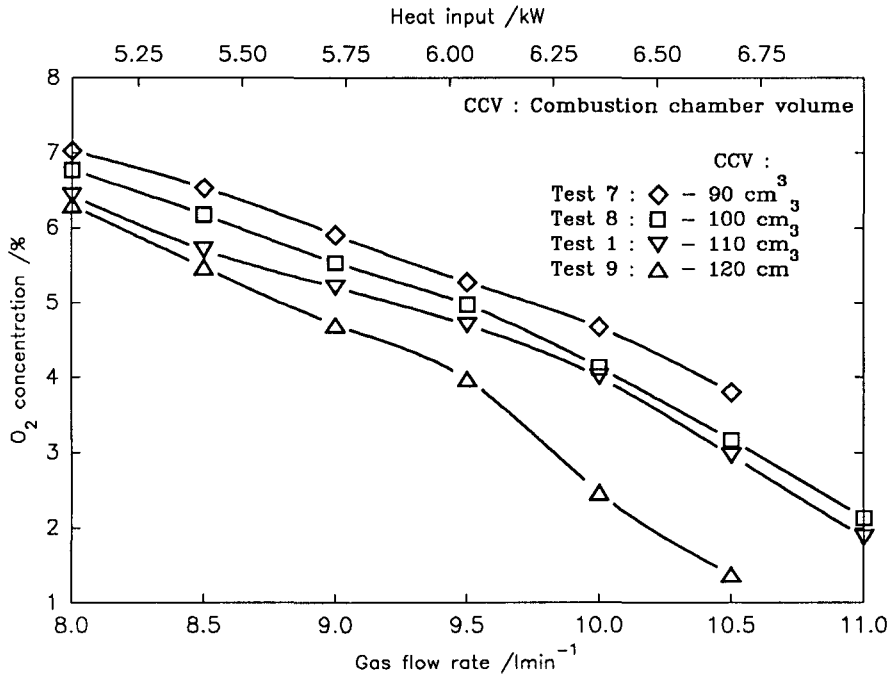

Figure 32 *Variation of oxygen concentration with gas flow rate for different combustion chamber volumes.*

Figure 34 shows the carbon monoxide concentrations in the combustion products as a function of gas flow rate for different combustion chamber volumes. CO curves once again resemble a 'U' shape or at least a part of it in the case of the smallest combustion chamber. The CO variation with load has been discussed earlier in section 4.3.3 and it can be seen that CO levels fell to a minimum before climbing again as gas input increased. The least CO concentration of 215 ppm was measured with the largest combustion chamber at GFR = 9.5 l min^{-1}. More importantly, Figure

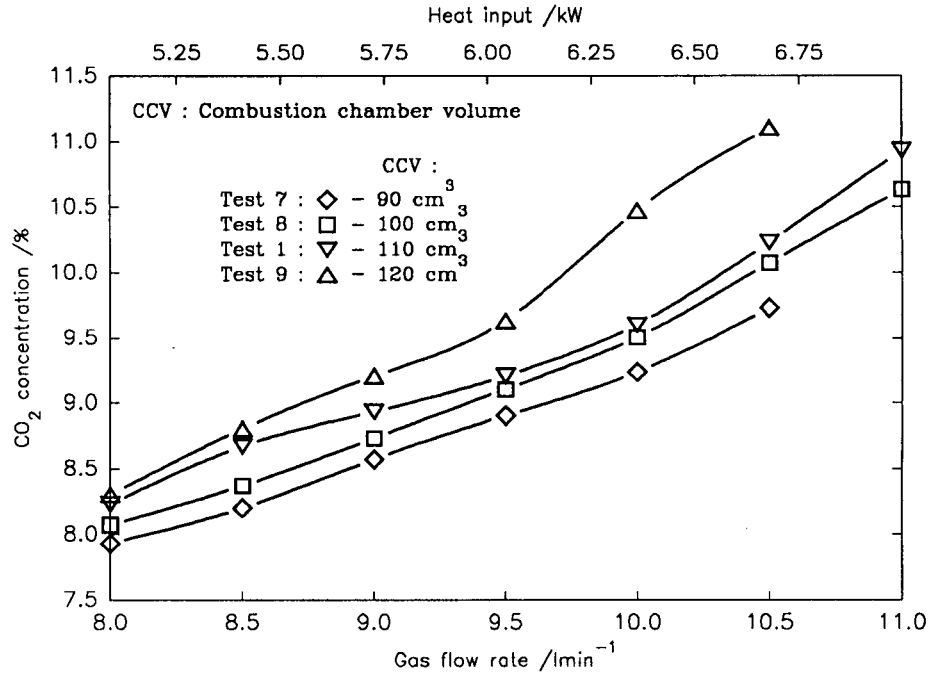

Figure 33 Variation of carbon dioxide concentration with gas flow rate for different combustion chamber volumes.

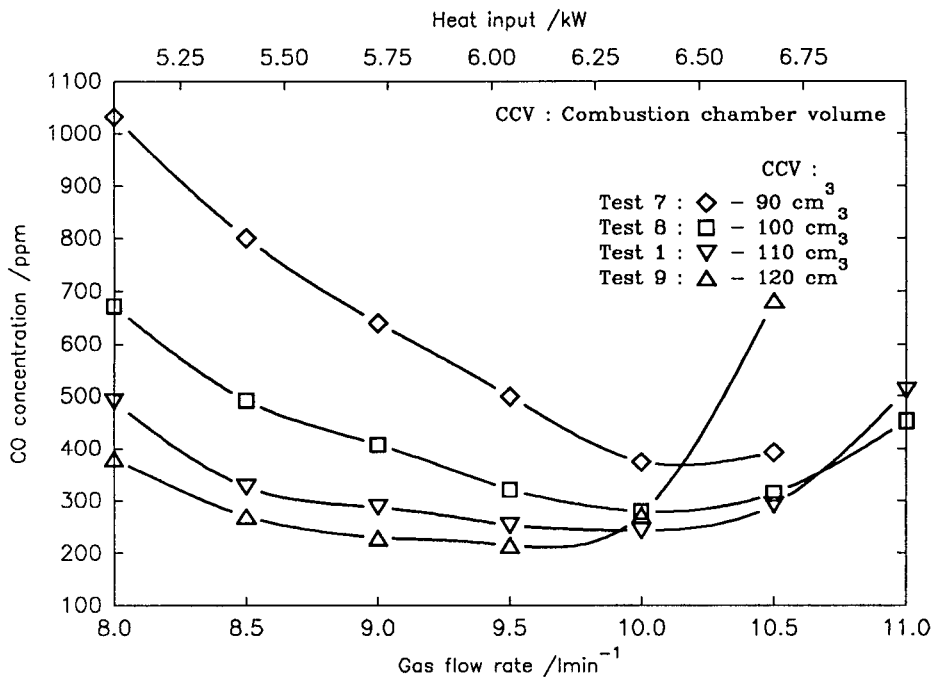

Figure 34 Variation of carbon monoxide concentration with gas flow rate for different combustion chamber volumes.

34 clearly exhibits a rise in CO formation in the lower and middle operating range of each combustion chamber as the combustion chamber size was reduced. We can explain such a trend by referring to the findings summarised in section 2.2.2. CO production is said to increase with a reduction in the flame temperature and residence time and with enhancement of the cooling rate of post combustion products. One can speculate that the latter two factors are, to some extent, dependent on operating frequency which is presumed to rise with combustion chamber volume decrease according to equation 2.1 (p. 41). Figure 35 shows that the lowest exhaust gas temperatures (which are related to the flame temperatures) are obtained with the smallest combustion chamber volume, which is also supposed to give the highest operating frequency (shortest residence time). This could explain the highest CO levels for CCV = 90 cm^3. In addition, the tailpipe Nusselt number, which determines the exhaust gas heat transfer rate (cooling rate), was found to increase with frequency [61]. This further supports the results depicted in Figure 34.

In order to examine the effect of the variation in combustion chamber volume on NO_x emissions we have to first consider the data summarised in Figure 35. This presents the variation of the exhaust gas temperature at combustion chamber exit with the gas flow rate for different combustion chamber volumes. It can be seen that t_{Exhl} rises as the mixture becomes less lean and the combustion chamber size increases. The reliability of the measured exhaust temperatures was validated by their comparison with the adiabatic flame temperatures (in case of CCV = 90 cm^3 and 110 cm^3). These were obtained in a similar fashion to those in Appendix F, for different tailpipe lengths.

Consequently, in Figure 36 we can observe nitrogen oxide levels diminishing with reduction in combustion chamber volume due to NO_x temperature dependency. Another factor which was said to influence NO_x emissions is residence time (see section 2.2.3). This can possibly also lead to lower NO_x levels for smaller combustion chamber volumes due to the higher frequency of operation for these sizes (refer to equation 2.1, p. 41).

The curves presented in Figure 37 show the variation of CO/CO_2 ratio with

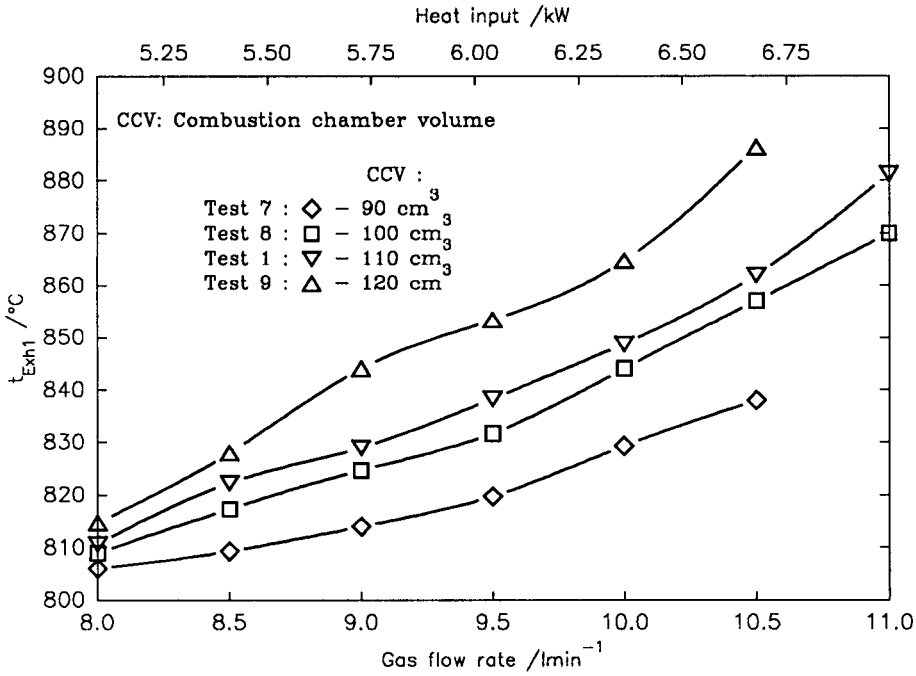

Figure 35 *Variation of exhaust gas temperature at combustion chamber exit (t_{Exh1}) with gas flow rate for different combustion chamber volumes.*

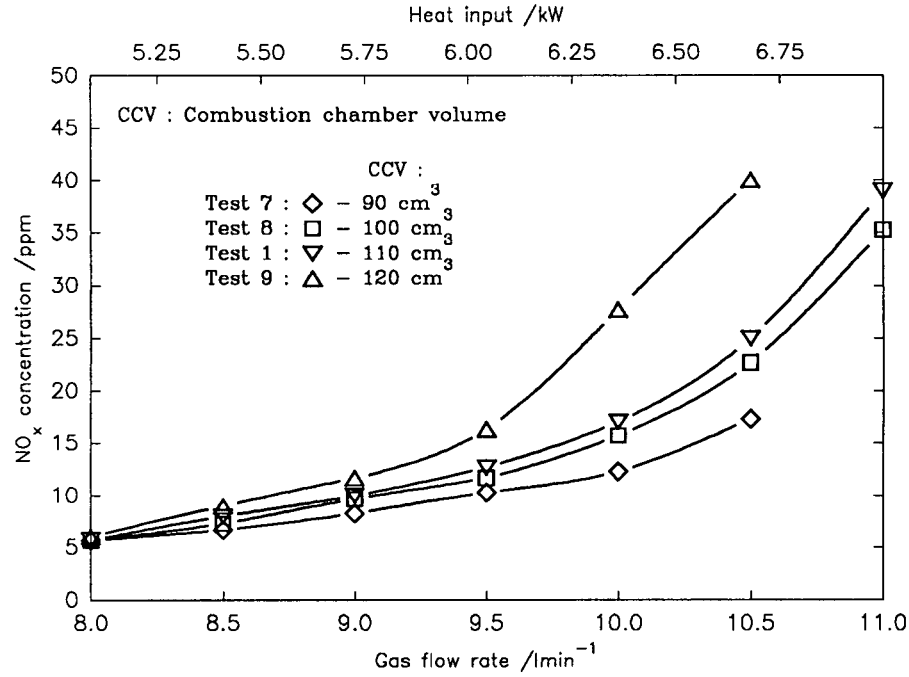

Figure 36 *Variation of nitrogen oxide concentration with gas flow rate for different combustion chamber volumes.*

gas input for the investigated combustion chamber volumes. As in case of CO concentrations shown in Figure 34, CO/CO_2 ratios also display a rise in the lower and middle operating range as the combustion chamber size was reduced. Furthermore, the combustion ratio (CO/CO_2) did not exceed the safety limit of 0.02 set by British Standard 5258 [78] for any of the examined combustion chamber volumes. The highest CO/CO_2 ratio of 0.013 was measured for the smallest combustion chamber at a gas input of 8 l min^{-1}. The minimum CO/CO_2 ratios of the two largest chambers are very close to those reported by Windmill [40].

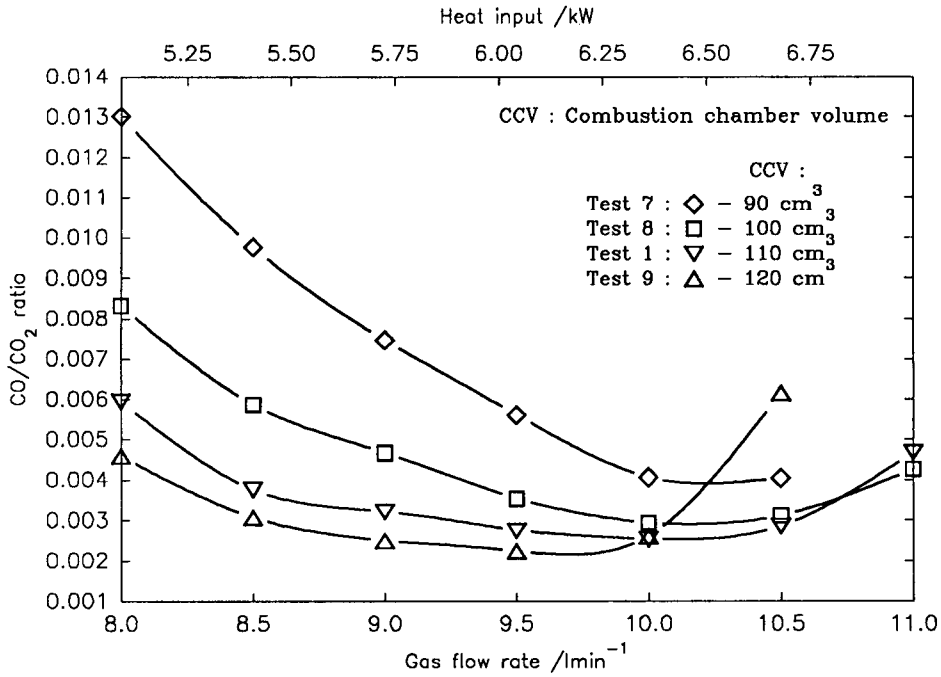

Figure 37 *Variation of CO/CO_2 ratio with gas flow rate for different combustion chamber volumes.*

Figures 38 and 39 are based on the results summarised in Appendix D and H and show the variation of air/fuel ratio (Figure 38) and percentage excess air levels (Figure 39) with gas flow rate for different combustion chamber volumes. These graphs show the air/fuel ratios and percentage excess air levels decreasing as the combustion chamber size increased in a similar pattern to that of O_2 exhaust emissions in Figure 32. The stoichiometric air/fuel ratio of 9.76, however, could not be reached since the combustion deteriorated due to oxygen starvation.

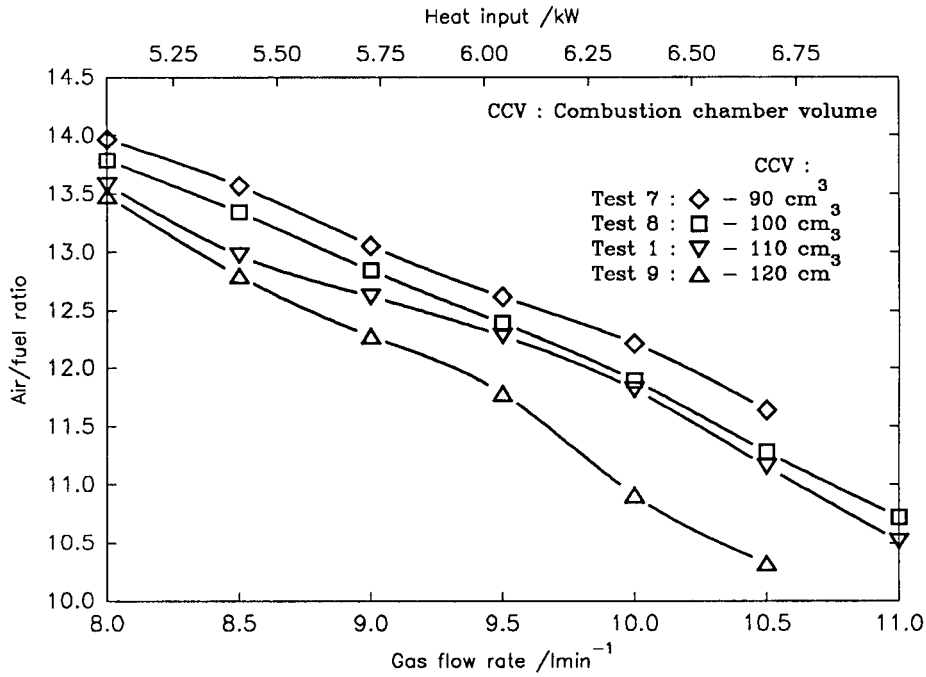

Figure 38 Variation of air/fuel ratio with gas flow rate for different combustion chamber volumes.

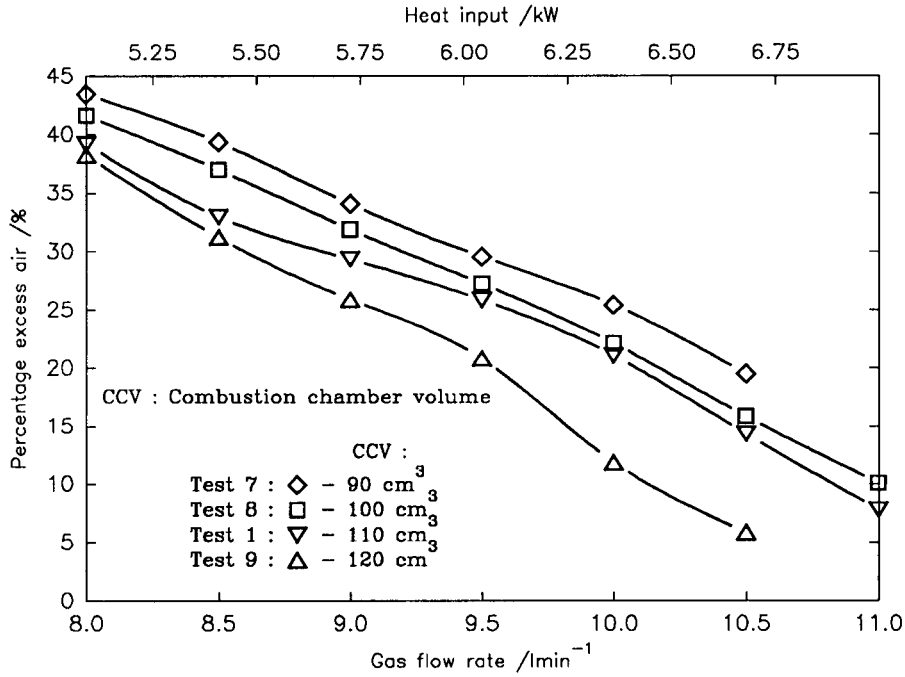

Figure 39 Variation of percentage excess air with gas flow rate for different combustion chamber volumes.

Consequently, CO emissions as well as operating frequency sharply increased and the combustor stalled. At high air/fuel ratios (and hence percentage excess air levels) the combustion process also tended to become unstable (below GFR = 8 l min^{-1}) with irregular pulsing. As fuel input was turned further down the hot gases from the previous cycle failed to ignite the too fuel-lean charge induced into the combustion chamber and the pulse burner ceased its operation probably due to insufficient energy available to drive the cycle.

4.6. EXHAUST GAS ANALYSIS FOR VARIOUS TEST GASES

4.6.1. General

This investigation was conducted in order to quantify the performance, emissions and fuel flexibility of the pulse combustor when running on family 2H test gases ie. NGA, NGB, NGC, NGD (see section 2.3.3) as well as on propane. NGA, which in general corresponds to the gas most usually distributed and for which the appliance has been specially designed, is known as the reference gas. The remaining three test gases, which correspond to the extreme variation of the characteristics of the mains distributed gas are referred to as limit gases. Since no specific guidelines are available to evaluate the effect of changes in fuel composition on performance of pulse combustors, the conventional interchangeability prediction based on the above gases was used in this study (refer to section 2.3.4). It should be mentioned that the compositions of the test gases which were used differed slightly from those specified in Reference 89 (compare Table 1 with Appendix J). However, according to BS 5386 [98] as long as the constitution of gases used for tests is as near as possible to those given in Table 1 and the Wobbe number of the mixture used is within ±2 % of the value in Table 1 for the corresponding test gas, these mixtures qualify as test gases.

Physical properties of the constituent and tested gases are summarised in Appendices I and K respectively. Where appropriate these appendices also quote

formulas used in calculation of the properties. Compositions of the tested gases obtained from British Gas are given in Appendix J.

Because the various gases used in this investigation were passed through a rotameter designed for natural gas (NGA), corrections were made in order to determine the actual flow rate of these gases. New rotameter scales were calibrated for NGB, NGC, NGD and propane according to the following formula [46] :

$$G2 = G1 \sqrt{\frac{RD_{G1}}{RD_{G2}}} \qquad (4.3)$$

where $G2$ is real value of volume flow rate of substituted gas,
$G1$ scale reading of volume flow rate of NGA,
RD_{G2} relative density of substituted gas
and RD_{G1} relative density of NGA.

Subsequently, the real gas flow rates obtained for the tested gases were expressed in terms of heat inputs (see Appendix K) so that the investigated parameters of the tested gases could be compared with each other.

Finally, it remains to be said that the proven optimum geometry of a 2.00 m long tailpipe and combustion chamber volume of 110 cm^3 was used in this study. It should be also noted that the pulse combustor was not able to run on propane since it stalled almost immediately after ignition (see section 4.6.4 for further details).

4.6.2. Experimental technique

NGB, NGC, NGD and propane were supplied by British Gas in high pressure cylinders which were connected one by one to the gas supply line as described in section 3.2.1 and Figure 17. The tests were carried out in the same way as the procedure outlined in section 4.3.2. However, use of the gas cylinders eliminated the necessity to use the booster pump.

4.6.3. Results and discussion

Figures 40 to 47 summarise the obtained data for the investigated gases shown as a function of the gas heat input rate. The curves were found to be located in three distinct regions according to the gross calorific values of the test gases. The left part of each graph (low heat inputs) includes limit gas NGC with the lowest GCV (30756 kJ m^{-3}), the middle part of the graphs contains limit gas NGD (GCV = 35601 kJ m^{-3}) and reference gas NGA (GCV = 38141 kJ m^{-3}) and finally, the area in the right part of the graphs (high heat inputs) embraces limit gas NGB with the highest GCV (46482 kJ m^{-3}).

Figure 40 shows the variation of oxygen concentration with heat input for the different types of natural gas. The four top horizontal axes display the load in terms of gas flow rates of the test gases. It can be seen that the pulse combustor was operated on NGA in the heat input range 5.1 - 7.0 kW (8 - 11 l min^{-1} of NGA), on NGB in the heat input range 6.2 - 9.3 kW (8 - 12 l min^{-1} of NGB), on NGC in the heat input range 3.6 - 4.6 kW (8 - 10 l min^{-1} of NGC) and on NGD in the heat input range 4.7 - 7.1 kW (8 - 12 l min^{-1} of NGD). The location of the curves as well as the values of oxygen concentrations in Figure 40 are reasonably similar to the results obtained by Suthenthiran [46] for a similar 15 kW pulse combustor.

The variation of carbon dioxide concentration with heat input rate for the test gases is shown in Figure 41. The apparent similarity to the previous figure is a result of the computation of CO_2 levels by the gas analyzer according to the formula : $CO_2 = CO_{2,Max}(21-O_2)/21$. However, $CO_{2,Max}$ refers to the mains gas (NGA) and its value of 11.9 % could not be used for the other test gases. Therefore $CO_{2,Max}$ values for NGB (12.5 %), NGC (10.9 %) and NGD (11.7 %) were computed by program "Gas" assuming stoichiometric combustion. Consequently, carbon dioxide concentrations for these three natural gases were calculated from the above formula now incorporating the corrected $CO_{2,Max}$ values. It should be also noted that the turn down ratios obtained (between 1.29 and 1.5) are very close to Suthenthiran's values [46] except for that for NGD which was found to be about 30 % higher in our study.

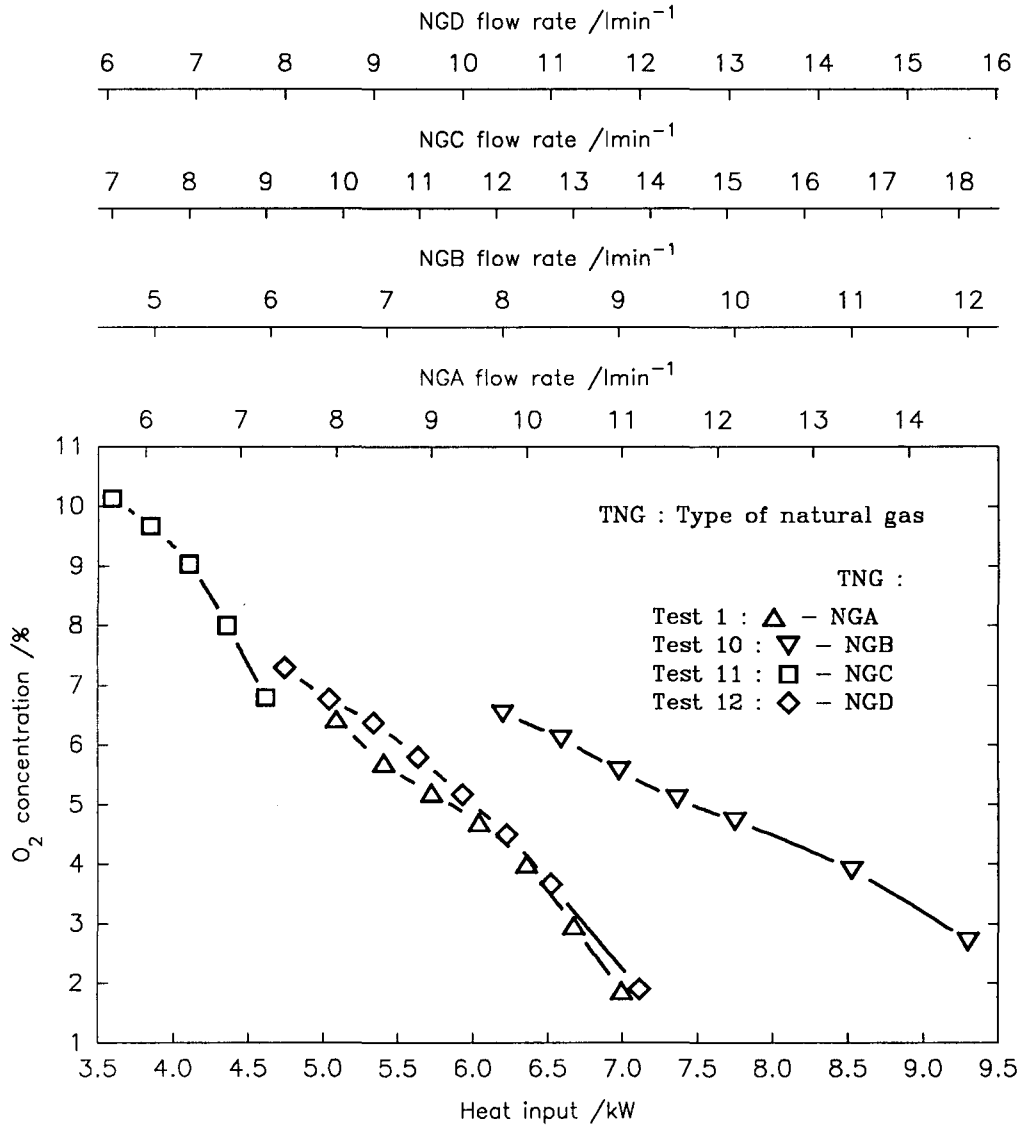

Figure 40 *Variation of oxygen concentration with heat input for different types of natural gas.*

Furthermore, turn down ratios observed by Windmill [42] are on average about 16 % higher than in our investigation. The operation of the pulse burner on NGB and NGD tended to be unstable near the upper operating limit of these gases and so it was decided to take readings in wider intervals of gas heat input rate in this region.

Figure 42 shows carbon monoxide concentration as a function of heat input

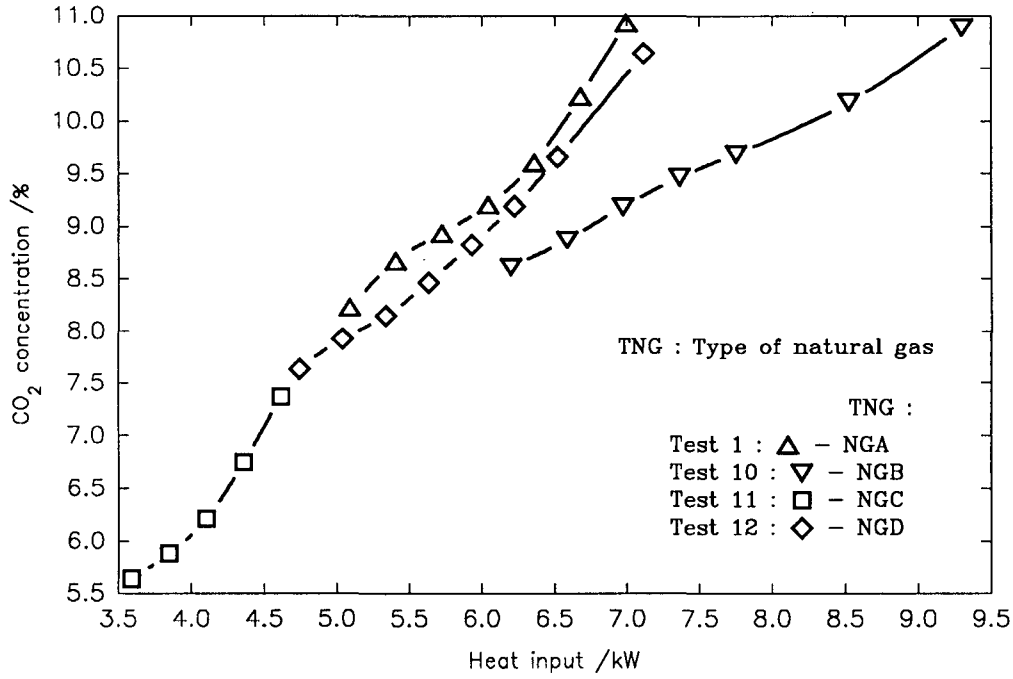

Figure 41 *Variation of carbon dioxide concentration with heat input for different types of natural gas.*

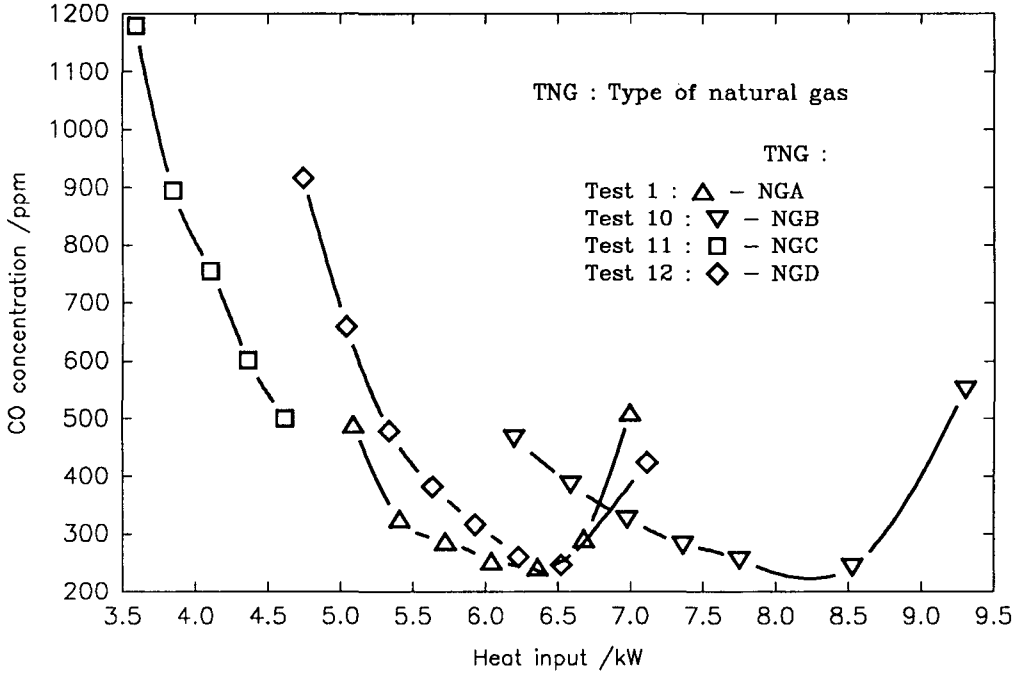

Figure 42 *Variation of carbon monoxide concentration with heat input for different types of natural gas.*

for the different types of natural gas. Apart from the limit gas NGC the rest of the tested gases show once again the typical 'U' shape curves for CO against load. It can also be seen that CO levels were considerably higher when using NGC as a fuel (500 - 1180 ppm) compared with the other investigated gases. This may be due to the lower flame temperatures obtained from burning NGC as indicated in Figure 44. Residence time and cooling rate may also affect the CO formation (see section 2.2.2) but the effect of these could not be assessed in the present study.

Figure 43 demonstrates one of the most important advantages of pulse combustion ie. low exhaust levels of nitrogen oxides. NO_x emissions, plotted here against heat input, show that the lowest value is obtained for the limit gas NGC (below 6 ppm), which is in agreement with Reference 46. Such NO_x levels most probably result from a reduction of the flame temperatures as indicated by the significantly lower exhaust temperatures shown in Figure 44. Further evidence of the temperature dependency of NO_x formation (see section 2.2.3) is given by very similar NO_x concentrations for NGA and NGD (below 40 ppm) which have similar exhaust gas temperatures.

The variation of the exhaust gas temperature at combustion chamber exit with load for the tested gases is shown in Figure 44. It can be seen that the exhaust temperatures for NGC are relatively low compared with values for the other test gases, probably because of the low gross calorific value of NGC (30756 kJ m^{-3}). However, NGB did not show any substantially higher exhaust gas temperatures than NGA (GCV = 38141 kJ m^{-3}) despite its higher gross calorific value of 46482 kJ m^{-3}. It should be also noted that unlike the work reported in Reference 46, this study showed no obvious influence of the increased flame speed, due to the high H_2 content of NGC (about 36 %) on the pulse combustor operation.

Figure 45 shows the variation of the CO/CO_2 ratio with the heat input rate of the combustor. A comparison can be made between these results and similar results reported by Windmill [42] on a 12 kW pulse combustor and by Suthenthiran [46] on a 15 kW pulse combustor respectively. Reference 42 reports an occurrence of the characteristic 'U' shaped curves for all four test gases and this investigation shows

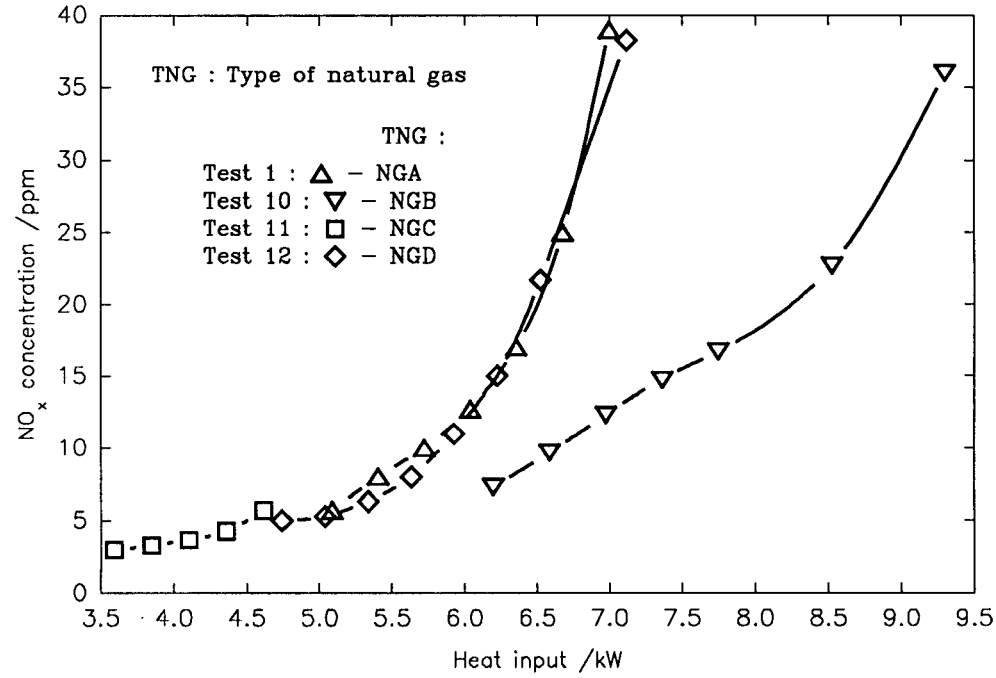

Figure 43 *Variation of nitrogen oxide concentration with heat input for different types of natural gas.*

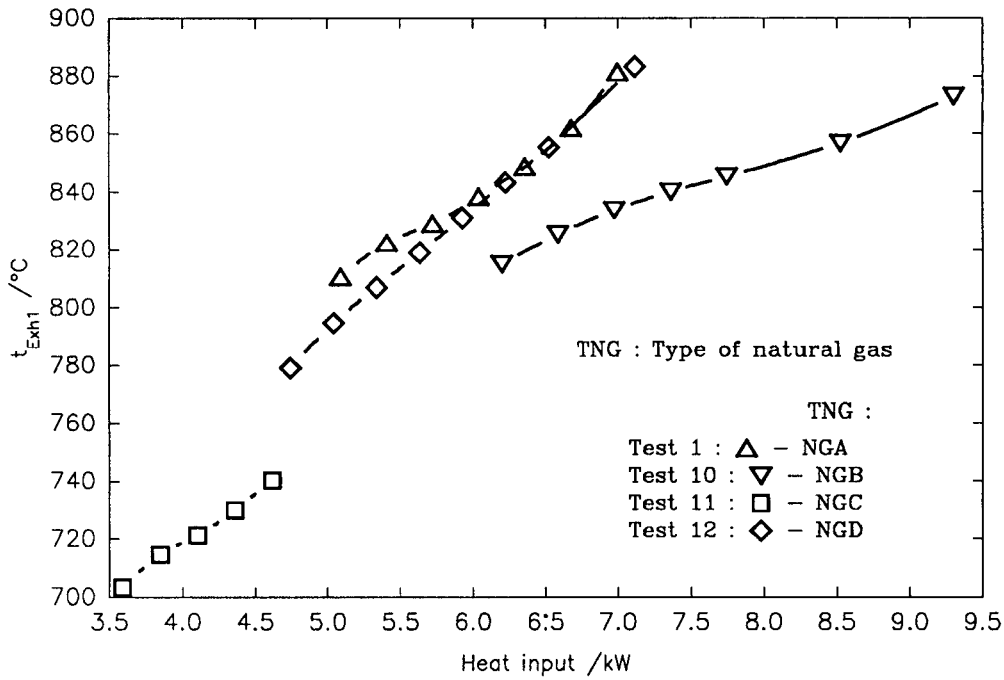

Figure 44 *Variation of exhaust gas temperature at combustion chamber exit (t_{Exh1}) with heat input for different types of natural gas.*

three 'U' shapes for NGA, NGB and NGD in contrast to Reference 46 which presents such a curve only for NGA. However, location of the curves in each graph ie. the low heat input region containing NGC, middle heat input region including NGA and NGD and high heat input region embracing NGB, is reasonably similar for all three works. This is most evident in Figure 45 and least apparent in Windmill's report which has highly overlapping curves. Another similarity shared between this investigation and the other two studies are the lowest measured CO/CO_2 ratios for NGA (0.0025, 0.0022 [42] and 0.0013 [46]) and the highest CO/CO_2 ratios for NGC (0.0197, 0.0164 [42] and 0.0128 [46]). The latter did not exceed the safety limit of 0.02 [78] in either this work or the others. In view of the very different burner geometries (this study : TPL = 2.00 m of 8 mm diam., CCV = 110 cm^3; Reference 42 : TPL = 7 x 0.90 m of 8 mm diam., CCV = 440 cm^3; Reference 46 : TPL = 2.50 m of 15 mm diam., CCV = 334 cm^3) one can draw a conclusion that emissions from the pulse combustors were more dependent on composition of the tested gases than on geometrical similarity of the burners.

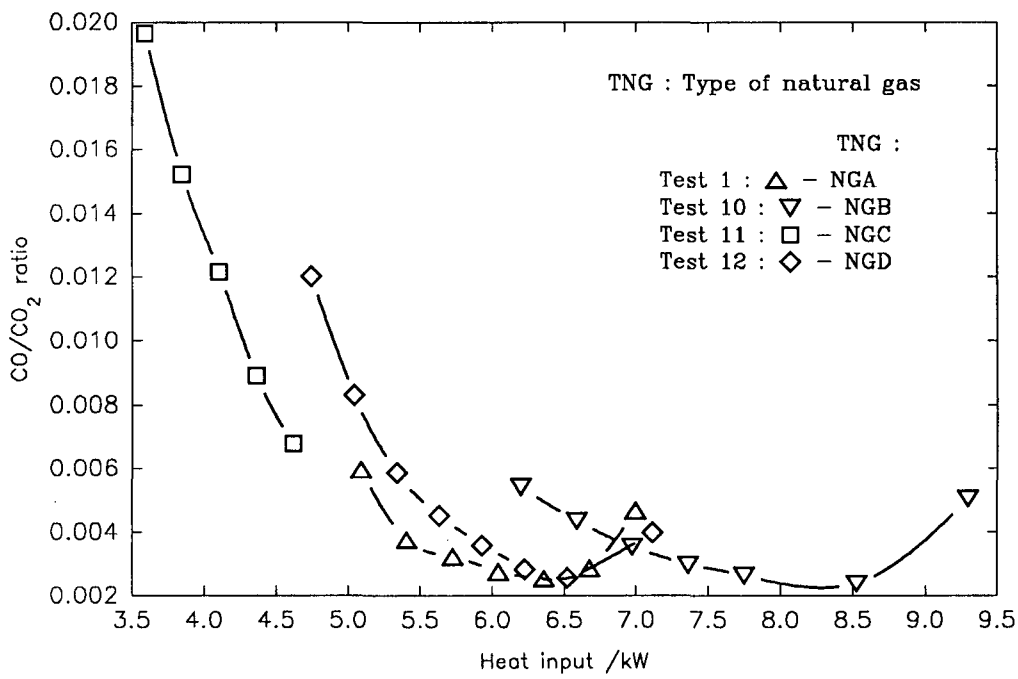

Figure 45 *Variation of CO/CO_2 ratio with heat input for different types of natural gas.*

From the comparison between results summarised in Figure 46 showing air/fuel ratios against load and data summarised in Appendices D and L we can conclude that stoichiometry conditions were not reached for any of the tested gases. The nearest stoichiometry operation of the pulse combustor was achieved by burning NGA (stoichiometric A/F ratio of 9.76) and NGD (stoichiometric A/F ratio of 9.08) with only about 8 % excess air (see figure 47) in either case. The lowest operational air/fuel ratios determined for NGB and NGC were about 17 % and 36 % above the stoichiometric values of 11.88 and 7.61 respectively.

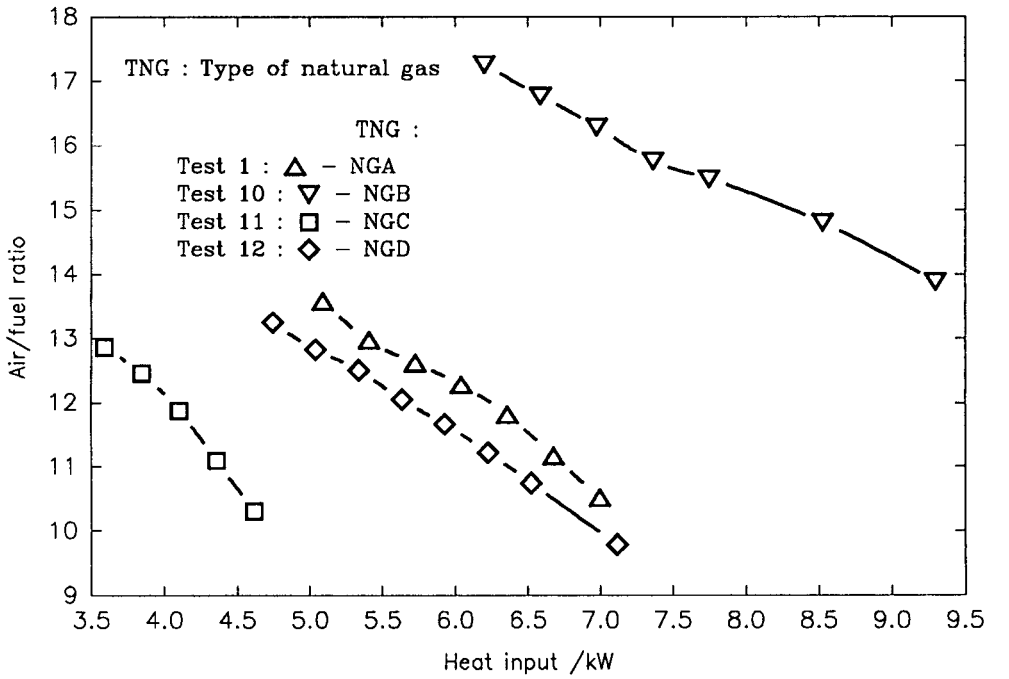

Figure 46 *Variation of air/fuel ratio with heat input for different types of natural gas.*

Figure 47 shows the variation of percentage excess air with heat input for different types of natural gas. It can be seen that PEA was greater than zero for all the investigated gases which implies that the pulse combustor was capable of operation only in a fuel-lean region. The highest percentage excess air level of about 69 % (corresponding to an A/F ratio of 12.86) was obtained by burning NGC at the lowest heat input. It should be mentioned that the only reference reporting excess air levels in the case of pulse combustion [42] states a PEA range of 2 - 39 % for NGA

which is consistent with these results ranging from 8 to 39 %.

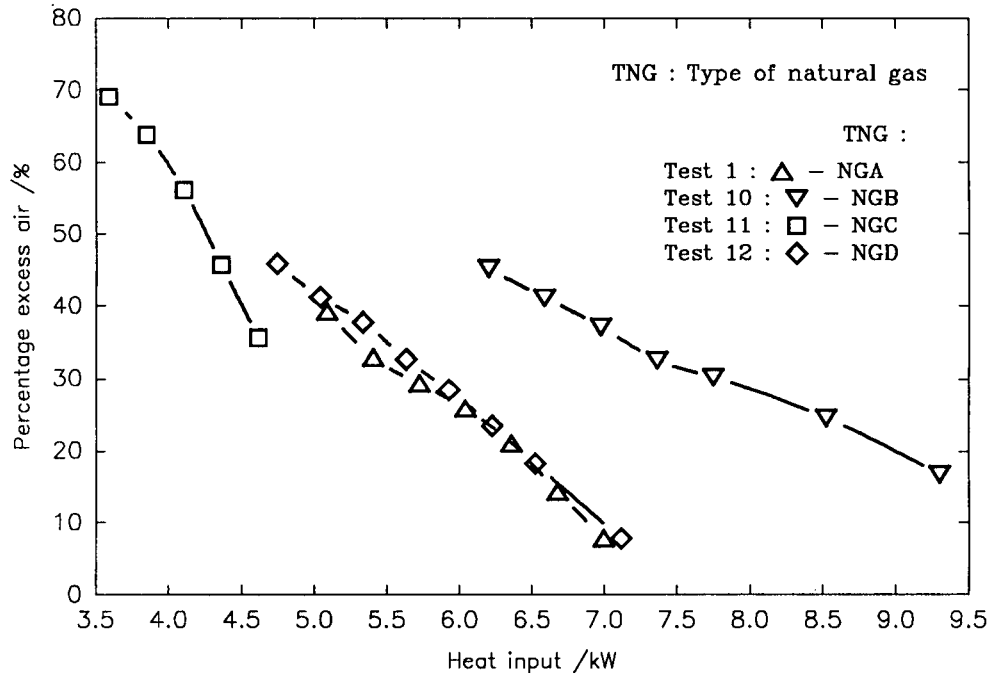

Figure 47 *Variation of percentage excess air with heat input for different types of natural gas.*

4.6.4. Interchangeability prediction

A prediction method based on the revised Harris & Lovelace diagram (see section 2.3.4) was used in this study to define an acceptable area within which all gases should be interchangeable. This technique, developed for conventional combustion systems, was used in this study because there is no interchangeability prediction available for pulse combustion systems. The pulse combustor was therefore treated as a conventional combustion device.

A modified Harris & Lovelace diagram (see Figure 48) was constructed for the investigated pulse combustor using the data summarised in Appendix K. Since the reference gas NGA and limit gases NGB, NGC and NGD, compositions of which are given in Appendix J, were successfully used as fuels for the tested pulse burner we can enclose an area of interchangeability in the diagram as shown by the dashed line. NGB was connected with NGC in Figure 48 by a straight line because

the limit gas NGC2 (see Table 1) was not available for this work.

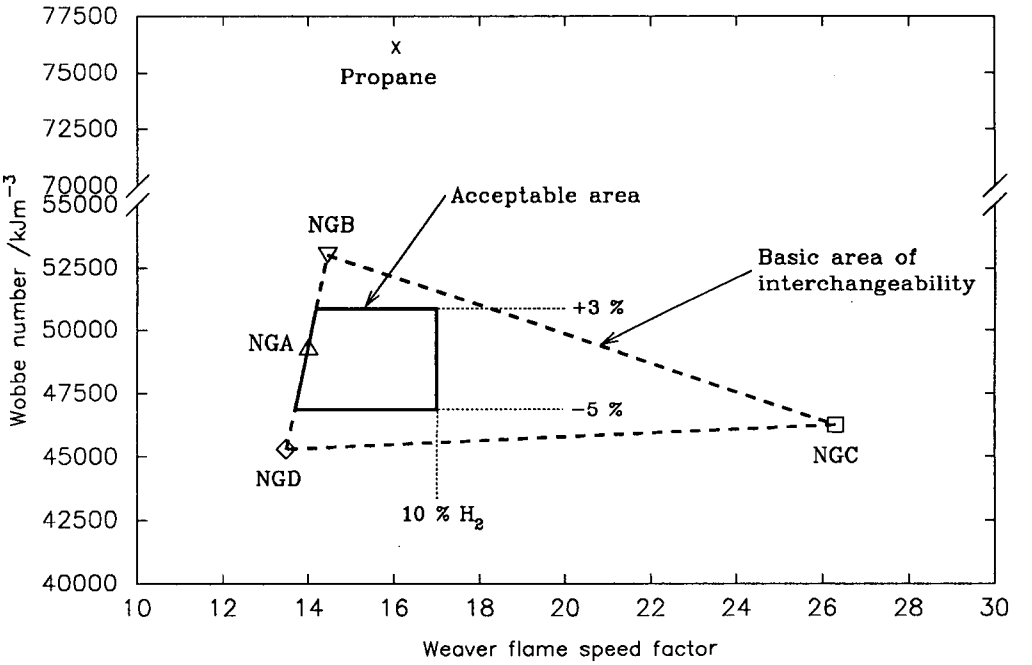

Figure 48 *Modified Harris and Lovelace diagram for the investigated pulse combustor.*

According to Reference 88 any natural gas of family 2H falling within an area bounded by the limit gases should give satisfactory performance on appliances adjusted for the reference gas. In another words, the studied pulse combustor, adjusted for NGA, should be capable of operation on any natural gas of family 2H falling into the basic area of interchangeability. However, as the result of industrial trials, tighter constraints on gas properties were imposed and the actual area of interchangeability today is smaller than originally envisaged. The acceptable area (enclosed by solid lines in Figure 48) is now bounded by Wobbe numbers of 3 % above and 5 % below that of the reference gas NGA and by a nearly-vertical line representing gases containing 10 % hydrogen [89]. One of the reasons for the introduction of the latter limit can be seen in Figure 45 which shows that if, for example, the combustor was rated for nominal heat input of 6.5 kW NGC with its high Weaver flame speed factor of 26.3 could be used as a fuel but the heat output of the burner would be drastically reduced. In view of the above it can be concluded

that natural gases of family 2H which fall within the acceptable area in Figure 48 and satisfy the criteria defined in section 2.3.4 are interchangeable with the existing mains supply. In addition, it can be concluded that assuming that a pulse combustor may be treated as a conventional combustor for fuel flexibility studies such gases should also ensure satisfactory operation of the pulse combustor without the need for any adjustment when being used as fuels.

Operation of the pulse burner on propane, which is a family 3 gas, was also investigated in this study. Despite altering the tailpipe length and combustion chamber volume it was impossible to maintain pulsations for more than five seconds. This is the result of a too high Wobbe number of propane (76090 kJ m^{-3}) which causes this gas to fall outside of the acceptable area shown in Figure 48. In other words, propane is not interchangeable with the reference gas NGA for the investigated pulse combustor.

4.7. MEASUREMENT OF OPERATING FREQUENCY

4.7.1. General

It was felt that this work would not be complete without at least a brief investigation of the operating frequency of the pulse combustor. As a fundamental characteristic of a pulsating device, operating frequency directly affects the tailpipe heat transfer rate which is one of the factors controlling system thermal efficiency (see section 2.1.2). Therefore, a test was conducted to evaluate the operating frequency variation with gas flow rate and a comparison was made between the measured and predicted frequencies.

Because a suitable pressure transducer for pulsating pressure monitoring was not available an alternative method based on the hot wire anemometer principle was utilized in this study for frequency measurement. The hot wire anemometer, which is basically a thermal transducer, has an excellent frequency response [100]. It employs a wire of high resistance which is heated up by a constant electric current

and exposed to a cross flow of gas. As the rate and temperature of the flow vary, the heat transfer from the wire varies. This causes a change in temperature of the wire which in turn results in a variation of its electrical resistance. The latter can be monitored with time as a voltage change across the wire by means of an oscilloscope.

If the wire is placed across the tailpipe exit of the pulse combustor, its resistance change with time would exhibit a frequency twice that of the pulsations due to the variations in the flow velocity during the exhaust and intake phase of each pulse. An experimental rig was built which employed the measuring circuit as shown in Figure 49. The rig, which was attached to the end of the exhaust silencer, consisted of a clamp-on collar and four terminal sockets two of which supported a platinum wire of 40 μm diameter. A readily available constant voltage power supply was used in this work and the variation in voltage V_r across the resistor r was monitored by the oscilloscope. It can be shown that the voltage V_r is almost a linear function of the resistance of the wire R_w, if this resistance is much greater than that of resistor r, R_r. In this case, the voltage V_r can be expressed as follows :

$$V_r = \frac{R_r V}{R_w} , \qquad (4.4)$$

where the numerator is a constant.

4.7.2. Experimental technique

The combustor was set up with its optimum geometry ie. 2.00 m long tailpipe and combustion chamber volume of 110 cm^3. The experimental procedure was very much the same as that given in section 4.3.2 except that only readings of the exhaust gas temperature at the combustion chamber exit (t_{Exh1}), exhaust gas temperature at the tailpipe exit (t_{Exh2}) and operating frequency were taken. The power supply of the measuring rig was set at a constant voltage of 5 V which heated the wire to a temperature of about 450 °C. This temperature was high enough to ensure clear

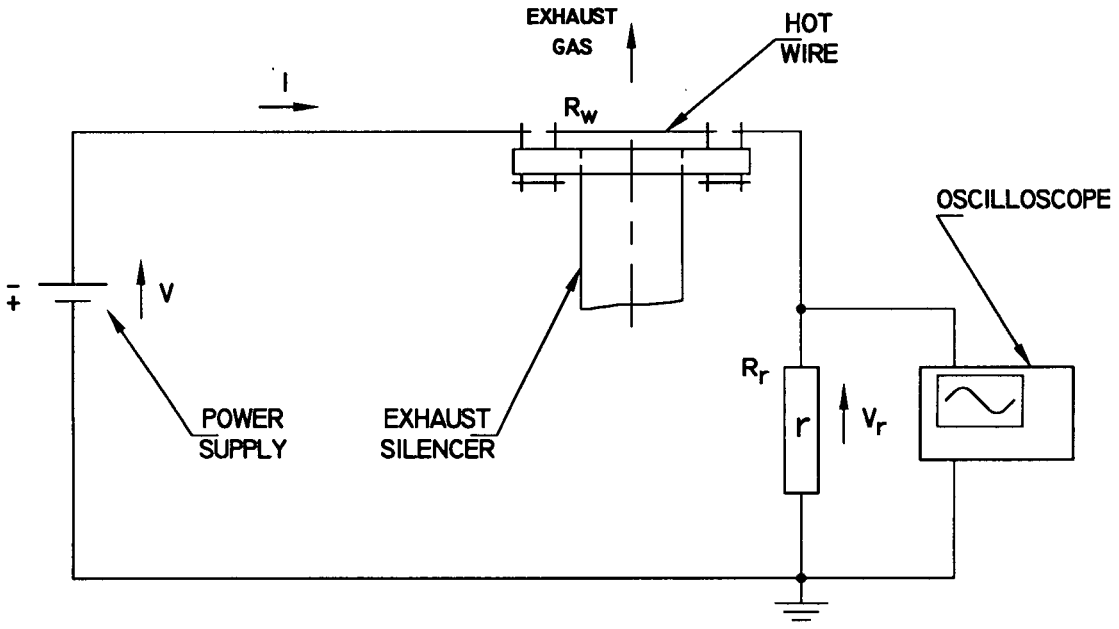

Figure 49 Schematic diagram of the frequency measuring circuit.

monitoring of the voltage V_r but did not cause any damage to the wire itself. The oscilloscope picture was first frozen and the peak to peak distance, read off in milliseconds, was then multiplied by factor of two and converted into frequency in hertz.

4.7.3. Results and discussion

Figure 50 shows the variation of the measured operating frequency, frequency predicted using equation 2.1 (p. 41) and mean temperature of the exhaust gas with gas flow rate. It can be observed that the operating frequency rose as the heat input was increased, which is in agreement with Keel's findings [51]. Minimum and maximum operating frequencies of 36.6 Hz and 60 Hz respectively were recorded. This means that these results fall into the lower region of the typical frequency range of a pulse combustor (see section 2.1.2).

There is a considerable difference between the predicted frequency, which is calculated in Appendix M, and the measured value. The measured frequency was

smaller than the predicted for gas flow rates below about 10.3 l min^{-1} and greater above this point. It is also seen that the predicted frequency (ranging from 50.1 to 53.5 Hz) rose with heat input increase but at a substantially lower rate than the measured frequency. The discrepancy between the two frequencies might be caused by the fact that the speed of sound varies along the tailpipe and using the mean temperature gives only a rough approximation to the actual speed. However, the phase relationship between the resonant pressure wave and the instantaneous energy release, which equation 2.1 (p. 41) does not account for, and which was probably varied in this test, is another factor affecting the operating frequency (see section 2.1.2). Consequently, we can conclude that the equation 2.1, derived from Helmholtz resonator model, can be used to predict only very roughly the operating frequency of a pulse combustor of this type.

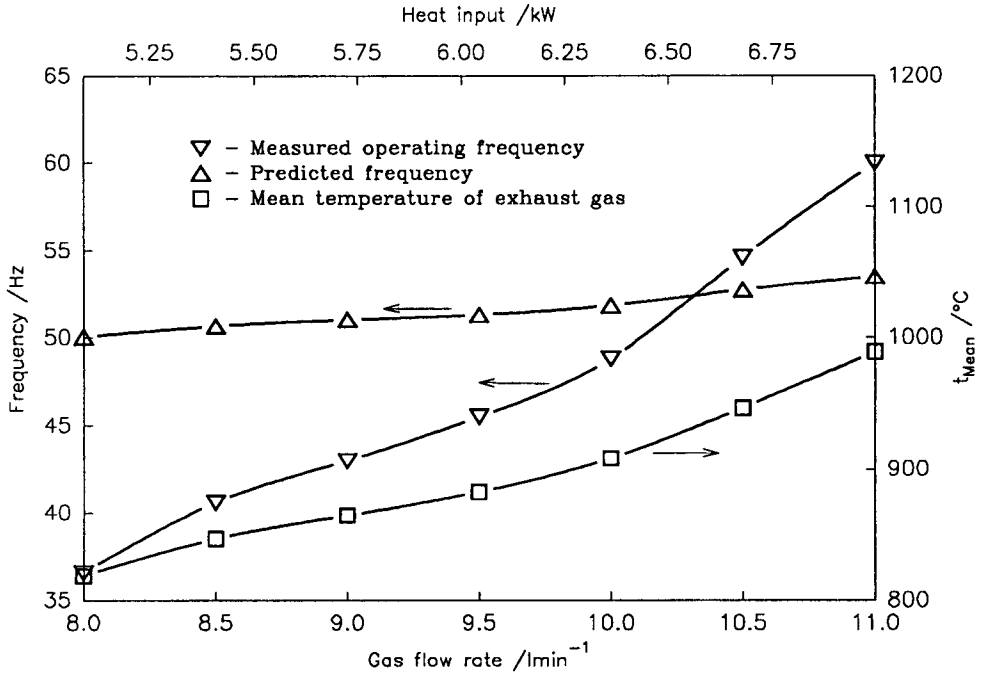

Figure 50 *Comparison of the operating frequency and the predicted value.*

CHAPTER 5 : CONCLUSIONS

5.1. SUMMARY OF MAJOR FINDINGS

It was found that the investigated pulse combustor was not capable of operation with an air-box inserted in the air-supply line prior to the air decoupler (see section 4.2.6). As a result, the essential requirement of ISO Technical report 3313 [93] was not satisfied (see section 3.2.2) which led to the conclusion that the pulsating flow of the aspirated combustion air could not be accurately measured by means of the orifice plate in this study. This was justified by considerable difference (mainly in the lower part of the gas flow range) between the air/fuel ratios obtained using the orifice plate without the air-box and those derived from an exhaust gas analysis (see Figure 21).

Combustion quality was assessed during the present investigations by monitoring the exhaust gas oxygen and carbon dioxide levels. The latter were computed from the former by the gas analyzer KM 9004. O_2 concentrations were reduced with increase in gas flow rate, tailpipe length and combustion chamber volume respectively (see Figures 18, 24 and 32). The recorded O_2 values for the aforementioned parameters fell typically in the range of 7 - 1 %, which implied that the combustor was burning a fuel-lean mixture. CO_2 levels ranging between about 8 - 11 % displayed a rise with increase in gas flow rate, tailpipe length and combustion chamber volume respectively (see Figures 18, 25 and 33). The trend for the last mentioned parameter was found to be consistent with Windmill's observations [42]. The exhaust gas analysis for combustion of NGC (high in hydrogen, low in calorific value) exhibited considerably higher O_2 (and hence lower CO_2) levels than for the rest of the test gases (see Figures 40 and 41). This is in agreement with Suthenthiran's results [46].

Other indicators of combustion quality and appliance safety, carbon monoxide levels and CO/CO_2 ratio, were found to decline in the lower and middle operating range only slightly with an increase in tailpipe length but had a greater reduction with increase in combustion chamber volume (see Figures 26, 29, 34 and 37). In view of the above findings we can conclude that the combustion chamber volume had a greater effect than the tailpipe length on CO formation. This appears to be

contradictory to Kassehchi's work [50]. The CO concentration and CO/CO_2 ratio variation with gas flow rate increase exhibited a typical 'U' shaped behaviour with the curve gently sloping down and reaching minimum CO level and CO/CO_2 ratio respectively, before rising steeply as stoichiometry was approached (see Figure 19 and 22). As stated in section 2.2.2, the reported levels of CO in pulse combustor exhaust gases do not generally exceed 400 ppm for optimum operating conditions. In our tests these conditions were achieved near the middle of the operating range where the CO concentrations dropped to about 100 ppm below the above mentioned value. Furthermore, CO/CO_2 ratios did not exceed the maximum permissible limit of 0.02 set by BS 5258 [78] for any of the conducted trials. CO/CO_2 ratios obtained for the burner operating on NGA, NGB, NGC and NGD revealed a reasonable degree of similarity between our results and those reported in References 42 and 46. In addition, it was concluded that emissions from the compared pulse combustors were more dependent on the composition of tested gases than on geometrical similarity of the burners (see section 4.6.3).

Our work showed NO_x levels below 60 ppm for all conducted tests and confirmed the most commonly cited advantage of pulse combustion systems ie. low production of nitrogen oxides [16, 36, 46 and 77]. Accordingly to References 46 and 85 it was observed that an increase in gas flow rate results in an increase in NO_x formation (see Figure 19). Furthermore, an increase in tailpipe length and combustion chamber volume respectively also led to an increase in NO_x concentrations in the studied combustion products (see Figures 27 and 36). Since the above trends were identical to those for the exhaust gas temperature at the combustion chamber exit, t_{Exhl}, (refer to Figures 20, 28 and 35) a conclusion was drawn that NO_x production is strongly temperature dependent, a fact which is emphasised throughout the literature. Our interchangeability work showed that when using NGC as a fuel the combustion products contained less NO_x than when burning the other test gases, which is in accord with Reference 46 (see Figure 43). Finally, since the pulse combustor operated only under fuel-lean conditions and the exhaust gases acquired high temperatures as indicated by measured t_{Exhl} (see also Appendix

F) it was concluded that the observed nitrogen oxides in our study consisted mainly of thermal NO formed by the Zeldovich mechanism.

Air/fuel ratios and percentage excess air levels were in the present work derived from the exhaust gas analysis by a specially written computer program (see Appendices A, B, C and D). It was shown that the air/fuel ratio and percentage excess air fell to low levels with an increase in gas flow rate, tailpipe length and combustion chamber volume (see Figure 21, 22, 30, 31, 38 and 39). This is the same response as that displayed by oxygen concentrations. In addition, since the obtained air/fuel ratios were greater than that for stoichiometric conditions and some percentage excess air was always present in the studied exhaust gas a conclusion was made that the pulse combustor was capable of operation only under fuel-lean conditions. Our fuel flexibility investigation revealed that the percentage excess air levels obtained when burning NGA were in the range of 8 - 39 %, which corresponds with data presented in Reference 42.

The pulse combustor was successfully operated on all four family 2H test gases ie. NGA, NGB, NGC (high in H_2) and NGD (high in N_2). It was found that the curves representing O_2, CO_2, CO, NO_x, t_{Exhl}, CO/CO_2 ratio, A/F ratio and PEA were in each plot located in three distinct regions according to the gross calorific values of the test gases. Furthermore, it was observed that the exhaust gas analysis for combustion of reference gas NGA and limit gas NGD were similar. A conclusion was made that the high H_2 content of NGC (and hence high flame speed) did not have any apparent effect on pulse combustor operation. Since there are no specific guidelines available to predict pulse combustor performance on different fuels a conventional interchangeability method based on the modified Harris & Lovelace diagram was used in this study. Consequently, an assumption was made that the pulse combustor could be treated as a conventional burner for our fuel flexibility study. As a result, a basic area of interchangeability bounded by the reference and limit gases was further restricted in order to define an acceptable area of interchangeability (see Figure 48). It was concluded that under the above assumption any natural gas of family 2H which falls within the acceptable area should be

interchangeable with the mains existing supply. Furthermore, such gas would also enable satisfactory operation of the pulse combustor without the need for any adjustments. Finally, it should be noted that the combustor was not able to run on propane. This finding supports the aforementioned conclusions since propane did not fall within the acceptable area of interchangeability.

In addition to the objectives of this study, a brief investigation of the operating frequency of the pulse combustor was conducted utilizing a hot wire anemometer technique. It was observed that the operating frequency rose with increase in gas flow rate and ranged from 36.6 - 60 Hz, which is consistent with values reported in the literature. The measured frequency was compared with the prediction based on equation 2.1 in section 2.1.2 (see Figure 50). As a result, a conclusion was made that the above equation, derived from the Helmholtz resonator model, can be used to predict only very roughly the operating frequency of a pulse combustor of the examined type.

Finally, it can be said that the investigated combustor was capable of safe operation over a range of different geometries, gave consistently low CO and NO_x emissions and appeared to be tolerant to the test gases. The audible noise of the burner was greatly reduced by the introduction of the motor car silencer. The low turn down ratios observed in our study confirmed one of the most commonly quoted disadvantage of pulse combustion systems.

5.2. SUGGESTIONS FOR FURTHER WORK

In view of the findings summarised above a different method of air flow measurement should be utilised in future work in order to compare actual air/fuel ratios with those based on the exhaust gas analysis. One of the possible ways is to record open and close responses of the flapper valve, as described by Keel and Shin [51].

In order to obtain a better understanding of the response of the pulse combustor exhaust gas emissions to changes in its geometry and when burning

various gaseous fuels, it is necessary to monitor operating frequency and pressure amplitude. According to the literature the latter two factors govern the resonant pressure wave formation within the combustor. It is the phase relationship between this resonant pressure wave and the release of energy from combustion processes which controls the operation of a pulse combustor (viz. Rayleigh's criterion, p. 20).

In our work an acceptable area of interchangeability based on the four test gases was defined. However, the only independent gas available, ie. propane, was found to be far from this area. It would be of much interest to evaluate the performance of the pulse combustor when burning a family 2H gas falling within or close to the limits of the acceptable area.

LIST OF REFERENCES

1. WOOD, A., *Acoustics*, Vol. II, Blackie & Son Ltd, London, 1950.

2. READER, G.T., The Pulse Jet 1906-1966, *Journal of Naval Science*, 3:226-232, 1977.

3. SKINNER, B., A New Concept in Air Conditioning, *Journal of the Institute of Gas Engineers*, Vol. 29, No. 1, January 1988.

4. KITCHEN, J.A., Canadian Development of Pulse-Combustion Heating Equipment, *Proceedings of the Symposium on Pulse Combustion Technology for Heating Applications*, Argone National Laboratory, 1979.

5. LORD RAYLEIGH, *The Theory of Sound*, Vol. II, MacMillan and Co., London, 1940.

6. REAY, D., The Thermal Efficiency, Silencing, and Practicability of Gas-Fired Industrial Pulsating Combustors, *Journal of the Institute of Fuel*, 42:135-142, 1969.

7. PUTNAM, A.A, *Combustion Driven Oscillations in Industry*, Elsevier, New York, 1971.

8. TYNDALL, J., *Sound*, D. Appleton & Company, New York, 1880.

9. STODOLA, A., *Steam and Gas Turbines*, Vol. II, Peter Smith, New York, 1945.

10. REYNST, F.H., *Pulsating Combustion - The Collected Works of F.H. Reynst* (N.W. Thring, Ed.), Pergamon Press, New York, 1961.

11. FOA, J.V., *Elements of Flight Propulsion*, John Willey & Sons, New York, 1960.

12. COX, H.R., *Gas Turbine Principles and Practice*, Van Nostrand, New York, 1955.

13. ZINN, B.T., *Advanced Combustion Methods* (F.J. Weinberg, Ed.), Academic Press, London, 1986.

14. ZINN, B.T., Pulsating Combustion, *Mechanical Engineering*, No. 8, August 1985.

15. PUTNAM, A.A., General Survey of Pulsed Combustion, *Proceedings of the first International Symposium on Pulsating Combustion* (D.J. Brown, Ed.), Sheffield, 1971.

16. PUTNAM, A.A., BELLES, F.E., AND KENTFIELD, J.A.C., Pulse Combustion, *Progress in Energy and Combustion Science*, 12:43-79, 1986.

17. PUTNAM, A.A., A Review of Pulse-Combustor Technology, *Proceedings of the Symposium on Pulse Combustion Technology for Heating Applications*, Argone National Laboratory, 1979.

18. SWITHENBANK, J., BROWN, D.J., AND SAUNDERS, R.J., The Application of Pulsating Combustion to Power Generation Using Gas Turbines, *Proceedings of the first International Symposium on Pulsating Combustion* (D.J. Brown, Ed.), Sheffield, 1971.

19. SERVANTY, P., Design and Testing of Harmonic Burners for Low Power Gas Turbines, *Proceedings of the first International Symposium on Pulsating Combustion* (D.J. Brown, Ed.), Sheffield, England, 1971.

20. MULLER, J.L., Theoretical and Practical Aspects of the Application of Resonant Combustion Chambers in Gas Turbines, *Journal of Mechanical Engineering Science*, 13:137-150, 1971.

21. KENTFIELD, J.A.C., Pressure-Gain Combustion, A Review of Recent Progress, *Proceedings of the Symposium on Pulse Combustion Technology for Heating Applications*, Argone National Laboratory, 1979.

22. SOMMERS, H., *Pulsating Combustion - The Collected Works of F.H. Reynst* (N.W. Thring, Ed.), Pergamon Press, New York, 1961.

23. BABKIN, Y.L., Pulsating Combustion Chambers as Furnaces for Steam Boilers, *Teploenergetika*, Moscow, 12:23-27, 1965.

24. KATSNEL'SON, B.D., MARONE, I.Y., AND TARAKANOVSKII, A.A., An Experimental Study of Pulsating Combustion, *Teploenergetika*, Moscow, 16:3-6, 1969.

25. HANBY, V.I., AND BROWN, D.J., A 50 lb/h Pulsating Combustor for Pulverised Coal, *Journal of the Institute of Fuel*, 41:423-426, 1968.

26. HANBY, V.I., *Journal of Fuel Society*, 18:44-49, 1967.

27. SEVERYANIN, V.S., The Combustion of Solid Fuel in a Pulsating Flow, *Teploenergetika*, Moscow, 16:6-8, 1969.

28. SEVERYANIN, V.S., Application of Pulsating Combustion in Industrial Installations, *Proceedings of the Symposium on Pulse Combustion Applications*, Vol. 1, Atlanta, 1982.

29. ZINN, B.T., MILLER, N., CARVALHO, J.A., AND DANIEL, B.R., Pulsating Combustion of Coal in a Rijke-Type combustor, *19th Symposium (International) on Combustion*, The Combustion Institute, Pittsburgh, 1982.

30. CARVALHO, J.A., WONG, M.R., MILLER, N., DANIEL, B.R., AND ZINN, B.T., Controlling Mechanisms and Performance of Coal Burning Rijke Type Pulsating Combustor, *20th Symposium (International) on Combustion*, The Combustion Institute, Pittsburgh, 1984.

31. HUBER, L., Central Heating, Air and Water Heating with Pulse Combustion, *Proceedings of the first International Symposium on Pulsating Combustion* (D.J. Brown, Ed.), Sheffield, 1971.

32. ALEBON, J., LEE, G.K, AND GELLER, L.B., A Pulsating Combustion System for Space Heating, *Proceedings of the Boyar Conference*, Montreal, 1963.

33. FRANCIS, W.E., HOGGARTH, M.L., AND REAY, D., A Study of Gas-Fired Pulsating Combustors for Industrial Applications, *Journal of the Institution of Gas Engineers*, 3:301-310, 1963.

34. LAWTON, E.A., IRWIN, L., AND LAWLER, A., Development of a Gas-Fired Pulse Combustion Commercial Water Heater, *Proceedings of the Symposium on Pulse Combustion Applications*, Vol. 1, Atlanta, 1982.

35. *G14/GSR14 Series Pulse Gas-fired Warm-air Heaters*, Engineering Data Brochure, Lennox Industries Ltd, June 1988.

36. THRASHER, W.H., Development of a Pulse Combustion Space Heater, *GRI-83/0061*, Gas Research Institute, Chicago, 1983.

37. MULLER, J.L., The Development of a Resonance Combustion Heater for Drying Applications, *South African Mechanical Engineer*, 16:137-146, 1967.

38. ELMAN, R.C., BELTER, J.W., AND DOCKTER, L., Adapting a Pulse-jet Combustion System to Entrained Drying of Lignite, *5th International Coal Preparation Congress*, October 1966.

39. FARNSWORTH, C.A., Pulse Combustion Deep Fat Fryer, *GRI 84/0037*, Gas Research Institute, Chicago, 1983.

40. HIMMEL, R.L., AND STACK, R.E., Commercial Cooking Equipment Improvement, Vol. 2, Deep Fat Fryers, *GRI 80/0079.2*, Gas Research Institute, Chicago, 1981.

41. GRIFFITHS, J.S., THRASHER, W.H., HIMMEL, R.L., AND FARNSWORTH, C.A., Development and Commercialization of an Integrated Commercial Cooking System with Ultra High Efficiency, *GRI 82/0090*, Gas Research Institute, Chicago, 1983.

42. WINDMILL, S.A., An Investigation of the Factors Affecting the Performance of an Experimental Pulsed Combustion Unit, *British Gas Report*, Watson House, August 1984.

43. SUTHENTHIRAN, A., Pulsed Combustion, *Report No.1*, Middlesex Polytechnic, 1988.

44. SUTHENTHIRAN, A., AND MASKELL, W.C., Pulsating Combustion, *Report No.2*, Middlesex Polytechnic, 1988.

45. SUTHENTHIRAN, A., AND MASKELL, W.C., Pulsed Combustion, *Report No.3*, Middlesex Polytechnic, 1988.

46. SUTHENTHIRAN, A., AND MASKELL, W.C., Pulsed Combustion - Mark 1 Combustor Operation with a Range of Test Gases, *Report No.4*, Middlesex Polytechnic, 1989.

47. SUTHENTHIRAN, A., AND MASKELL, W.C., Pulsed Combustion - Modification to the Mark 1, *Report No.5*, Middlesex Polytechnic, 1990.

48. SUTHENTHIRAN, A., AND MASKELL, W.C., Pulsed Combustion - Noise Levels During Mark 1 Combustion Operation, *Report No.6*, Middlesex Polytechnic, 1990.

49. SUTHENTHIRAN, A., Construction of Mark 2 Pulsed Combustor, *Report No.7*, Middlesex Polytechnic, 1990.

50. KASSEHCHI, D., Pulsating Combustion, *MSc Report*, Middlesex Polytechnic, 1990.

51. KEEL, S.I., AND SHIN, H.D., A Study of the Operating Characteristics of a Helmholtz-type Pulsating Combustor, *Journal of the Institute of Energy*, 64:99-106, 1991.

52. KELLER, J.O., BRAMLETTE, T.T, DEC, J.E., AND WESTBROOK, C.K., Pulse Combustion : The Importance of Characteristic Times, *Combustion and Flame*, 75:33-44, 1989.

53. HARGRAVE, G.K., KILHAM, J.K., AND WILLIAMS, A., Operating Characteristics and Convective Heat Transfer of a Natural-Gas-Fired Combustor, *Journal of the Institute of Energy*, 59:63-69, 1986.

54. GRIFFITHS, J.C., THOMPSON, C.W, AND WEBER, E.J., New or Unusual Burners and Combustion Processes, *American Gas Association Research Bulletin*, No. 96, 1963.

55. GRIFFITHS, J.C., AND WEBER, E.J., The design of Pulse Combustion Burners, *American Gas Association Research Bulletin*, No. 107, 1969.

56. BAIRD, M.H.I., Vibration and Pulsations : Bane or Blessing?, *British Chemical Engineering*, Vol. 11., No. 1, January 1966.

57. ZARTMAN, W.N., AND CURCHILL, S.W., Heat Transfer from Acoustically Resonating Gas Flames in a Cylindrical Burner, *American Institute of Chemical Engineers Journal*, 7:588-592, 1961.

58. WEST, F.B., AND TAYLOR, A.T., The Effects of Flow Pulsations on Heat Transfer, *Chemical Engineering Progress*, 48:39-43, 1952.

59. HANBY, V.I., Basic Considerations on the Operation of a Simple Pulse Combustor, *Journal of the Institute of Fuel*, 44:595-598, 1971.

60. HANBY, V.I., Convective Heat Transfer in a Gas-Fired Pulsating Combustor, *Journal of Engineering for Power*, 91:48-52, 1969.

61. DEC, J.E., AND KELLER, J.O., Pulse Combustor Tail-Pipe Heat-Transfer Dependence on Frequency, Amplitude, and Mean Flow Rate, *Combustion and Flame*, 77:359-374, 1989.

62. ALHADDAD, A.A., AND COULMAN, G.A., Experimental and Theoretical Study of Heat Transfer in Pulse-Combustion Heaters, *Proceedings of the Symposium on Pulse Combustion Applications*, Vol. 1, Atlanta, 1982.

63. BLOMQUIST, C.A., AND CLINCH, J.M., Operational and Heat-Transfer Results from an Experimental Pulse-Combustion Burner, *Proceedings of the Symposium on Pulse Combustion Applications*, Vol. 1, Atlanta, 1982.

64. INCROPERA, F.P., AND DEWITT, D.P., *Fundamentals of Heat Transfer*, Willey, New York, 1981.

65. PRITCHARD, R., GUY J.J., AND CONNOR N.E., *Industrial Gas Utilization*, Bowker, Essex, 1978.

66. *BS 845*, Methods for Assessing Thermal Performance of Boilers for Steam, Hot Water and High Temperature Heat Transfer Fluids, BSI, 1987.

67. JONES., H.R.N., *Domestic Burners Design*, British Gas Plc., London, 1989.

68. EDELMAN, R.B., TURAN, A., AND FRANCE, D.H., Modelling of the Pulse-Combustion Process, *Proceedings of the Symposium on Pulse Combustion Technology for Heating Applications*, Argone National Laboratory, 1979.

69. CHIU, H.H., AND CROKE, E.J., Combustion Performance and Noise Emission Characteristics of Pulse Combustion, *Proceedings of the Symposium on Pulse Combustion Technology for Heating Applications*, Argone National Laboratory, 1979.

70. BARR, P.K., KELLER, J.O., BRAMLETTE, T.T, WESTBROOK, C.K., AND DEC, J.E., Pulse Combustor Modelling : Demonstration of the Importance of Characteristic Times, *Combustion and Flame*, 82:252-269, 1990.

71. STREHLOW, R.A., *Combustion Fundamentals*, McGraw-Hill, New York, 1984.

72. CERNY, V., *Spalovaci zarizeni a vymeniky tepla*, CVUT, Prague, 1988.

73. CHIGIER, N.A., Pollution Formation and Destruction in Flames-Introduction, *Progress in Energy and Combustion Science*, 1:3-15, 1976.

74. STARKMAN, E.S., Theory, Experiment, and Rationale in the Generation of Pollutants by Combustion, *12th Symposium (International) on Combustion*, The Combustion Institute, Pittsburgh, 1969.

75. BOWMAN, C.T., Kinetics of Pollutant Formation and Destruction in Combustion, *Progress in Energy and Combustion Science*, 1:33-45, 1976.

76. ZINN, B.T., Pulse Combustion : Recent Applications and Research Issues, *24th Symposium (International) on Combustion*, The Combustion Institute, Pittsburgh, 1992.

77. GRIFFITHS, J.C., CONNELLEY, S.M., AND DEREMER, R.B., Effect of Fuel Composition on Appliance Performance, *GRI 82/0037*, Gas Research Institute, Chicago, 1982.

78. *BS 5258*, Specification for Safety of Domestic Gas Appliances, BSI, 1986.

79. ZELDOVICH, Y.B., SADOVNIKOV, P.Y., AND FRANK-KAMENTSKII, D.A., *Oxidation of Nitrogen in Combustion* (M. Shelef, transl.), Academy of Sciences of USSR, Moscow-Leningrad, 1947.

80. FENIMORE, C.P., Formation of Nitric Oxide in Premixed Hydrocarbon Flames, *13th Symposium (International) on Combustion*, The Combustion Institute, Pittsburgh, 1971.

81. THOMSON, D., BROWN T.D., AND BEER, J.M., Formation of NO in a Methane-air Flame, *14th Symposium (International) on Combustion*, The Combustion Institute, Pittsburgh, 1973.

82. SAROFIM, A.F., AND POHL, J.H., *14th Symposium (International) on Combustion*, The Combustion Institute, Pittsburgh, 1973.

83. IVERACH, D., BASDEN, K.S., AND KIROV, N.Y., Formation of Nitric Oxide in Fuel-lean and Fuel-rich Flames, *14th Symposium (International) on Combustion*, The Combustion Institute, Pittsburgh, 1973.

84. MURPHY, M.J., AND PUTNAM, A.A, Control of NO_x Emissions from Residential Gas Appliances, *GRI 85/0132*, Gas Research Institute, Chicago, 1985.

85. CORLISS, J.M., PUTNAM, A.A., AND MURPHY, M.J., NO_x Emissions from Several Pulse Combustors, *Paper No. 84-JPGC-APC-2*, 105th ASME Winter Annual Meeting, New Orleans, 1984.

86. KELLER, J.O., AND HONGO, I., Pulse Combustion : The Mechanisms of NO_x Production, *Combustion and Flame*, 80:219-237, 1990.

87. HARRIS, J.A., AND LOVELACE, D.E., Combustion Characteristic of Natural Gas and Manufactured Substitutes, *Journal of the Institution of Gas Engineers*, 8:169-185, 1968.

88. JESSEN, P.F., LAMBERT, G.M.S., AND SOUTH, R., Interchangeability of Gases-the Mixture as before?, *Communications 1055*, The Institution of Gas Engineers, London, 1978.

89. DUTTON, B.C., HARRIS, J.A., AND SOUTH, R., Interchangeability of Gases-the Past, Present and Future, *Paper IGU/EI-82*, 15th World Gas Conference, Lausanne, 1982.

90. DUTTON, B.C., Interchangeability Prediction-the Framework for a New Approach, *Journal of the Institute of Fuel*, 225-229, December 1978.

91. DUTTON, B.C., A New Dimension to Gas Interchangeability, *Communications 1246*, The Institute of Gas Engineers, London, 1984.

92. KELLER, J.O., AND WESTBROOK, C.K., Response of a Pulse Combustor to Changes in Fuel Composition, *SAND 86-8631*, Sandia Report, 1986.

93. *ISO Technical Report 3313*, Measurement of Pulsating Fluid Flow in a Pipe by Means of Orifice Plates, Nozzles or Venturi Tubes, in Particular in the Case of Sinusoidal or Square Wave Intermittent Periodic-Type Fluctuation, 1974.

94. *BS 1042*, Measurement of Fluid Flow in Closed Conduits, BSI, 1981.

95. KALCIK, J., AND SYKORA, K., *Technicka termomechanica*, Academia, Prague, 1972.

96. JANEBA, B., AND KARTAK J., *Tepelne vypocty kotlu a parnich generatoru*, CVUT, Prague, 1989.

97. RAZNJEVIC, K., *Handbook of Thermodynamic Tables and Charts*, Hemisphere, Washington, 1976.

98. *CSN 385509*, Gaseous Fuels-Physical Constants, Vydavatelstvi norem, Prague, 1991.

99. *BS 5386*, Specification for Gas-burning Appliances, BSI, 1981.

100. LOMAS, C.G., *Fundamentals of Hot Wire Anemometry*, Cambridge University Press, Cambridge, 1986.

APPENDICES

APPENDIX A : Method of calculation of air/fuel ratios

Air/fuel ratios in this study were determined from the analysis of combustion products and known fuel gas compositions by a specially written computer program "Gas". The technique of calculation of air/fuel ratios and other combustion characteristics used in program "Gas" is outlined in this appendix. Appendices B, C and D show the program's flow chart, program "Gas" written in Turbo Pascal 5.5 and a specimen of a print-out from the program for Test 1. Exhaust analysis for the same test is summarised in Appendix E and the fuel gas composition is given in Appendix J.

This example describes the procedure for obtaining the air/fuel ratios from an exhaust gas analysis measured in Test 1 for the pulse combustor operating with the optimum geometry ie. TPL = 2.00 m and CCV = 110 cm^3 (see Appendix E).

Natural gas from the mains (NGA) of the following volumetric composition : 92.88 % CH_4, 2.86 % C_2H_6, 0.59 % C_3H_8, 0.23 % C_4H_{10}, 0.3 % C_5H_{12}, 2.8 % N_2 and 0.34 % CO_2 was burnt in the pulse combustor at a firing rate of 9 l min^{-1}. The products of combustion contained (dry basis) : 5.2 % O_2, 0.0287 % CO, 8.93 % CO_2 and 85.84 % N_2 (by difference). The content of NO_x in the exhaust gas was neglected in this calculation. An air relative humidity of 50 % was measured at an ambient temperature of 19 °C at the beginning of the test.

We can write the following stoichiometric equation for 1 mole of NGA burning with A moles of air :

$$\begin{aligned} &1 \text{ mole NGA} + A \text{ moles Air} \rightarrow \\ &m1 \text{ moles } CO_2 + m2 \text{ moles } N_2 + Z \text{ moles Water} . \end{aligned} \qquad (1)$$

Since moist air enters the reaction (1) the second term of the left side becomes :

$$A\,[0.21\ O_2 + 0.79\ N_2] + A\,[\chi H_2O] , \qquad (2)$$

where 0.21 O_2 + 0.79 N_2 is the composition of 1 mole of dry air and χ represents the moist air coefficient which expresses the water content accompanying 1 mole of

dry air. According to Cerny [72] χ is a function of relative air humidity φ, atmospheric pressure p_a and pressure of saturated water vapour p'' at ambient temperature ie.

$$\chi = \frac{\varphi}{100} \frac{p''}{p_a - \frac{\varphi}{100} p''} . \qquad (3)$$

Upon substituting 50 % for relative humidity, 100000 Pa for atmospheric pressure (assumption) and 2196 Pa for p'' [96] in the above relationship we can rewrite equation (2) as follows :

$$A\ [0.21\ O_2 + 0.79\ N_2 + 0.0111\ H_2O] . \qquad (4)$$

Consequently, the stoichiometric equation (1) can be expressed in full as shown below :

$$\begin{aligned} &[\ 0.9288\ CH_4 + 0.0286\ C_2H_6 + 0.0059\ C_3H_8 + 0.0023\ C_4H_{10} + \\ &0.003\ C_5H_{12} + 0.0034\ CO_2 + 0.028\ N_2\ ] + A\ [\ 0.21\ O_2 + \\ &0.79\ N_2 + 0.0111\ H_2O\ ] \rightarrow m1\ CO_2 + m2\ N_2 + Z\ H_2O\ . \end{aligned} \qquad (5)$$

The unknowns m1, A, Z and m2 are calculated from carbon, oxygen, hydrogen and nitrogen balances and are 1.0313, 9.6483, 2.1036 and 7.6507 respectively. Thus the stoichiometric air/fuel ratio on dry basis equals value of A which is 9.6483 and stoichiometric air/fuel ratio on wet basis being defined as $A(1 + \chi)$ is 9.7554.

In real situation, however, the perfect combustion, outlined above, is not possible and the stoichiometric equation (1) has to be changed as follows :

$$\begin{aligned} &1\ \text{mole NGA} + A\ \text{moles Air} \rightarrow \\ &V\ \text{moles Dry Exhaust Gas} + Z\ \text{moles Water} . \end{aligned} \qquad (6)$$

After substituting the exhaust gas analysis in the products side of the above equation we obtain a reaction equation such as :

$$[\ 0.9288\ CH_4 + 0.0286\ C_2H_6 + 0.0059\ C_3H_8 + 0.0023\ C_4H_{10} + 0.003\ C_5H_{12} + 0.0034\ CO_2 + 0.028\ N_2\ ] + A\ [\ 0.21\ O_2 + 0.79\ N_2 + 0.0111\ H_2O\ ] \rightarrow V\ [\ 0.052\ O_2 + 0.000287\ CO + 0.0893\ CO_2 + 0.8584\ N_2\ ] + Z\ H_2O\ . \quad (7)$$

The unknowns V, A and Z are calculated from carbon, oxygen and hydrogen balances and are 11.5117, 12.491 and 2.1352 respectively. The value of A, determined from a nitrogen balance, is 12.473. It should be noted that the values of the air/fuel ratio by the oxygen (A/F_O) and nitrogen (A/F_N) balances do not agree. This reflects inaccuracies in the measurement of the exhaust gas analysis*. As a result the actual air/fuel ratio on a dry bases is obtained as an average of A/F_O + A/F_N which equals 12.482. In the similar way, the actual averaged air/fuel ratio on a wet basis is 12.6206 when the air/fuel ratios by the oxygen and nitrogen balances are defined as $A/F_O(1 + \chi)$ and $A/F_N(1 + \chi)$ respectively.

In the final step, the equation presented below gives a percentage excess air value of 29.37 % for this worked example.

$$Percentage\ excess\ air = \frac{A/F_{actual} - A/F_{stoichiometric}}{A/F_{stoichiometric}} 100\ . \quad (8)$$

* CO_2 content was calculated by the gas analyzer from O_2 concentration in the exhaust gas.

APPENDIX B : Flow chart for program "Gas"

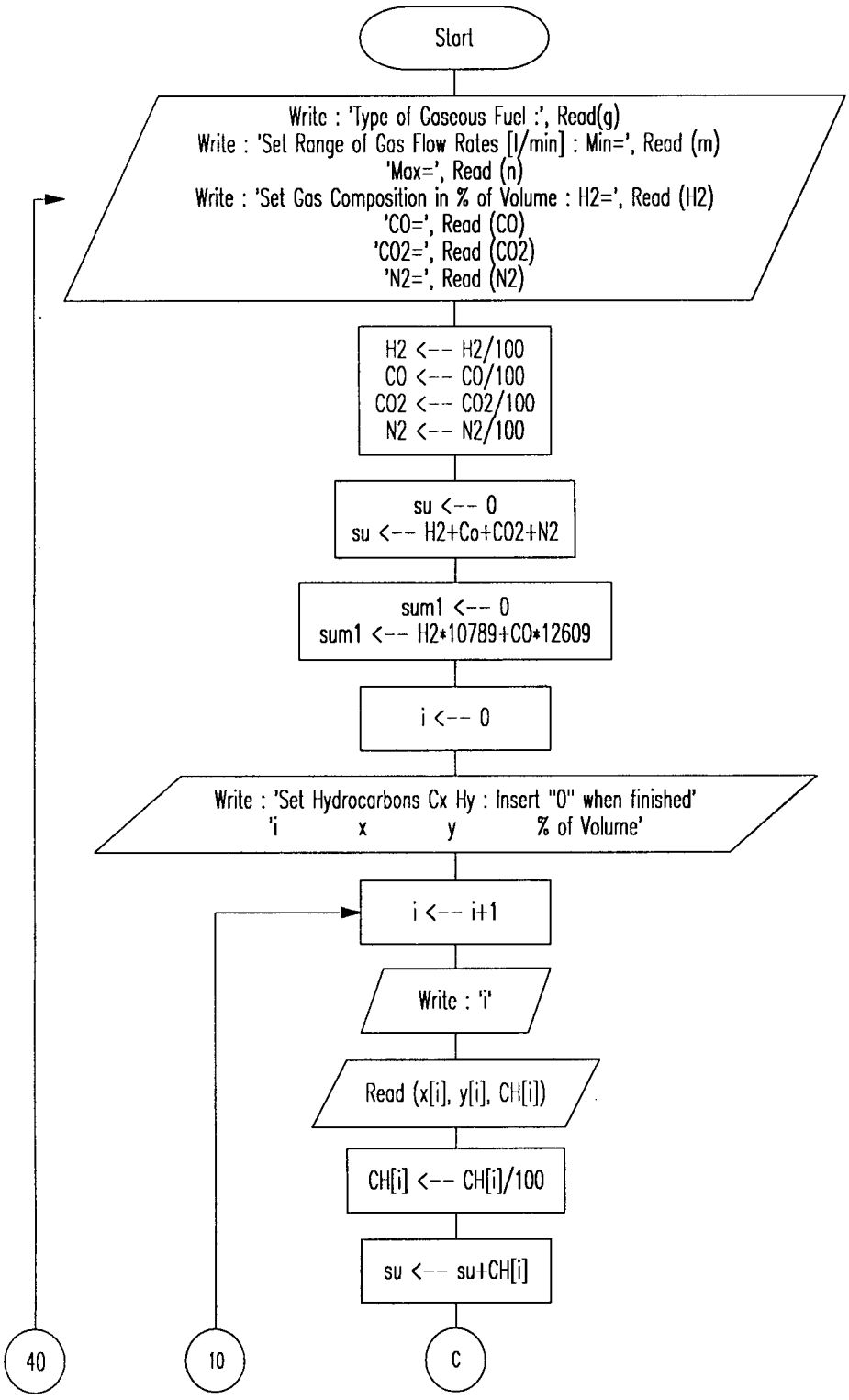

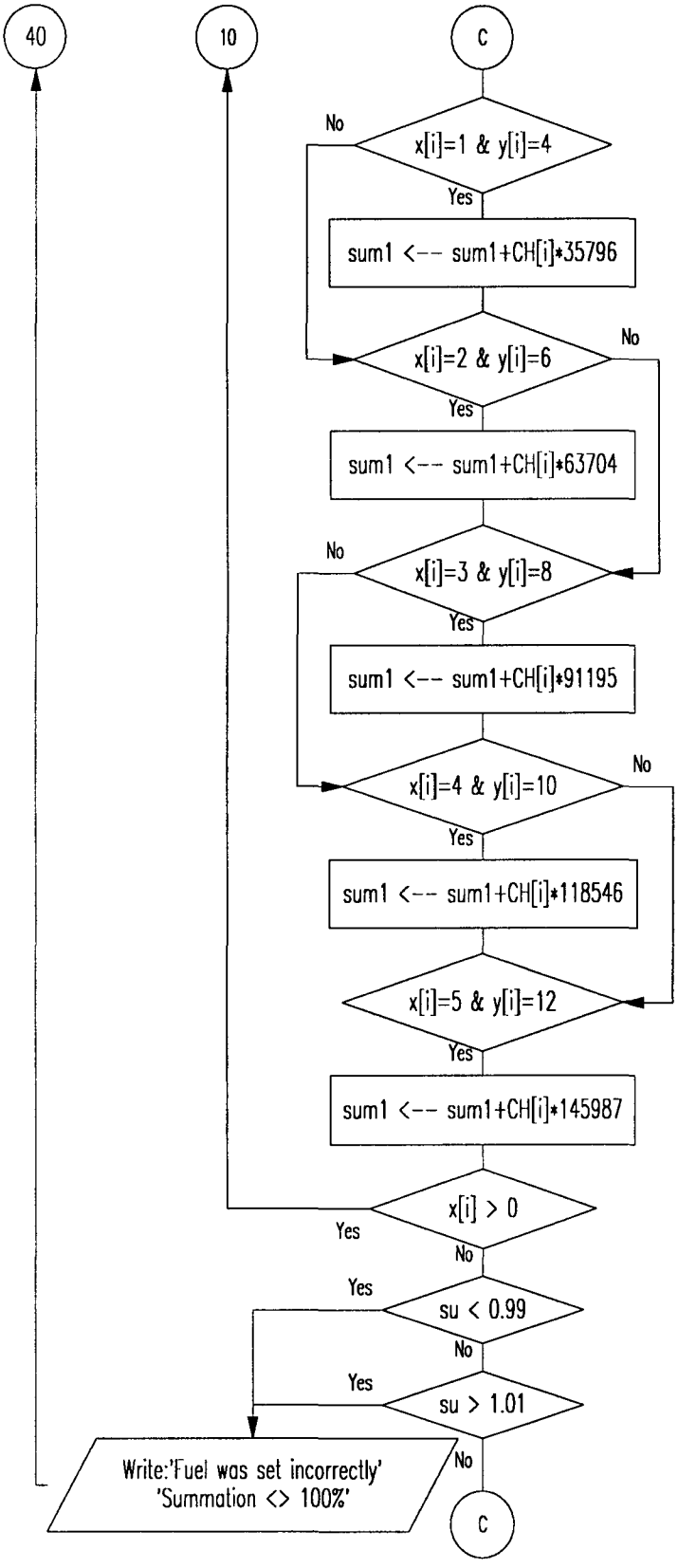
40
10
C
No
x[i]=1 & y[i]=4
Yes
sum1 <-- sum1+CH[i]*35796
No
x[i]=2 & y[i]=6
Yes
sum1 <-- sum1+CH[i]*63704
No
x[i]=3 & y[i]=8
Yes
sum1 <-- sum1+CH[i]*91195
No
x[i]=4 & y[i]=10
Yes
sum1 <-- sum1+CH[i]*118546
x[i]=5 & y[i]=12
Yes
sum1 <-- sum1+CH[i]*145987
x[i] > 0
Yes
No
Yes
su < 0.99
No
Yes
su > 1.01
Write:'Fuel was set incorrectly'
'Summation <> 100%'
No
C

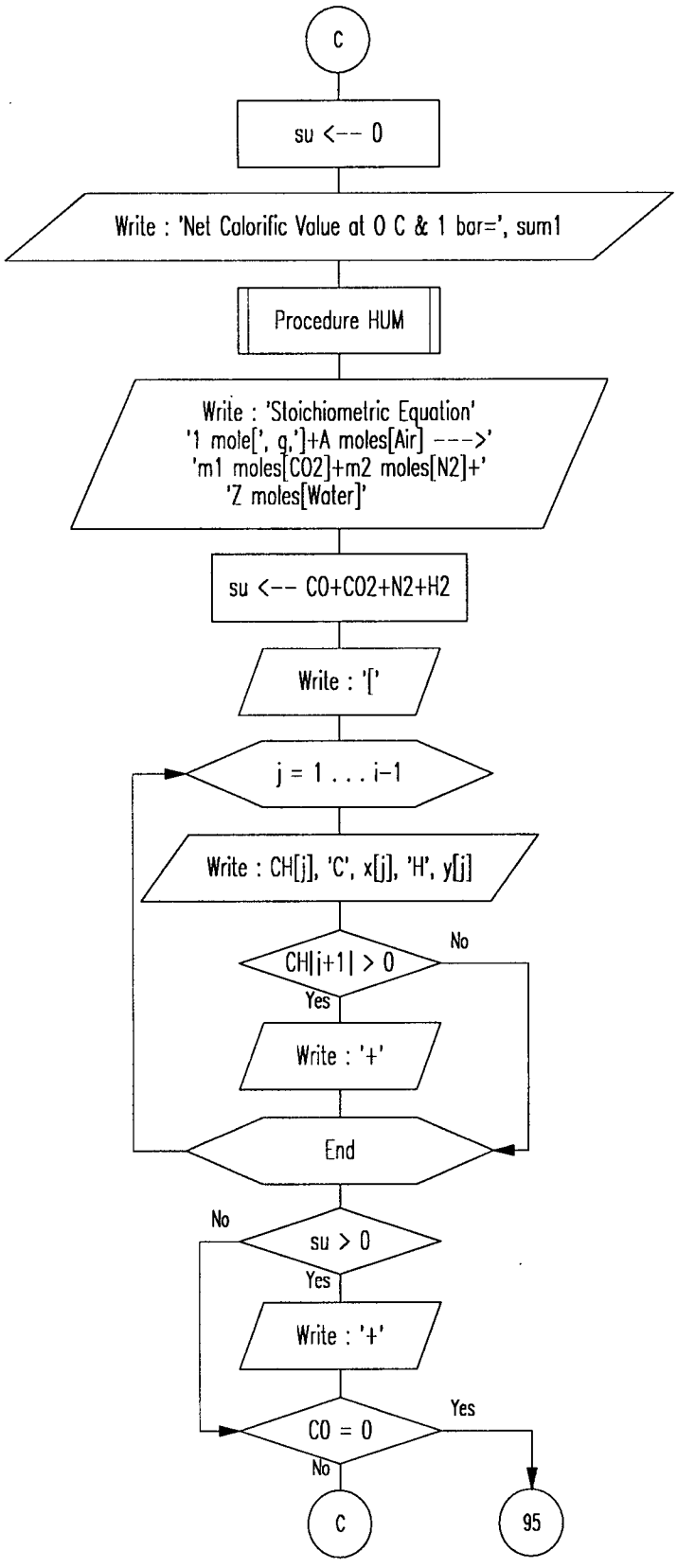
C
su <-- 0
Write : 'Net Colorific Value at 0 C & 1 bar=', sum1
Procedure HUM
Write : 'Stoichiometric Equation'
'1 mole[', q,']+A moles[Air] --->'
'm1 moles[CO2]+m2 moles[N2]+'
'Z moles[Water]'
su <-- CO+CO2+N2+H2
Write : '['
j = 1 . . . i-1
Write : CH[j], 'C', x[j], 'H', y[j]
CH[j+1] > 0
No
Yes
Write : '+'
End
No
su > 0
Yes
Write : '+'
CO = 0
Yes
No
C
95

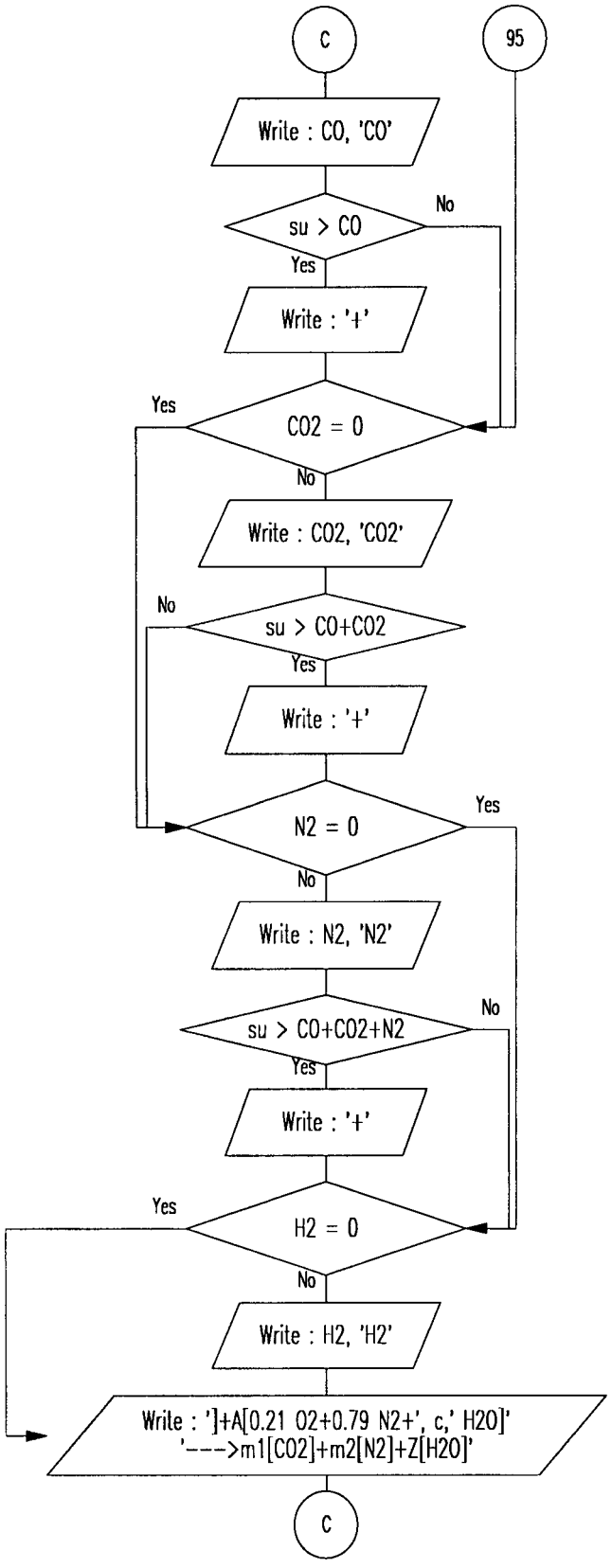
C
95
Write : CO, 'CO'
su > CO
No
Yes
Write : '+'
Yes
CO2 = 0
No
Write : CO2, 'CO2'
No
su > CO+CO2
Yes
Write : '+'
N2 = 0
Yes
No
Write : N2, 'N2'
su > CO+CO2+N2
No
Yes
Write : '+'
Yes
H2 = 0
No
Write : H2, 'H2'
Write : ']+A[0.21 O2+0.79 N2+', c,' H2O]'
'--->m1[CO2]+m2[N2]+Z[H2O]'
C

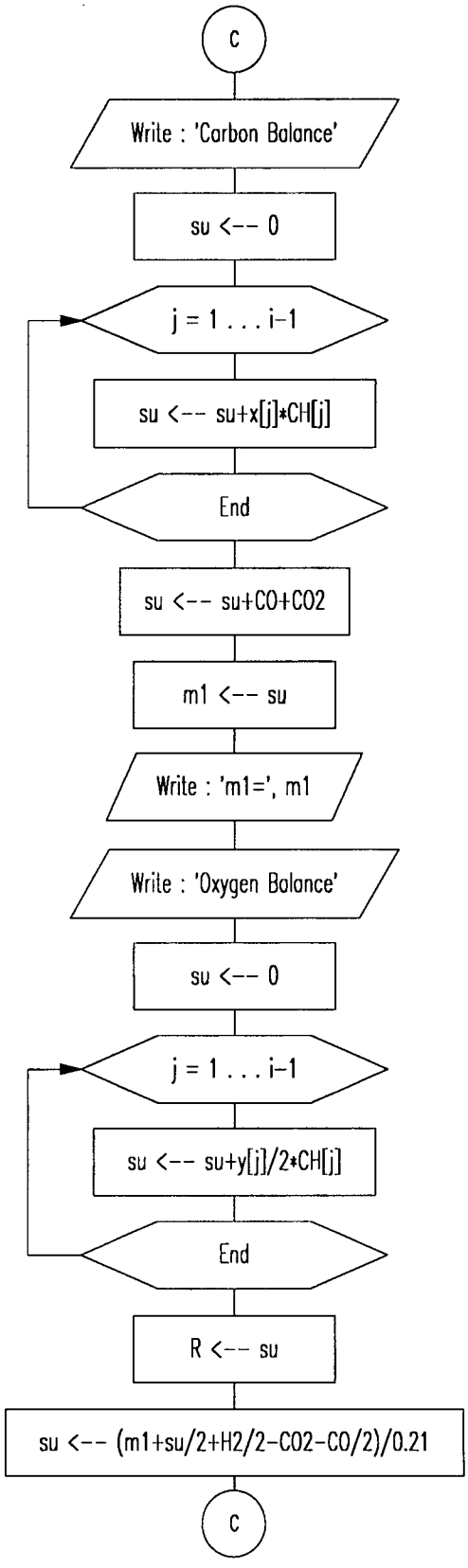
C
Write : 'Carbon Balance'
su <-- 0
j = 1 . . . i-1
su <-- su+x[j]*CH[j]
End
su <-- su+CO+CO2
m1 <-- su
Write : 'm1=', m1
Write : 'Oxygen Balance'
su <-- 0
j = 1 . . . i-1
su <-- su+y[j]/2*CH[j]
End
R <-- su
su <-- (m1+su/2+H2/2-CO2-CO/2)/0.21
C

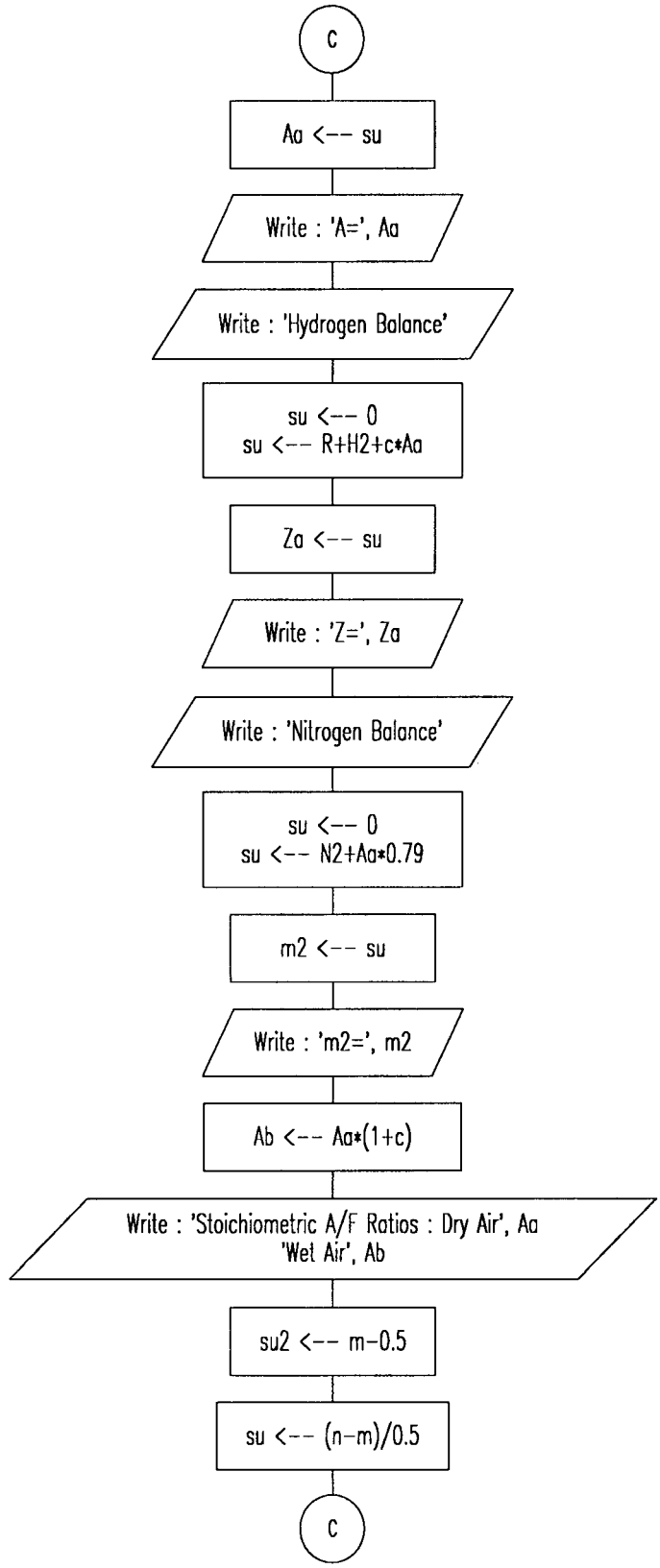
c
Aa <-- su
Write : 'A=', Aa
Write : 'Hydrogen Balance'
su <-- 0
su <-- R+H2+c*Aa
Za <-- su
Write : 'Z=', Za
Write : 'Nitrogen Balance'
su <-- 0
su <-- N2+Aa*0.79
m2 <-- su
Write : 'm2=', m2
Ab <-- Aa*(1+c)
Write : 'Stoichiometric A/F Ratios : Dry Air', Aa
'Wet Air', Ab
su2 <-- m-0.5
su <-- (n-m)/0.5
c

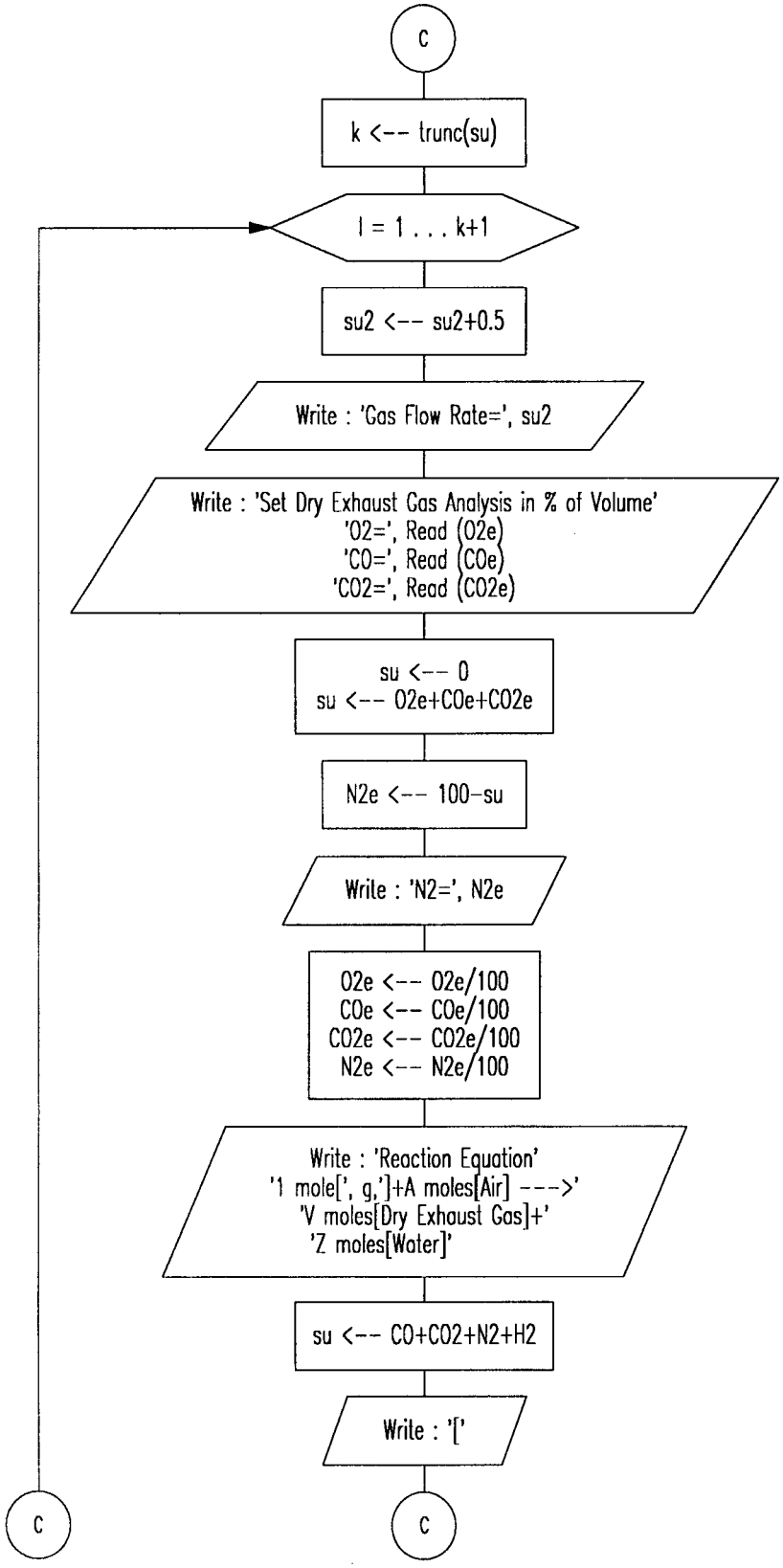
C
k <-- trunc(su)
I = 1 . . . k+1
su2 <-- su2+0.5
Write : 'Gas Flow Rate=', su2
Write : 'Set Dry Exhaust Gas Analysis in % of Volume'
'O2=', Read (O2e)
'CO=', Read (COe)
'CO2=', Read (CO2e)
su <-- 0
su <-- O2e+COe+CO2e
N2e <-- 100-su
Write : 'N2=', N2e
O2e <-- O2e/100
COe <-- COe/100
CO2e <-- CO2e/100
N2e <-- N2e/100
Write : 'Reaction Equation'
'1 mole[', g,']+A moles[Air] --->'
'V moles[Dry Exhaust Gas]+'
'Z moles[Water]'
su <-- CO+CO2+N2+H2
Write : '['
C
C

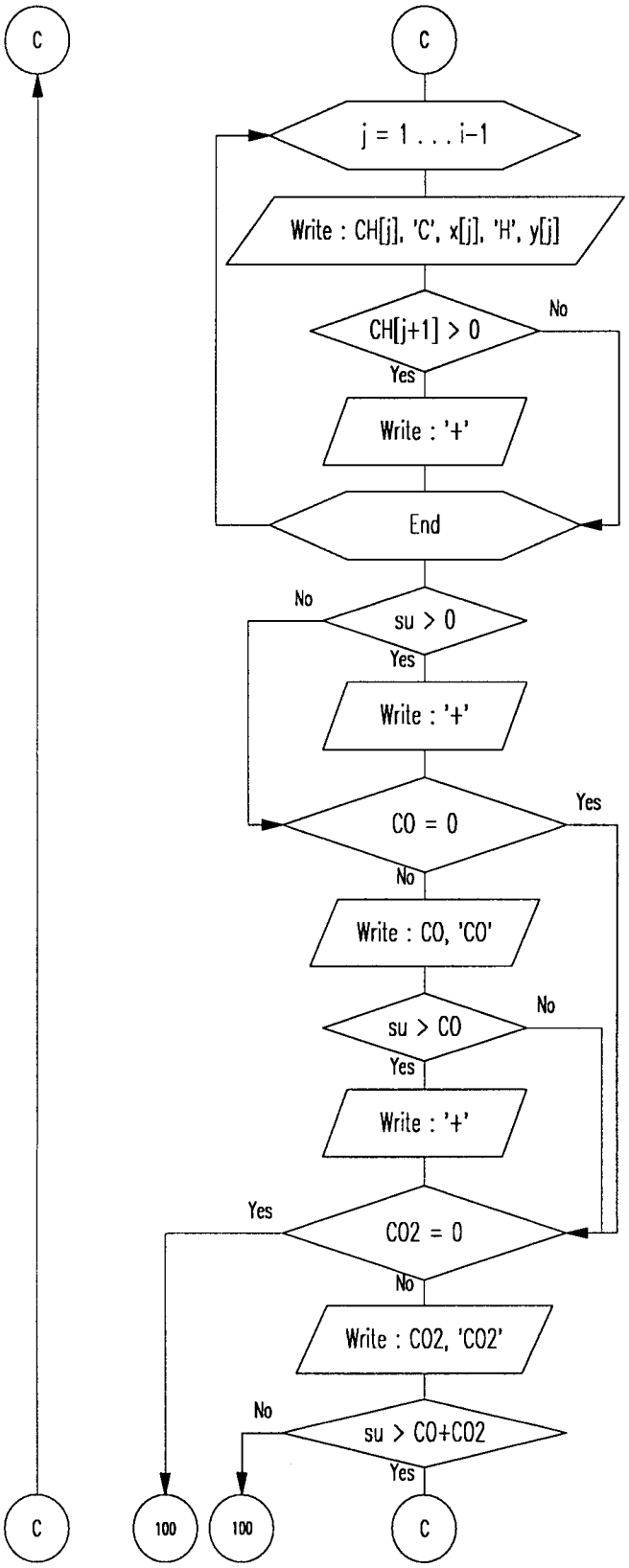
C
C
j = 1 . . . i-1
Write : CH[j], 'C', x[j], 'H', y[j]
CH[j+1] > 0
No
Yes
Write : '+'
End
No
su > 0
Yes
Write : '+'
CO = 0
Yes
No
Write : CO, 'CO'
su > CO
No
Yes
Write : '+'
CO2 = 0
Yes
No
Write : CO2, 'CO2'
su > CO+CO2
No
Yes
C
100
100
C

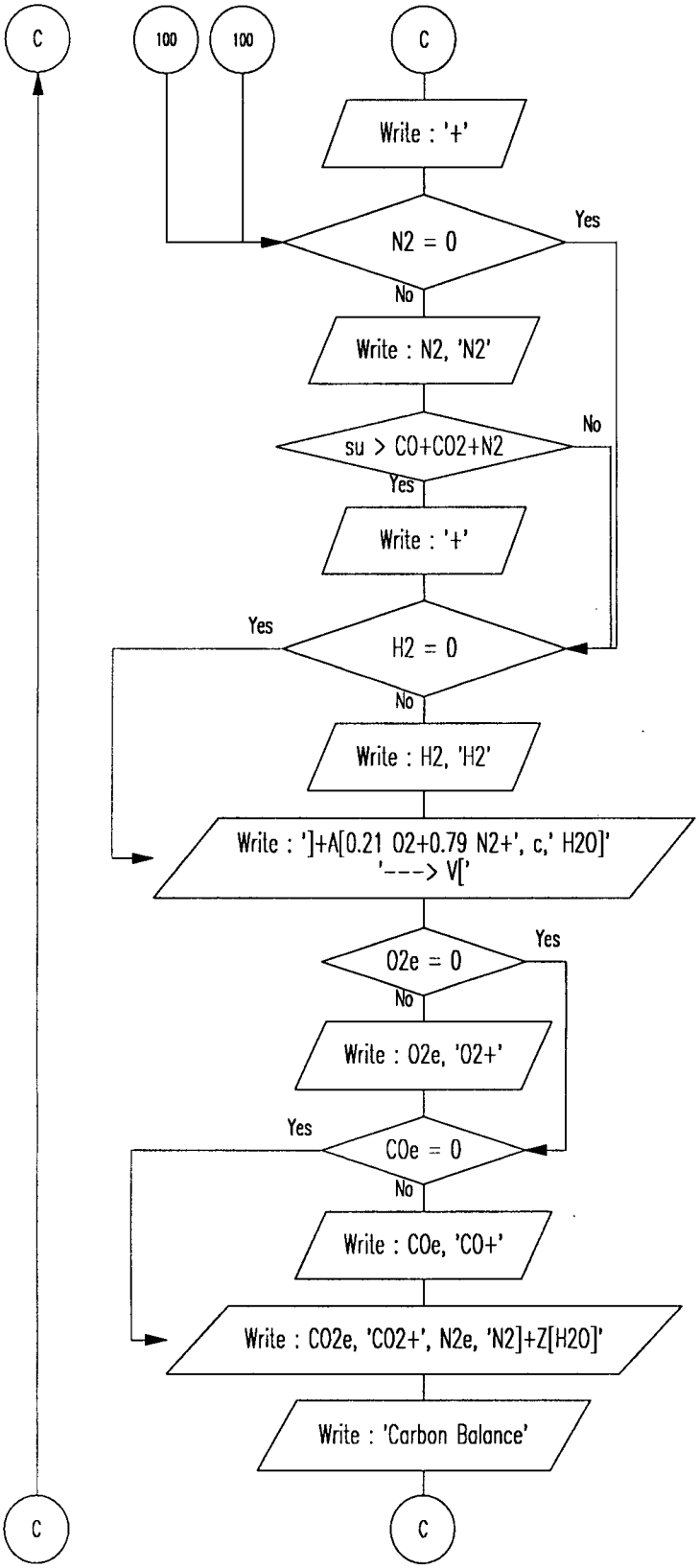
C
100
100
C
Write : '+'
N2 = 0
Yes
No
Write : N2, 'N2'
su > CO+CO2+N2
No
Yes
Write : '+'
H2 = 0
Yes
No
Write : H2, 'H2'
Write : ']+A[0.21 O2+0.79 N2+', c,' H2O]'
'---> V['
O2e = 0
Yes
No
Write : O2e, 'O2+'
COe = 0
Yes
No
Write : COe, 'CO+'
Write : CO2e, 'CO2+', N2e, 'N2]+Z[H2O]'
Write : 'Carbon Balance'
C
C

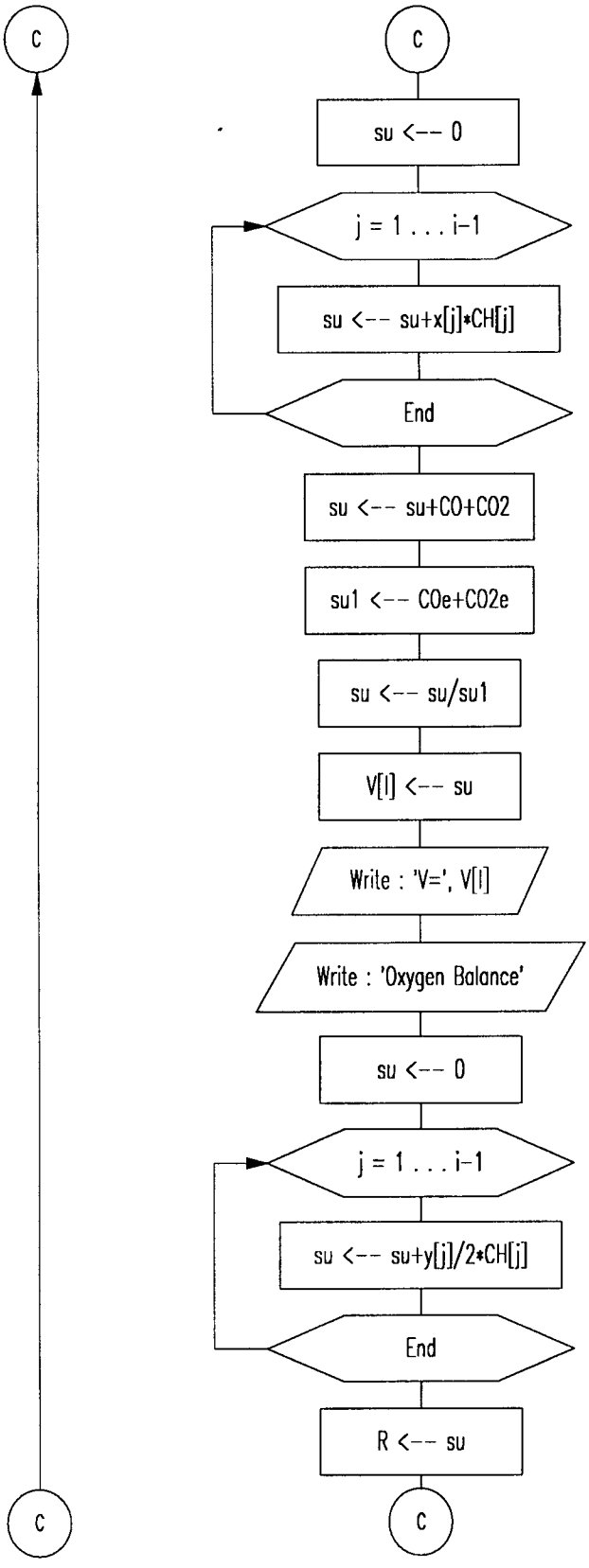
C
C
su <-- 0
j = 1 . . . i-1
su <-- su+x[j]*CH[j]
End
su <-- su+CO+CO2
su1 <-- COe+CO2e
su <-- su/su1
V[I] <-- su
Write : 'V=', V[I]
Write : 'Oxygen Balance'
su <-- 0
j = 1 . . . i-1
su <-- su+y[j]/2*CH[j]
End
R <-- su
C
C

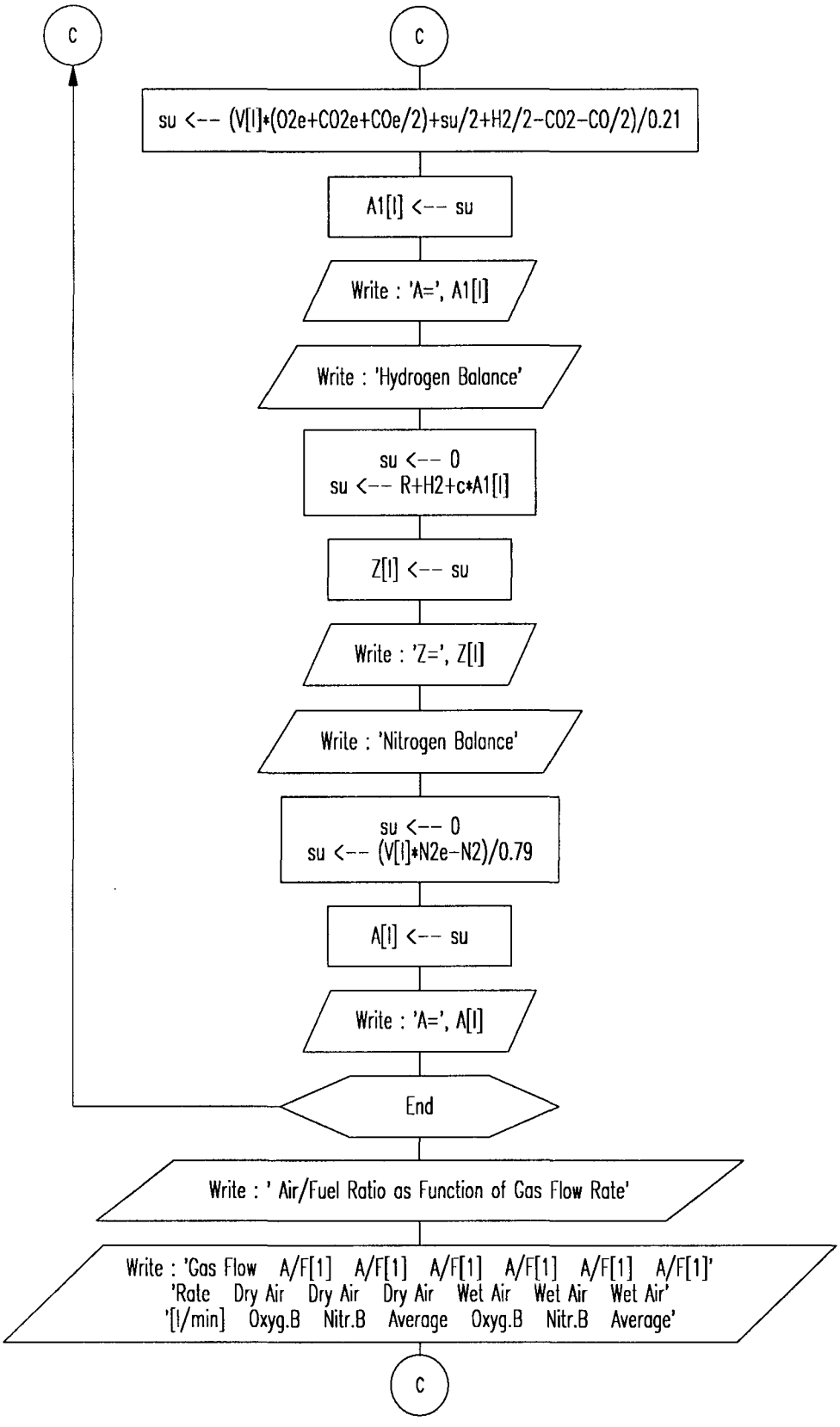
C
C
su <-- (V[I]*(O2e+CO2e+COe/2)+su/2+H2/2-CO2-CO/2)/0.21
A1[I] <-- su
Write : 'A=', A1[I]
Write : 'Hydrogen Balance'
su <-- 0
su <-- R+H2+c*A1[I]
Z[I] <-- su
Write : 'Z=', Z[I]
Write : 'Nitrogen Balance'
su <-- 0
su <-- (V[I]*N2e-N2)/0.79
A[I] <-- su
Write : 'A=', A[I]
End
Write : ' Air/Fuel Ratio as Function of Gas Flow Rate'
Write : 'Gas Flow A/F[1] A/F[1] A/F[1] A/F[1] A/F[1] A/F[1]'
'Rate Dry Air Dry Air Dry Air Wet Air Wet Air Wet Air'
'[l/min] Oxyg.B Nitr.B Average Oxyg.B Nitr.B Average'
C

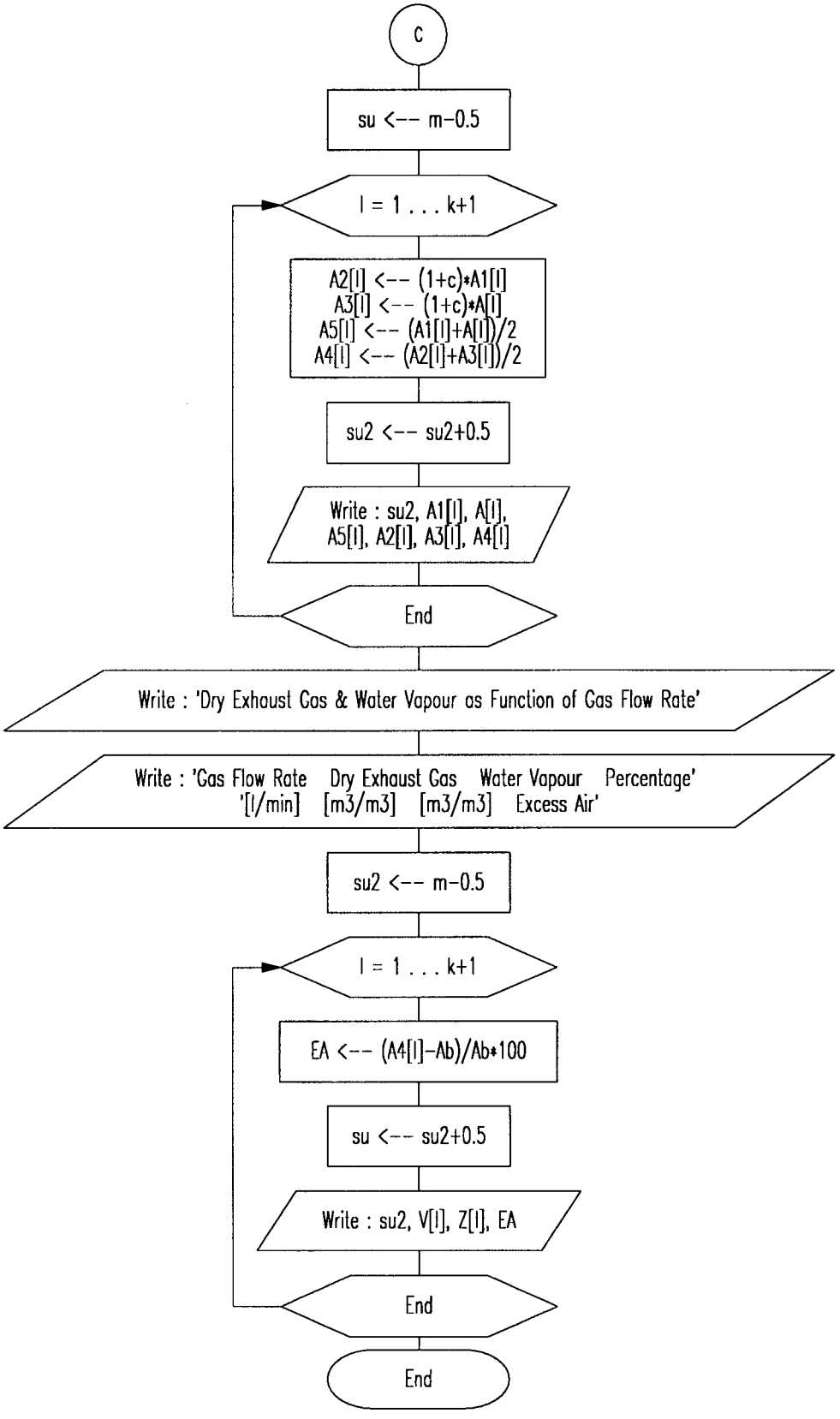
c
su <-- m-0.5
I = 1 . . . k+1
A2[I] <-- (1+c)*A1[I]
A3[I] <-- (1+c)*A[I]
A5[I] <-- (A1[I]+A[I])/2
A4[I] <-- (A2[I]+A3[I])/2
su2 <-- su2+0.5
Write : su2, A1[I], A[I],
A5[I], A2[I], A3[I], A4[I]
End
Write : 'Dry Exhaust Gas & Water Vapour as Function of Gas Flow Rate'
Write : 'Gas Flow Rate Dry Exhaust Gas Water Vapour Percentage'
'[l/min] [m3/m3] [m3/m3] Excess Air'
su2 <-- m-0.5
I = 1 . . . k+1
EA <-- (A4[I]-Ab)/Ab*100
su <-- su2+0.5
Write : su2, V[I], Z[I], EA
End
End

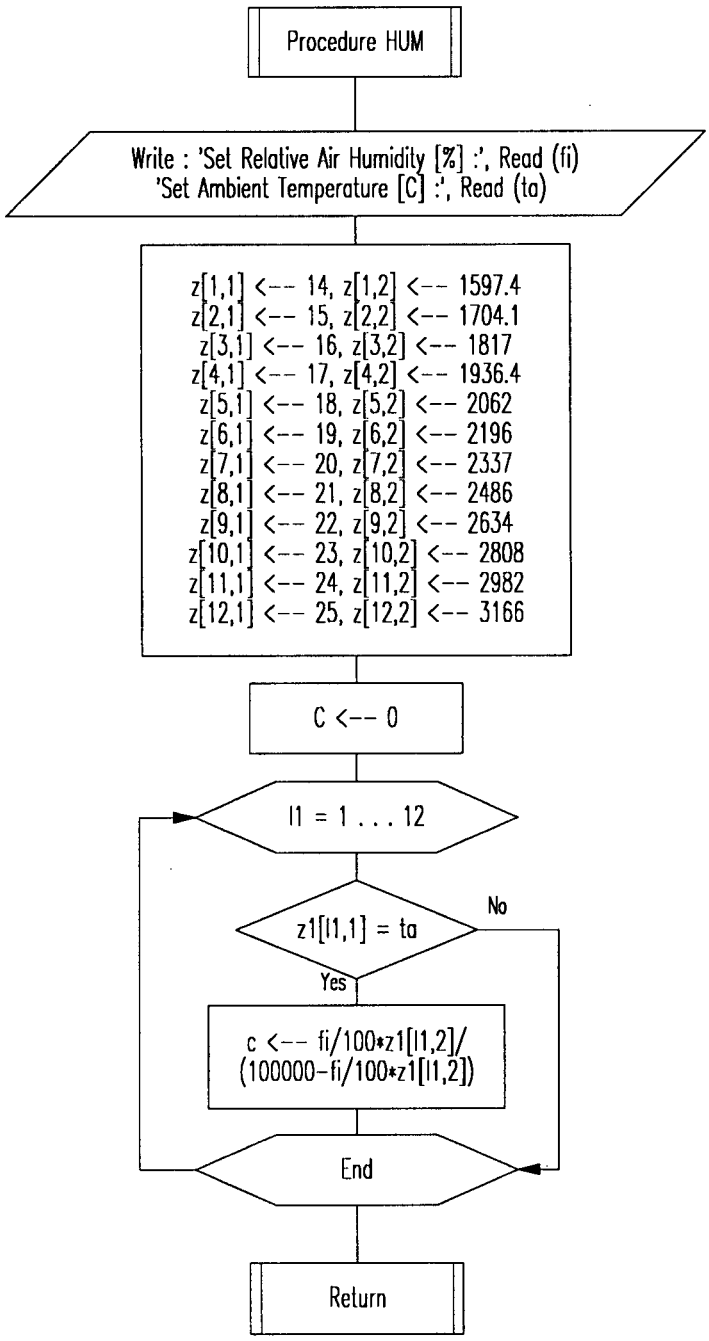
Procedure HUM
Write : 'Set Relative Air Humidity [%] :', Read (fi)
'Set Ambient Temperature [C] :', Read (ta)
z[1,1] <-- 14, z[1,2] <-- 1597.4
z[2,1] <-- 15, z[2,2] <-- 1704.1
z[3,1] <-- 16, z[3,2] <-- 1817
z[4,1] <-- 17, z[4,2] <-- 1936.4
z[5,1] <-- 18, z[5,2] <-- 2062
z[6,1] <-- 19, z[6,2] <-- 2196
z[7,1] <-- 20, z[7,2] <-- 2337
z[8,1] <-- 21, z[8,2] <-- 2486
z[9,1] <-- 22, z[9,2] <-- 2634
z[10,1] <-- 23, z[10,2] <-- 2808
z[11,1] <-- 24, z[11,2] <-- 2982
z[12,1] <-- 25, z[12,2] <-- 3166
C <-- 0
I1 = 1 . . . 12
z1[I1,1] = ta
No
Yes
c <-- fi/100*z1[I1,2]/
(100000-fi/100*z1[I1,2])
End
Return

APPENDIX C : Computer program "Gas"

```
Program Gas;
uses CRT;
Label 5,10,20,30,40,80,90,95,100,105,110,115,120,125,130,140;
Var
  H2,CO,CO2,N2,O2,O2e,COe,CO2e,N2e,su,su1,su2,sum1,m,n,R:real;
  ta,m1,m2,Aa,Za,EA,Ab,c:real;
  i,j,k,l,i1,j1:integer;
  O:boolean;
  P:char;
  g:string[15];
  x:array [1..10] of integer;
  y:array [1..10] of integer;
  CH:array [1..10] of real;
  V:array [1..10] of real;
  A:array [1..10] of real;
  A1:array [1..10] of real;
  A2:array [1..10] of real;
  A3:array [1..10] of real;
  A4:array [1..10] of real;
  A5:array [1..10] of real;
  Z:array [1..10] of real;
Procedure Hum;
Var
  fi,p:real;
  z1:array[1..12,1..2] of real;
  l1:integer;
Begin
 Write ('Set Relative Air Humidity [%] : '); Readln (fi);
 Write ('Set Ambient Temperature  [',char(248),'C] : '); Readln (ta);
 z1[1,1]:=14; z1[1,2]:=1597.4; z1[2,1]:=15; z1[2,2]:=1704.1;
 z1[3,1]:=16; z1[3,2]:=1817; z1[4,1]:=17; z1[4,2]:=1936.4;
 z1[5,1]:=18; z1[5,2]:=2062; z1[6,1]:=19; z1[6,2]:=2196;
 z1[7,1]:=20; z1[7,2]:=2337; z1[8,1]:=21; z1[8,2]:=2486;
 z1[9,1]:=22; z1[9,2]:=2643; z1[10,1]:=23; z1[10,2]:=2808;
 z1[11,1]:=24; z1[11,2]:=2982; z1[12,1]:=25; z1[12,2]:=3166;
 c:=0;
 for l1:=1 to 12 do
  Begin
   if z1[l1,1]=ta then c:=fi/100*z1[l1,2]/(100000-fi/100*z1[l1,2])
else;
  End;
End;
Begin
 ClrScr;
 su:=0;
 Write ('Type of Gaseous Fuel          :  '); ReadLn (g);
 WriteLn;
 Write ('Set Range of Gas Flow Rates [l/min] : Min = '); Readln (m);
 Write ('                                      Max = '); Readln (n);
 Writeln;
 40: Write ('Set Gas Composition in % of Volume  :    H2   = ');
 ReadLn (H2); H2:=H2/100;
 Write ('                                          CO   = ');
 ReadLn (CO); CO:=CO/100;
 Write ('                                          CO2  = ');
 ReadLn (CO2); CO2:=CO2/100;
 Write ('                                          N2   = ');
```

```
Readln (N2); N2:=N2/100;
Writeln;
su:=0;
su:=H2+CO+CO2+N2;
sum1:=0;
sum1:=H2*10789+CO*12609;
i:=0;
Writeln ('Set Hydrocarbons Cx Hy  :  Insert "0" when finished');
Writeln ('    i          x          y        % of Volume');
Writeln ('-------------------------------------------------');
10: i:=i+1;
Write ('    ',i,'          '); Read (x[i]); GotoXY (27,13+i);
Read(y[i]); GotoXY(36,13+i); Readln (CH[i]);CH[i]:=CH[i]/100;
su:=su+CH[i];
if (x[i]=1) and (y[i]=4) then sum1:=sum1+CH[i]*35796;
if (x[i]=2) and (y[i]=6) then sum1:=sum1+CH[i]*63704;
if (x[i]=3) and (y[i]=8) then sum1:=sum1+CH[i]*91195;
if (x[i]=4) and (y[i]=10) then sum1:=sum1+CH[i]*118546;
if (x[i]=5) and (y[i]=12) then sum1:=sum1+CH[i]*145987;
if x[i]>0 then goto 10;
if su<0.99 then goto 20;
if su>1.01 then goto 20 else goto 30;
20: ClrScr; Writeln ('Fuel was set incorrectly.');
WriteLn ('Summation of constituents = ',su*100:6:2,'% <> 100%.');
Writeln; Writeln; Writeln; goto 40;
30: su:=0;
Writeln;
Write ('*** Net Calorific Value at 0',char(248));
Writeln ('C & 1bar  =  ',sum1:5:0,' KJ/m3 ***');
Writeln;
Begin
 Hum;
End;
i1:=WhereX ; j1:=WhereY;
GotoXY(60,24); TextColor(10); Write ('Type "c" to continue.');
GotoXY(i1,j1);
TextColor(7);
 Begin
  Repeat
  Until Readkey=Char(99);
  ClrScr;
 End;
Writeln ('Stoichiometric Equation');
Writeln ('************************');
Writeln;
Writeln ('1 mole [ ',g,' ] + A moles [ Air ] ------->');
Writeln ('m1 moles [ CO2 ] + m2 moles [ N2] + Z moles [ Water ]');
Writeln;
su:=CO+CO2+N2+H2;
Write ('[ ');
For j:=1 to i-1 do
 Begin
  Write (CH[j]:6:4,' C',x[j]:1,'H',y[j]:1);
  if CH[j+1]>0 then Write (' + ');
 End;
if su>0 then Write (' + ');
if CO=0 then goto 95;
Write (CO:5:4,' CO'); if su>CO then Write (' + ') else ;
95: if CO2=0 then goto 105;
Write (CO2:5:4,' CO2'); if su>CO+CO2 then Write (' + ') else ;
105: if N2=0 then goto 115;
```

```
Write (N2:5:4,' N2'); if su>CO+CO2+N2 then Write (' + ') else ;
115: if H2=0 then goto 125;
Write (H2:5:4,' H2');
125: Writeln (' ] + A [ 0.21 O2 + 0.79 N2 + ',c:2:4,' H2O ]
------->');
Writeln ('m1 [ CO2 ] + m2 [ N2 ] + Z [ H2O ]');
Writeln;
Writeln ('*** Carbon Balance ***');
Writeln;
su:=0;
For j:=1 to i-1 do
 Begin
  su:=su+x[j]*CH[j];
 End;
su:=su+CO+CO2;
m1:=su;
Writeln ('     m1 = ',m1:6:4);
Writeln;
Writeln ('*** Oxygen Balance ***');
Writeln;
su:=0;
For j:=1 to i-1 do
 Begin
  su:=su+y[j]/2*CH[j];
 End;
R:=su;
su:=(m1+su/2+H2/2-CO2-CO/2)/0.21;
Aa:=su;
Writeln ('     A = ',Aa:6:4);
Writeln;
Writeln ('*** Hydrogen Balance ***');
Writeln;
su:=0;
su:=R+H2+c*Aa;
Za:=su;
Writeln ('     Z = ',Za:6:4);
i1:=WhereX ; j1:=WhereY;
Gotoxy(60,24); TextColor(10); Write ('Type "c" to continue.');
Gotoxy(i1,j1);
TextColor(7);
 Begin
  Repeat
  Until Readkey=Char(99);
  ClrScr;
 End;
Writeln ('*** Nitrogen Balance ***');
Writeln;
su:=0;
su:=N2+Aa*0.79;
m2:=su;
Writeln ('     m2 = ',m2:6:4);
Writeln;
Ab:=Aa*(1+c);
Write ('*** Stoichiometric A/F Ratios :   Dry Air     ');
Writeln ('|     Wet Air ***');
Write ('                                    ',Aa:6:4);
Writeln ('      |     ',Ab:7:4);
Writeln; Writeln;
su2:=m-0.5;
su:=(n-m)/0.5;
k:=trunc(su);
```

```
For l:=1 to k+1 do
 Begin
  su2:=su2+0.5;
  Writeln ('*** Gas Flow Rate = ',su2:3:1,' ***');
  Write ('============================');
  if su2>9.5 then Writeln ('=') else Writeln;
  Writeln;
  Write ('Set Dry Exhaust Gas Analysis in % of Volume : O2  = ');
  Readln (O2e);
  Write ('                                              CO  = ');
  Readln (COe);
  Write ('                                              CO2 = ');
  Readln (CO2e);
  su:=0;
  su:=O2e+COe+CO2e;
  N2e:=100-su;
  Write ('                                              N2  = ');
  Writeln (N2e:6:3);
  O2e:=O2e/100;
  COe:=COe/100;
  CO2e:=CO2e/100;
  N2e:=N2e/100;
  i1:=WhereX ; j1:=WhereY;
  Gotoxy(60,24); TextColor(10); Write ('Type "c" to continue.');
  Gotoxy(i1,j1);
  TextColor(7);
   Begin
    Repeat
    Until Readkey=Char(99);
    ClrScr;
   End;
  Writeln ('Reaction Equation');
  Writeln ('******************');
  Writeln;
  Writeln ('1 mole [ ',g,' ] + A moles [ Air ] ------->');
  Writeln ('V moles [ Dry Exhaust Gas ] + Z moles [ Water ]');
  Writeln;
  su:=CO+CO2+N2+H2;
  Write ('[ ');
  For j:=1 to i-1 do
   Begin
    Write (CH[j]:6:4,' C',x[j]:1,'H',y[j]:1);
    if CH[j+1]>0 then Write (' + ');
   End;
  if su>0 then Write (' + ');
  if CO=0 then goto 90;
  Write (CO:5:4,' CO'); if su>CO then Write (' + ') else ;
  90: if CO2=0 then goto 100;
  Write (CO2:5:4,' CO2'); if su>CO+CO2 then Write (' + ') else ;
  100: if N2=0 then goto 110;
  Write (N2:5:4,' N2'); if su>CO+CO2+N2 then Write (' + ') else ;
  110: if H2=0 then goto 120;
  Write (H2:5:4,' H2');
  120: Writeln (' ] + A [ 0.21 O2 + 0.79 N2 + ',c:2:4,' H2O ]
  ------->');
  if O2e=0 then goto 130;
  Write ('V [ ',O2e:5:4,' O2 + ');
  130: if COe=0 then goto 140;
  Write (COe:7:6,' CO + ');
  140: Writeln (CO2e:5:4,' CO2 + ',N2e:8:6,' N2 ] + Z [ H2O ]');
  Writeln;
```

```
   Writeln ('*** Carbon Balance ***');
   Writeln;
   su:=0;
   For j:=1 to i-1 do
    Begin
     su:=su+x[j]*CH[j];
    End;
   su:=su+CO+CO2;
   su1:=COe+CO2e;
   su:=su/su1;
   V[1]:=su;
   Writeln ('     V = ',V[1]:6:4);
   Writeln;
   Writeln ('*** Oxygen Balance ***');
   Writeln;
   su:=0;
   For j:=1 to i-1 do
    Begin
     su:=su+y[j]/2*CH[j];
    End;
   R:=su;
   su:=(V[1]*(O2e+CO2e+COe/2)+su/2+H2/2-CO2-CO/2)/0.21;
   A1[1]:=su;
   Writeln ('     A = ',A1[1]:6:4);
   Writeln;
   Writeln ('*** Hydrogen Balance ***');
   Writeln;
   su:=0;
   su:=R+H2+c*A1[1];
   Z[1]:=su;
   Writeln ('     Z = ',Z[1]:6:4);
   i1:=WhereX ; j1:=WhereY;
   Gotoxy(60,24); TextColor(10); Write ('Type "c" to continue.');
   Gotoxy(i1,j1);
   TextColor(7);
    Begin
     Repeat
     Until Readkey=Char(99);
     ClrScr;
    End;
   Writeln ('*** Nitrogen Balance ***');
   Writeln;
   su:=0;
   su:=(V[1]*N2e-N2)/0.79;
   A[1]:=su;
   Writeln ('     A = ',A[1]:6:4);
   i1:=WhereX ; j1:=WhereY;
   Gotoxy(60,24); TextColor(10); Write ('Type "c" to continue.');
   Gotoxy(i1,j1);
   TextColor(7);
    Begin
     Repeat
     Until Readkey=Char(99);
     ClrScr;
    End;
  End;
Writeln ('Air/Fuel Ratio as Function of Gas Flow Rate');
Writeln ('****************************************');
Writeln;
Write ('+----------+---------+---------+---------+---------+');
Writeln ('---------+---------+');
```

```
Write ('| Gas Flow | A/F [1] | A/F [1] | A/F [1] | A/F [1] |');
Writeln (' A/F [1] | A/F [1] |');
Write ('| Rate     | Dry Air | Dry Air | Dry Air | Wet Air |');
Writeln (' Wet Air | Wet Air |');
Write ('| [l/min]  | Oxyg.B. | Nitr.B. | Average | Oxyg.B. |');
Writeln (' Nitr.B. | Average |');
Write ('+----------+---------+---------+---------+---------+');
Writeln ('---------+---------+');
su2:=m-0.5;
For l:=1 to k+1 do
 Begin
  A2[l]:=(1+c)*A1[l];
  A3[l]:=(1+c)*A[l];
  A5[l]:=(A1[l]+A[l])/2;
  A4[l]:=(A2[l]+A3[l])/2;
  su2:=su2+0.5;
  Write ('|    ',su2:4:1,'    | ',A1[l]:7:4,' | ',A[l]:7:4,' | ');
  Write (A5[l]:7:4,' | ',A2[l]:7:4,' | ',A3[l]:7:4,' | ');
  Writeln (A4[l]:7:4,' |');
 End;
Write ('+----------+---------+---------+---------+---------+');
Writeln ('---------+---------+');
i1:=WhereX ; j1:=WhereY;
Gotoxy(60,24); TextColor(10); Write ('Type "c" to continue.');
Gotoxy(i1,j1);
TextColor(7);
 Begin
  Repeat
  Until Readkey=Char(99);
  ClrScr;
 End;
Write ('Dry Exhaust Gas & Water Vapour as Function of Gas Flow
Rate');
Writeln;
Write ('**********************************************************
****');
Writeln; Writeln;
Write ('+---------------+-----------------+--------------+');
Writeln ('------------+');
Write ('| Gas Flow Rate | Dry Exhaust Gas | Water Vapour |');
Writeln (' Percentage |');
Write ('| [l/min]       | [m3/m3]         | [m3/m3]      |');
Writeln (' Excess Air |');
Write ('+---------------+-----------------+--------------+');
Writeln ('------------+');
su2:=m-0.5;
For l:=1 to k+1 do
 Begin
  EA:=(A4[l]-Ab)/Ab*100;
  su2:=su2+0.5;
  Write ('|    ',su2:4:1,'       |    ',V[l]:7:4,'      |   ');
  Writeln (Z[l]:7:3,'    |   ',EA:6:3,'   |');
 End;
Write ('+---------------+-----------------+--------------+');
Writeln ('------------+');
i1:=WhereX ; j1:=WhereY;
Gotoxy(60,24); TextColor(10); Write ('Type "c" to continue.');
Gotoxy(i1,j1);
TextColor(7);
 Begin
  Repeat
```

```
   Until Readkey=Char(99);
   ClrScr;
  End;
End.


{NOMENCLATURE}

{fi : relative air humidity}
{ta : ambient temperature}
{z1[1,2]..z1[12,2] : pressures of saturated water vapour at}
{temperatures z1[1,1]..z1[12,1]}
{c : moist air coefficient}
{g : type of gaseous fuel}
{m : minimum gas flow rate}
{n : maximum gas flow rate}
{H2 : hydrogen content in gaseous fuel}
{CO : carbon monoxide content in gaseous fuel}
{CO2 : carbon dioxide content in gaseous fuel}
{N2 : nitrogen content in gaseous fuel}
{x[i], x[j] : number of carbon atoms of hydrocarbon i}
{y[i], y[j] : number of hydrogen atoms of hydrocarbon i}
{CH[i], CH[j] : volumetric concentration of hydrocarbon i in gaseous}
{fuel}
{O2e : volumetric concentration of oxygen in exhaust gas}
{COe : volumetric concentration of carbon monoxide in exhaust gas}
{CO2e : volumetric concentration of carbon dioxide in exhaust gas}
{N2e : volumetric concentration of nitrogen in exhaust gas}
{m1 : moles of carbon dioxide leaving stoichiometric equation}
{Aa : air/fuel ratio on dry basis}
{Za : moles of water leaving stoichiometric equation}
{m2 : moles of nitrogen leaving stoichiometric equation}
{Ab : air/fuel ratio on wet basis}
{V[1] : moles of dry exhaust gas leaving reaction equation}
{A1[1] : air/fuel ratio on dry basis derived from oxygen balance}
{Z[1] : moles of water leaving reaction equation}
{A[1] : air/fuel ratio on dry basis derived from nitrogen balance}
{A2[1] : air/fuel ratio on wet basis derived from oxygen balance}
{A3[1] : air/fuel ratio on wet basis derived from nitrogen balance}
{A4[1] : average air/fuel ratio on dry basis}
{A5[1] : average air/fuel ratio on wet basis}
{EA : percentage excess air}
```

APPENDIX D : Specimen of a print-out from program "Gas"

```
Type of Gaseous Fuel          :  Natural Gas NGA

Set Range of Gas Flow Rates [l/min] : Min =  8.0
                                      Max = 11.0

Set Gas Composition in % of Volume  :    H2  = 0.00
                                         CO  = 0.00
                                         CO2 = 0.34
                                         N2  = 2.80

Set Hydrocarbons Cx Hy  :  Insert "0" when end
i          x          y        % of Volume
-----------------------------------------------
1                     4          92.88
2                     6          2.86
3                     8          0.59
4                    10          0.23
5                    12          0.30
6                     0          0.00

*** Net Calorific Value at 0°C & 1bar  =  36318 KJ/m3 ***

Set Relative Air Humidity [%] : 50
Set Ambient Temperature  [°C] : 19

Stoichiometric Equation
***********************

1 mole [ Natural Gas NGA ] + A moles [ Air ] ------->
m1 moles [ CO2 ] + m2 moles [ N2] + Z moles [ Water ]

[ 0.9288 C1H4 + 0.0286 C2H6 + 0.0059 C3H8 + 0.0023 C4H10 +
0.0030 C5H12 + 0.0034 CO2 + 0.0280 N2 ] + A [ 0.21 O2 +
0.79 N2 +0.0111 H2O ] ------->
m1 [ CO2 ] + m2 [ N2 ] + Z [ H2O ]

*** Carbon Balance ***
     m1 = 1.0313

*** Oxygen Balance ***
      A = 9.6483

*** Hydrogen Balance ***
      Z = 2.1036

*** Nitrogen Balance ***
     m2 = 7.6502

*** Stoichiometric A/F Ratios :  Dry Air   |   Wet Air ***
                                 9.6483    |   9.7554

*** Gas Flow Rate = 8.0 ***
===========================

Set Dry Exhaust Gas Analysis in % of Volume : O2  =  6.4300
                                              CO  =  0.0490
                                              CO2 =  8.2300
```

```
                                                    N2   = 85.2910

Reaction Equation
*****************

1 mole [ Natural Gas NGA ] + A moles [ Air ] ------->
V moles [ Dry Exhaust Gas ] + Z moles [ Water ]

[ 0.9288 C1H4 + 0.0286 C2H6 + 0.0059 C3H8 + 0.0023 C4H10 +
0.0030 C5H12 + 0.0034 CO2 + 0.0280 N2 ] + A [ 0.21 O2 +
0.79 N2 + 0.0111 H2O ] ------->
V [ 0.0643 O2 + 0.000490 CO + 0.082 CO2 + 0.852910 N2 ] +
Z [ H2O ]

*** Carbon Balance ***
     V = 12.4569

*** Oxygen Balance ***
     A = 13.4480

*** Hydrogen Balance ***
     Z = 2.1458

*** Nitrogen Balance ***
     A = 13.4134

*** Gas Flow Rate = 8.5 ***
===========================

Set Dry Exhaust Gas Analysis in % of Volume : O2   =  5.7000
                                              CO   =  0.0326
                                              CO2  =  8.6700
                                              N2   = 85.5974

Reaction Equation
*****************

1 mole [ Natural Gas NGA ] + A moles [ Air ] ------->
V moles [ Dry Exhaust Gas ] + Z moles [ Water ]

[ 0.9288 C1H4 + 0.0286 C2H6 + 0.0059 C3H8 + 0.0023 C4H10 +
0.0030 C5H12 + 0.0034 CO2 + 0.0280 N2 ] + A [ 0.21 O2 +
0.79 N2 + 0.0111 H2O ] ------->
V [ 0.0570 O2 + 0.000326 CO + 0.087 CO2 + 0.855974 N2 ] +
Z [ H2O ]

*** Carbon Balance ***
     V = 11.8505

*** Oxygen Balance ***
     A = 12.8557

*** Hydrogen Balance ***
     Z = 2.1392

*** Nitrogen Balance ***
     A = 12.8047

*** Gas Flow Rate = 9.0 ***
===========================
```

```
Set Dry Exhaust Gas Analysis in % of Volume : O2  =  5.2000
                                              CO  =  0.0287
                                              CO2 =  8.9300
                                              N2  = 85.8413

Reaction Equation
*****************

1 mole [ Natural Gas NGA ] + A moles [ Air ] ------->
V moles [ Dry Exhaust Gas ] + Z moles [ Water ]

[ 0.9288 C1H4 + 0.0286 C2H6 + 0.0059 C3H8 + 0.0023 C4H10 +
0.0030 C5H12 + 0.0034 CO2 + 0.0280 N2 ] + A [ 0.21 O2 +
0.79 N2 + 0.0111 H2O ] ------->
V [ 0.0520 O2 + 0.000287 CO + 0.089 CO2 + 0.858413 N2 ] +
Z [ H2O ]

*** Carbon Balance ***
     V = 11.5117

*** Oxygen Balance ***
     A = 12.4910

*** Hydrogen Balance ***
     Z = 2.1352

*** Nitrogen Balance ***
     A = 12.4731

*** Gas Flow Rate = 9.5 ***
===========================

Set Dry Exhaust Gas Analysis in % of Volume : O2  =  4.7000
                                              CO  =  0.0253
                                              CO2 =  9.2000
                                              N2  = 86.0747

Reaction Equation
*****************

1 mole [ Natural Gas NGA ] + A moles [ Air ] ------->
V moles [ Dry Exhaust Gas ] + Z moles [ Water ]

[ 0.9288 C1H4 + 0.0286 C2H6 + 0.0059 C3H8 + 0.0023 C4H10 +
0.0030 C5H12 + 0.0034 CO2 + 0.0280 N2 ] + A [ 0.21 O2 +
0.79 N2 + 0.0111 H2O ] ------->
V [ 0.0470 O2 + 0.000253 CO + 0.092 CO2 + 0.860747 N2 ] +
Z [ H2O ]

*** Carbon Balance ***
     V = 11.1791

*** Oxygen Balance ***
     A = 12.1436

*** Hydrogen Balance ***
     Z = 2.1313

*** Nitrogen Balance ***
     A = 12.1448
```

```
*** Gas Flow Rate = 10.0 ***
============================

Set Dry Exhaust Gas Analysis in % of Volume : O2  =  4.0000
                                              CO  =  0.0243
                                              CO2 =  9.6000
                                              N2  = 86.3757

Reaction Equation
*****************

1 mole [ Natural Gas NGA ] + A moles [ Air ] ------->
V moles [ Dry Exhaust Gas ] + Z moles [ Water ]

[ 0.9288 C1H4 + 0.0286 C2H6 + 0.0059 C3H8 + 0.0023 C4H10 +
0.0030 C5H12 + 0.0034 CO2 + 0.0280 N2 ] + A [ 0.21 O2 +
0.79 N2 + 0.0111 H2O ] ------->
V [ 0.0400 O2 + 0.000243 CO + 0.096 CO2 + 0.863757 N2 ] +
Z [ H2O ]

*** Carbon Balance ***
     V = 10.7156

*** Oxygen Balance ***
     A = 11.6832

*** Hydrogen Balance ***
     Z = 2.1262

*** Nitrogen Balance ***
     A = 11.6806

*** Gas Flow Rate = 10.5 ***
============================

Set Dry Exhaust Gas Analysis in % of Volume : O2  =  2.9600
                                              CO  =  0.0292
                                              CO2 = 10.2300
                                              N2  = 86.7808

Reaction Equation
*****************

1 mole [ Natural Gas NGA ] + A moles [ Air ] ------->
V moles [ Dry Exhaust Gas ] + Z moles [ Water ]

[ 0.9288 C1H4 + 0.0286 C2H6 + 0.0059 C3H8 + 0.0023 C4H10 +
0.0030 C5H12 + 0.0034 CO2 + 0.0280 N2 ] + A [ 0.21 O2 +
0.79 N2 + 0.0111 H2O ] ------->
V [ 0.0296 O2 + 0.000292 CO + 0.102 CO2 + 0.867808 N2 ] +
Z [ H2O ]

*** Carbon Balance ***
     V = 10.0525

*** Oxygen Balance ***
     A = 11.0583

*** Hydrogen Balance ***
     Z = 2.1193
```

```
*** Nitrogen Balance ***
     A = 11.0071

*** Gas Flow Rate = 11.0 ***
============================

Set Dry Exhaust Gas Analysis in % of Volume : O2  =  1.8700
                                              CO  =  0.0510
                                              CO2 = 10.9300
                                              N2  = 87.1490

Reaction Equation
*****************

1 mole [ Natural Gas NGA ] + A moles [ Air ] ------->
V moles [ Dry Exhaust Gas ] + Z moles [ Water ]

[ 0.9288 C1H4 + 0.0286 C2H6 + 0.0059 C3H8 + 0.0023 C4H10 +
0.0030 C5H12 + 0.0034 CO2 + 0.0280 N2 ] + A [ 0.21 O2 +
0.79 N2 + 0.0111 H2O ] ------->
V [ 0.0187 O2 + 0.000510 CO + 0.109 CO2 + 0.871490 N2 ] +
Z [ H2O ]

*** Carbon Balance ***
     V = 9.3917

*** Oxygen Balance ***
     A = 10.4732

*** Hydrogen Balance ***
     Z = 2.1128

*** Nitrogen Balance ***
     A = 10.3250
```

Air Fuel Ratio as Function of Gas Flow Rate

Gas Flow Rate [l/min]	A/F [1] Dry Air Oxyg.B.	A/F [1] Dry Air Nitr.B.	A/F [1] Dry Air Average	A/F [1] Wet Air Oxyg.B.	A/F [1] Wet Air Nitr.B.	A/F [1] Wet Air Average
8.0	13.4480	13.4134	13.4307	13.5973	13.5623	13.5798
8.5	12.8557	12.8047	12.8302	12.9984	12.9469	12.9727
9.0	12.4910	12.4731	12.4820	12.6296	12.6116	12.6206
9.5	12.1436	12.1448	12.1442	12.2784	12.2796	12.2790
10.0	11.6832	11.6806	11.6819	11.8129	11.8103	11.8116
10.5	11.0583	11.0071	11.0327	11.1810	11.1293	11.1552
11.0	10.4732	10.3250	10.3991	10.5895	10.4396	10.5145

Dry Exhaust Gas & Water Vapour as Function of Gas Flow Rate

Gas Flow Rate [l/min]	Dry Exhaust Gas [m3/m3]	Water Vapour [m3/m3]	Percentage Excess Air
8.0	12.4569	2.146	39.202
8.5	11.8505	2.139	32.979
9.0	11.5117	2.135	29.370
9.5	11.1791	2.131	25.868
10.0	10.7156	2.126	21.077
10.5	10.0525	2.119	14.348
11.0	9.3917	2.113	7.781

APPENDIX E : Specimen of measured data

TEST 1

Type of gas : natural gas NGA (mains) t_{Amb} = 19 °C

Tailpipe length = 2.00 m t_{Water} = 65 °C

Immersed length = 1.76 m t_{Exh2} = 70 -75 °C

Volume of combustion chamber = 110 cm^3 Rel. air humidity = 50 %

Volume of water in the tank = 38.5 l Silencer : on

Type of gas analyzer : KM 9004 (port 1) and Lancom 3200 (port 2)

Gas flow Rate / l min^{-1}	No.	Δp / mm H_2O	t_{Exh1} / °C	O_2 / vol %	CO / ppm	CO_2 / vol %	NO_x / ppm
8.0	1	41.0	812	6.4	483	8.3	5
	2	41.0	811	6.4	474	8.2	6
	3	40.0	809	6.5	512	8.2	6
	Aver.	**40.7**	**810.7**	**6.43**	**489.7**	**8.23**	**5.7**
8.5	1	39.0	824	5.7	332	8.6	7
	2	38.0	822	5.7	313	8.7	8
	3	38.0	821	5.7	332	8.7	9
	Aver.	**38.3**	**822.3**	**5.7**	**325.7**	**8.67**	**8.0**
9.0	1	38.0	830	5.3	301	8.9	9
	2	36.0	828	5.2	278	8.9	10
	3	37.0	829	5.1	283	9.0	11
	Aver.	**37.0**	**829.0**	**5.2**	**287.3**	**8.93**	**10.0**
9.5	1	36.0	835	4.7	252	9.2	12
	2	35.0	840	4.6	244	9.3	13
	3	35.0	840	4.8	262	9.1	13
	Aver.	**35.3**	**838.3**	**4.7**	**252.7**	**9.2**	**12.7**
10.0	1	34.0	847	3.9	250	9.7	17
	2	32.0	850	4.0	232	9.6	16
	3	33.0	849	4.1	246	9.5	18
	Aver.	**33.0**	**848.7**	**4.0**	**242.7**	**9.6**	**17.0**
10.5	1	31.0	861	2.9	317	10.3	25
	2	30.0	862	3.0	275	10.2	24
	3	31.0	863	3.0	283	10.2	26
	Aver.	**30.7**	**862.0**	**2.96**	**291.7**	**10.23**	**25.0**
11.0	1	29.0	879	1.8	520	10.9	39
	2	30.0	881	1.8	499	10.9	38
	3	28.0	884	1.7	512	10.0	40
	Aver.	**29.0**	**881.3**	**1.87**	**510.3**	**10.93**	**39.0**

All gas analysis refer to dry bases.

APPENDIX F : Graphical determination of adiabatic flame temperature

Adiabatic flame temperature is a theoretical temperature of combustion products based on the assumption that no heat is radiated from the flame and no heat losses occur. This temperature can be graphically determined from the diagram of heat content of combustion products and of air versus temperature [96]. A H-t diagram was constructed for natural gas (NGA) assuming stoichiometric combustion of the gas consisting purely of methane at ambient temperature 18 °C and relative air humidity 60 % (see Figure 51). The heat contents have been obtained from the volumetric enthalpies of the constituent gases tabulated in [97] according to the

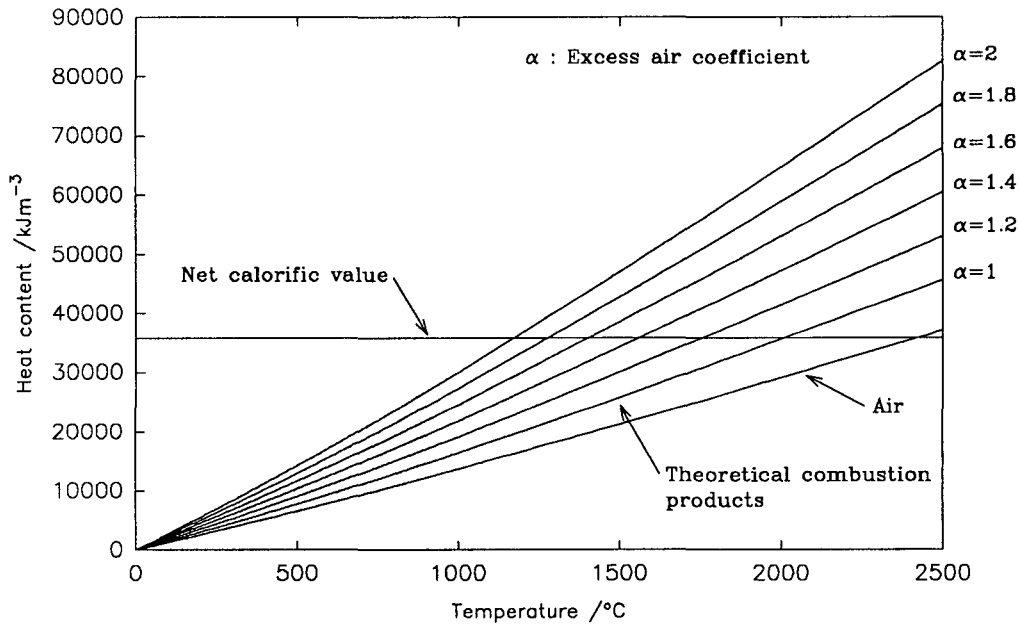

Figure 51 Heat content of combustion products of NGA (100 % CH_4) and of air.

following formulas [65, 96] :

a) for stoichiometric combustion products :

$$H_{SCP} = \sum_i V_i h_i \,, \qquad (1)$$

where H_{SCP} is heat content of stoichiometric combustion products for given

temperature,

i constituent of wet stoichiometric combustion products ie. CO_2, N_2, H_2O,

V_i theoretical volume of i-th constituent of wet stoichiometric combustion products

and h_i enthalpy of i-th constituent of wet stoichiometric combustion products for given temperature;

b) for theoretical combustion air :

$$H_{CA} = V_{DA} h_{DA} + V_W h_W \ , \qquad (2)$$

where H_{CA} is combustion air heat content for given temperature,

V_{DA} theoretical volume of dry air,

h_{DA} enthalpy of dry air for given temperature,

V_W water vapour content of combustion air

and h_W enthalpy of water vapour for given temperature;

c) for combustion with excess air :

$$H_{EA} = H_{SCP} + (\alpha - 1) H_{CA} \ , \qquad (3)$$

where H_{EA} is heat content of combustion products for combustion with excess air for given temperature

and α excess air coefficient = air/fuel ratio divided by stoichiometric air/fuel ratio.

Figure 51 shows the curve of the theoretical combustion products (equation 1), of the air (equation 2) and the curves of five different excess air coefficients (equation 3). Additionally, net calorific value of methane (35796 kJ m^{-3} [98]) is also depicted by a horizontal line. It is the intersection of this line and the heat content curve at the investigated equivalence ratio which gives us the adiabatic flame temperature [96] as demonstrated in Figure 52. This diagram is an enlarged section of Figure 51 and gives the heat content curves of combustion products at the equivalence ratios calculated for the 2.00 m long tailpipe. The adiabatic flame temperatures were read off by projecting the intersections of the net calorific value line and the heat content curves to the temperature axis. The adiabatic flame temperatures for the 2.30 m long exhaust tube were determined in a similar way. Figure 53 presents the obtained theoretical flame temperatures as well as the exhaust

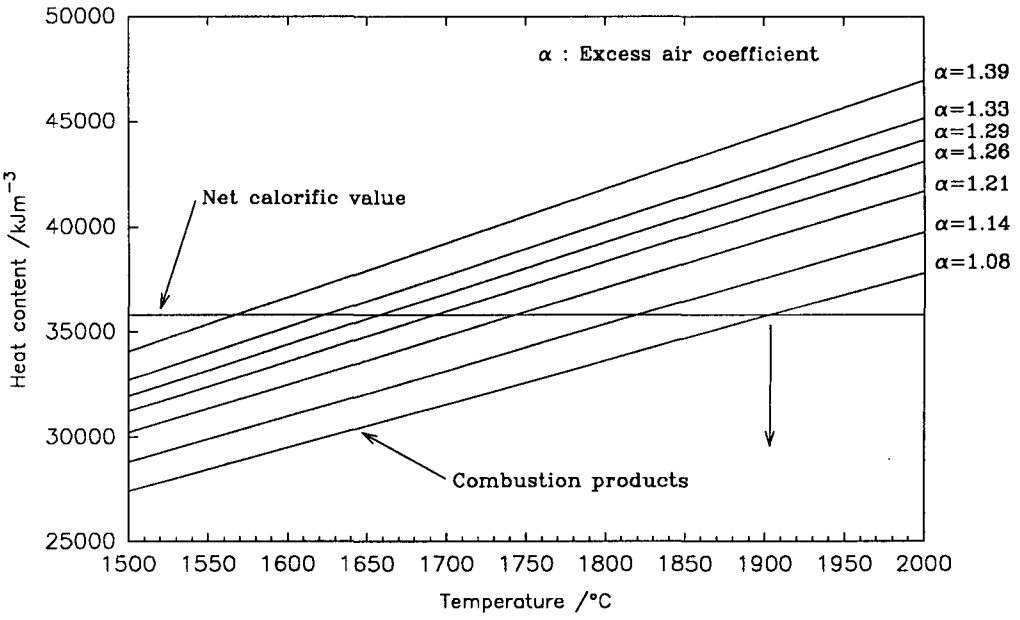

Figure 52 *H-t diagram of NGA (100 % CH_4) for 2.00 m long tailpipe.*

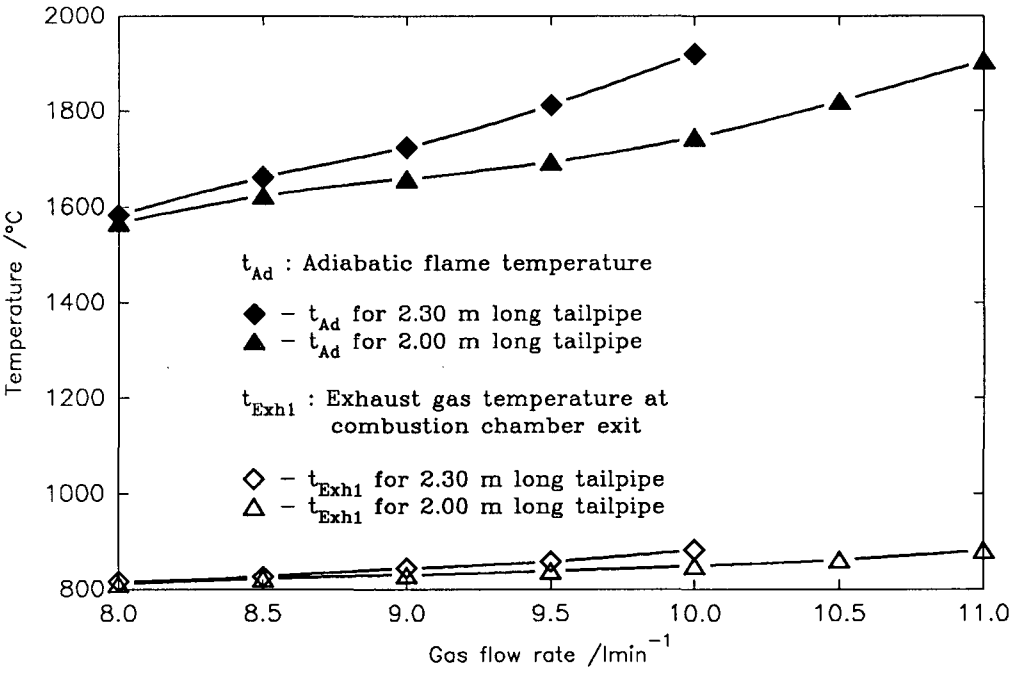

Figure 53 *Exhaust gas temperature (t_{Exh1}) and adiabatic flame temperature (t_{Ad}) against gas flow rate for 2.00 m and 2.30 m long tailpipes.*

temperatures at combustion chamber exit against gas flow rate. Adiabatic flame temperatures of the longer pipe were found to be greater than those of the shorter pipe which is in agreement with the measured exhaust gas temperatures for the two tailpipes.

APPENDIX G : Summary of data computed by program "Gas" for different tailpipe lengths

Test 2 : Tailpipe length = 1.90 m

*** Stoichiometric A/F Ratios : Dry Air | Wet Air ***
9.6483 | 9.7570

Air/Fuel Ratio as Function of Gas Flow Rate

Gas Flow Rate [l/min]	A/F [1] Dry Air Oxyg.B.	A/F [1] Dry Air Nitr.B.	A/F [1] Dry Air Average	A/F [1] Wet Air Oxyg.B.	A/F [1] Wet Air Nitr.B.	A/F [1] Wet Air Average
9.0	13.4411	13.3971	13.4191	13.5924	13.5479	13.5702
9.5	13.2203	13.1565	13.1884	13.3692	13.3047	13.3369
10.0	12.9086	12.7809	12.8448	13.0539	12.9248	12.9894
10.5	12.5531	12.4988	12.5260	12.6945	12.6395	12.6670
11.0	12.2674	12.2125	12.2399	12.4055	12.3500	12.3777
11.5	11.8971	11.9077	11.9024	12.0311	12.0418	12.0364
12.0	11.5970	11.5653	11.5811	11.7276	11.6955	11.7116
12.5	11.3531	11.3147	11.3339	11.4809	11.4421	11.4615

Dry Exhaust Gas & Water Vapour as Function of Gas Flow Rate

Gas Flow Rate [l/min]	Dry Exhaust Gas [m3/m3]	Water Vapour [m3/m3]	Percentage Excess Air
9.0	12.4431	2.148	39.082
9.5	12.2061	2.145	36.691
10.0	11.8431	2.142	33.129
10.5	11.5452	2.138	29.825
11.0	11.2588	2.135	26.860
11.5	10.9401	2.130	23.362
12.0	10.6063	2.127	20.033
12.5	10.3573	2.124	17.470

Test 3 : Tailpipe length = 2.10 m

*** Stoichiometric A/F Ratios : Dry Air | Wet Air ***
9.6483 | 9.7570

Air/Fuel Ratio as Function of Gas Flow Rate

Gas Flow Rate [l/min]	A/F [1] Dry Air Oxyg.B.	A/F [1] Dry Air Nitr.B.	A/F [1] Dry Air Average	A/F [1] Wet Air Oxyg.B.	A/F [1] Wet Air Nitr.B.	A/F [1] Wet Air Average
8.0	13.4481	13.3392	13.3936	13.5995	13.4894	13.5445
8.5	12.8299	12.7658	12.7978	12.9744	12.9095	12.9419
9.0	12.3920	12.3470	12.3695	12.5315	12.4860	12.5088
9.5	11.9433	11.9472	11.9452	12.0778	12.0817	12.0797
10.0	11.0572	10.9568	11.0070	11.1817	11.0802	11.1310
10.5	10.1975	10.0840	10.1407	10.3123	10.1975	10.2549

Dry Exhaust Gas & Water Vapour as Function of Gas Flow Rate

Gas Flow Rate [l/min]	Dry Exhaust Gas [m3/m3]	Water Vapour [m3/m3]	Percentage Excess Air
8.0	12.3982	2.148	38.818
8.5	11.8141	2.141	32.643
9.0	11.3909	2.136	28.203
9.5	10.9807	2.131	23.806
10.0	10.0126	2.121	14.082
10.5	9.1445	2.111	5.103

Test 4 : Tailpipe length = 2.20 m

*** Stoichiometric A/F Ratios : Dry Air | Wet Air ***
9.6483 | 9.7772

Air/Fuel Ratio as Function of Gas Flow Rate

Gas Flow Rate [l/min]	A/F [1] Dry Air Oxyg.B.	A/F [1] Dry Air Nitr.B.	A/F [1] Dry Air Average	A/F [1] Wet Air Oxyg.B.	A/F [1] Wet Air Nitr.B.	A/F [1] Wet Air Average
8.0	13.3285	13.2625	13.2955	13.5065	13.4396	13.4730
8.5	12.6941	12.6863	12.6902	12.8636	12.8557	12.8597
9.0	12.0683	12.1242	12.0963	12.2294	12.2861	12.2578
9.5	11.6911	11.7258	11.7084	11.8472	11.8823	11.8648
10.0	10.9212	10.7929	10.8571	11.0671	10.9370	11.0021
10.5	10.0846	9.9756	10.0301	10.2193	10.1088	10.1640

Dry Exhaust Gas & Water Vapour as Function of Gas Flow Rate

Gas Flow Rate [l/min]	Dry Exhaust Gas [m3/m3]	Water Vapour [m3/m3]	Percentage Excess Air
8.0	12.3124	2.174	37.801
8.5	11.7227	2.166	31.527
9.0	11.1469	2.158	25.372
9.5	10.7528	2.153	21.352
10.0	9.8548	2.142	12.528
10.5	9.0367	2.131	3.957

Test 5 : Tailpipe length = 2.30 m

*** Stoichiometric A/F Ratios : Dry Air | Wet Air ***
9.6483 | 9.7692

Air/Fuel Ratio as Function of Gas Flow Rate

Gas Flow Rate [l/min]	A/F [1] Dry Air Oxyg.B.	A/F [1] Dry Air Nitr.B.	A/F [1] Dry Air Average	A/F [1] Wet Air Oxyg.B.	A/F [1] Wet Air Nitr.B.	A/F [1] Wet Air Average
8.0	13.2709	13.2057	13.2383	13.4372	13.3711	13.4041
8.5	12.4638	12.4208	12.4423	12.6199	12.5763	12.5981
9.0	11.8521	11.8255	11.8388	12.0005	11.9737	11.9871
9.5	11.1209	11.0699	11.0954	11.2602	11.2086	11.2344
10.0	10.2842	10.2508	10.2675	10.4131	10.3792	10.3961

Dry Exhaust Gas & Water Vapour as Function of Gas Flow Rate

Gas Flow Rate [l/min]	Dry Exhaust Gas [m3/m3]	Water Vapour [m3/m3]	Percentage Excess Air
8.0	12.2553	2.163	37.208
8.5	11.4644	2.153	28.958
9.0	10.8654	2.145	22.703
9.5	10.1151	2.136	14.998
10.0	9.2941	2.125	6.418

APPENDIX H : Summary of data computed by program "Gas" for different combustion chamber volumes

Test 7 : Combustion chamber volume = 90 cm^3

```
*** Stoichiometric A/F Ratios :  Dry Air   |   Wet Air ***
                                 9.6483    |   9.7368
```

Air/Fuel Ratio as Function of Gas Flow Rate

Gas Flow Rate [l/min]	A/F [1] Dry Air Oxyg.B.	A/F [1] Dry Air Nitr.B.	A/F [1] Dry Air Average	A/F [1] Wet Air Oxyg.B.	A/F [1] Wet Air Nitr.B.	A/F [1] Wet Air Average
8.0	13.9145	13.7673	13.8409	14.0420	13.8935	13.9678
8.5	13.4976	13.3957	13.4466	13.6213	13.5185	13.5699
9.0	12.9860	12.8869	12.9365	13.1051	13.0050	13.0551
9.5	12.5264	12.4765	12.5015	12.6412	12.5909	12.6161
10.0	12.1131	12.0876	12.1004	12.2242	12.1985	12.2113
10.5	11.5487	11.5141	11.5314	11.6546	11.6196	11.6371

Dry Exhaust Gas & Water Vapour as Function of Gas Flow Rate

Gas Flow Rate [l/min]	Dry Exhaust Gas [m3/m3]	Water Vapour [m3/m3]	Percentage Excess Air
8.0	12.8380	2.124	43.454
8.5	12.4552	2.120	39.367
9.0	11.9447	2.116	34.080
9.5	11.5230	2.111	29.571
10.0	11.1282	2.108	25.414
10.5	10.5566	2.102	19.517

Test 8 : combustion chamber volume = 100 cm^3

*** Stoichiometric A/F Ratios : Dry Air | Wet Air ***
9.6483 | 9.7368

Air/Fuel Ratio as Function of Gas Flow Rate

Gas Flow Rate [l/min]	A/F [1] Dry Air Oxyg.B.	A/F [1] Dry Air Nitr.B.	A/F [1] Dry Air Average	A/F [1] Wet Air Oxyg.B.	A/F [1] Wet Air Nitr.B.	A/F [1] Wet Air Average
8.0	13.7139	13.6160	13.6649	13.8396	13.7408	13.7902
8.5	13.2330	13.2081	13.2206	13.3543	13.3292	13.3418
9.0	12.7333	12.7201	12.7267	12.8501	12.8367	12.8434
9.5	12.3124	12.2438	12.2781	12.4253	12.3560	12.3907
10.0	11.7699	11.7945	11.7822	11.8778	11.9027	11.8902
10.5	11.1819	11.1729	11.1774	11.2844	11.2754	11.2799
11.0	10.6178	10.6274	10.6226	10.7151	10.7248	10.7200

Dry Exhaust Gas & Water Vapour as Function of Gas Flow Rate

Gas Flow Rate [l/min]	Dry Exhaust Gas [m3/m3]	Water Vapour [m3/m3]	Percentage Excess Air
8.0	12.6739	2.122	41.630
8.5	12.2495	2.118	37.024
9.0	11.7584	2.113	31.906
9.5	11.2932	2.109	27.256
10.0	10.8240	2.104	22.116
10.5	10.2095	2.099	15.848
11.0	9.6607	2.094	10.098

Test 9 : Combustion chamber volume = 120 cm^3

*** Stoichiometric A/F Ratios : Dry Air | Wet Air ***
9.6483 | 9.7522

Air/Fuel Ratio as Function of Gas Flow Rate

Gas Flow Rate [l/min]	A/F [1] Dry Air Oxyg.B.	A/F [1] Dry Air Nitr.B.	A/F [1] Dry Air Average	A/F [1] Wet Air Oxyg.B.	A/F [1] Wet Air Nitr.B.	A/F [1] Wet Air Average
8.0	13.3477	13.3292	13.3384	13.4914	13.4727	13.4820
8.5	12.6841	12.6393	12.6617	12.8206	12.7754	12.7980
9.0	12.1449	12.1482	12.1465	12.2756	12.2790	12.2773
9.5	11.6629	11.6479	11.6554	11.7885	11.7733	11.7809
10.0	10.7975	10.7880	10.7928	10.9137	10.9041	10.9089
10.5	10.2358	10.1879	10.2118	10.3460	10.2976	10.3218

Dry Exhaust Gas & Water Vapour as Function of Gas Flow Rate

Gas Flow Rate [l/min]	Dry Exhaust Gas [m3/m3]	Water Vapour [m3/m3]	Percentage Excess Air
8.0	12.3686	2.140	38.246
8.5	11.6834	2.133	31.232
9.0	11.1819	2.127	25.893
9.5	10.6854	2.122	20.802
10.0	9.8245	2.113	11.861
10.5	9.2343	2.107	5.840

APPENDIX I : Physical properties of constituent gases

	GCV_0† / kJ m^{-3}	NCV_0† / kJ m^{-3}	GCV / kJ m^{-3}	RD† dry air=1	W / kJ m^{-3}	TAR‡	F‡
CH_4	39724	35796	37653	0.5539	50592	9.52	148
C_2H_6	69595	63704	65967	1.0382	64742	16.67	301
C_3H_8	99048	91195	93884	1.5224	76090	23.81	398
C_4H_{10}	128363	118546	121673	2.0067	85891	30.95	513
C_5H_{12}	157768	145987	149543	2.4910	94750	38.09	*
H_2	12753	10789	12088	0.0696	45819	2.38	339
N_2	0	0	0	0.9672	0	0	0
CO_2	0	0	0	1.5198	0	0	0

* F for C_5H_{12} is not stated in the literature; in further calculations it was assumed to be like that of C_4H_{10}.
† Source : [98].
‡ Source : Jones [67].

Nomenclature :

GCV_0 - Gross calorific value at normal conditions (0 °C, 1013.25 mbar)
NCV_0 - Net calorific value at normal conditions (0 °C, 1013.25 mbar)
GCV - Gross calorific value at standard conditions (15 °C and 1013.25 mbar)
RD - Relative density (dry gas relative to dry air)
W - Wobbe number based on GCV
TAR - Theoretical air requirement
F - Weaver coefficient

Gross calorific values at normal conditions (0 °C, 1013.25 mbar) are converted to gross calorific values at standard conditions (15 °C, 1013.25 mbar) according to Cerny [72] as follows :

$$GCV = GCV_0 \frac{273+t_0}{273+t} \frac{p}{p_0} , \quad (1)$$

where t_0 is temperature at normal conditions (0 °C),
t temperature at standard conditions(15 °C),
p_0 pressure at normal conditions (1013.25 mbar)
and p pressure at standard conditions (1013.25 mbar).

Wobbe numbers at standard conditions are calculated using the following formula [65] :

$$W = \frac{GCV}{\sqrt{RD}} , \quad (2)$$

where GCV is the gross calorific value at standard conditions (15 °C, 1013.25 mbar) and RD stands for the relative density.

APPENDIX J : Composition of tested gases

	NGA V_i / % vol	NGB V_i / % vol	NGC V_i / % vol	NGD V_i / % vol	Propane V_i / % vol
CH_4	92.88	73.78	55.84	87.20	0
C_2H_6	2.86	2.57	2.23	2.54	0
C_3H_8	0.59	17.31	3.63	0.49	100
C_4H_{10}	0.23	0.35	0.28	0.2	0
C_5H_{12}	0.3	0.22	0.12	0.26	0
H_2	0	0	35.83	0	0
N_2	2.8	5.5	1.94	9.31	0
CO_2	0.34	0.27	0.13	0	0

Above compositions were obtained from British Gas.
Mole fractions can be calculated as volumetric compositions divided by 100.

APPENDIX K : Physical properties of tested gases

	GCV / kJ m^{-3}	RD dry air=1	W / kJ m^{-3}	TAR	S	Q_h / kW
NGA	38141	0.5975	49343	9.64	14	0.636
NGB	46482	0.7687	53016	11.77	14.45	0.775
NGC	30756	0.442	46261	7.54	26.3	0.513
NGD	35601	0.6174	45308	9	13.47	0.593
Propane	93884	1.5224	76090	23.81	16.04	1.565

Nomenclature :

GCV - Gross calorific value at standard conditions (15 °C, 1013.25 mbar)
RD - Relative density (dry mixture relative to dry air)
W - Wobbe number based on GCV
TAR - Theoretical air requirement
S - Weaver flame speed factor
Q_h - Heat input corresponding to one l min^{-1} of tested gas

Natural gas is a multicomponent mixture and its gross calorific value, relative density and theoretical required air can be derived as follows [67] :

$$P = \sum_i x_i P_i \,, \qquad (1)$$

where P is parameter for gas mixture,
x_i mole fraction of component i obtained from Appendix J as %vol/100,
and P_i parameter for component i obtained from Appendix I.

Wobbe numbers (standard conditions) for tested gases are calculated using the following formula [49] :

$$W = \frac{\sum_i x_i GCV_i}{\sqrt{\sum_i x_i RD_i}}, \qquad (2)$$

where W is wobbe number of gas mixture,
x_i mole fraction of component i obtained from Appendix J,
GCV_i gross calorific value of component i obtained from Appendix I
and RD_i relative density of component i obtained from Appendix I.

According to Jones [49] Weaver flame speed factor can be determined as :

$$S = \frac{\sum_i x_i F_i}{1+TAR+5x_N-18.8x_O}, \qquad (3)$$

where S is Weaver flame speed factor of gas mixture,
x_i mole fraction of component i obtained from Appendix J,
F_i Weaver coefficient of component i obtained from Appendix I,
TAR theoretical air requirement of gas mixture obtained from Appendix I
x_N, x_O mole fractions of inerts and oxygen respectively obtained from Appendix J.

The heat input (kW) corresponding to one l min^{-1} of tested gas as a function of gross calorific value (kJ m^{-3}) of gas mixture is given by equation 4.

$$Q_h = GCV\frac{1}{60000} \qquad (4)$$

APPENDIX L : Summary of data computed by program "Gas" for different types of natural gas

Test 11 : Type of natural gas = B (NGB)

```
*** Stoichiometric A/F Ratios :  Dry Air   |   Wet Air ***
                                 11.7686   |   11.8808
```

Air/Fuel Ratio as Function of Gas Flow Rate

Gas Flow Rate [l/min]	A/F [1] Dry Air Oxyg.B.	A/F [1] Dry Air Nitr.B.	A/F [1] Dry Air Average	A/F [1] Wet Air Oxyg.B.	A/F [1] Wet Air Nitr.B.	A/F [1] Wet Air Average
8.0	16.7889	17.4098	17.0994	16.9491	17.5758	17.2625
8.5	16.3158	16.9051	16.6105	16.4715	17.0663	16.7689
9.0	15.8014	16.4665	16.1340	15.9522	16.6236	16.2879
9.5	15.3256	15.8817	15.6036	15.4717	16.0332	15.7525
10.0	15.0108	15.6472	15.3290	15.1540	15.7964	15.4752
11.0	14.3204	15.0059	14.6631	14.4570	15.1490	14.8030
12.0	13.4060	14.0861	13.7461	13.5339	14.2205	13.8772

Dry Exhaust Gas & Water Vapour as Function of Gas Flow Rate

Gas Flow Rate [l/min]	Dry Exhaust Gas [m3/m3]	Water Vapour [m3/m3]	Percentage Excess Air
8.0	16.2030	2.436	45.297
8.5	15.7042	2.431	41.143
9.0	15.2491	2.427	37.094
9.5	14.6867	2.422	32.587
10.0	14.4353	2.419	30.254
11.0	13.7834	2.412	24.596
12.0	12.8666	2.404	16.803

Test 12 : Type of natural gas = C (NGC)

```
*** Stoichiometric A/F Ratios :  Dry Air   |   Wet Air ***
                                 7.5395    |   7.6073
```

Air/Fuel Ratio as Function of Gas Flow Rate

Gas Flow Rate [l/min]	A/F [1] Dry Air Oxyg.B.	A/F [1] Dry Air Nitr.B.	A/F [1] Dry Air Average	A/F [1] Wet Air Oxyg.B.	A/F [1] Wet Air Nitr.B.	A/F [1] Wet Air Average
7.0	13.1458	12.3495	12.7477	13.2639	12.4605	12.8622
7.5	12.7222	11.9799	12.3511	12.8365	12.0876	12.4620
8.0	12.1352	11.4095	11.7723	12.2442	11.5120	11.8781
8.5	11.3212	10.6550	10.9881	11.4229	10.7508	11.0869
9.0	10.5148	9.9307	10.2228	10.6092	10.0199	10.3146

Dry Exhaust Gas & Water Vapour as Function of Gas Flow Rate

Gas Flow Rate [l/min]	Dry Exhaust Gas [m3/m3]	Water Vapour [m3/m3]	Percentage Excess Air
7.0	11.6901	1.826	69.078
7.5	11.3074	1.823	63.818
8.0	10.7324	1.817	56.142
8.5	9.9644	1.810	45.741
9.0	9.2222	1.803	35.589

Test 13 : Type of natural gas = D (NGD)

```
*** Stoichiometric A/F Ratios :  Dry Air   |   Wet Air ***
                                 9.0057    |   9.0800
```

Air/Fuel Ratio as Function of Gas Flow Rate

Gas Flow Rate [l/min]	A/F [1] Dry Air Oxyg.B.	A/F [1] Dry Air Nitr.B.	A/F [1] Dry Air Average	A/F [1] Wet Air Oxyg.B.	A/F [1] Wet Air Nitr.B.	A/F [1] Wet Air Average
8.0	13.2389	13.0485	13.1437	13.3480	13.1561	13.2520
8.5	12.8039	12.6407	12.7223	12.9094	12.7449	12.8272
9.0	12.4880	12.3263	12.4071	12.5910	12.4279	12.5094
9.5	12.0497	11.8541	11.9519	12.1490	11.9518	12.0504
10.0	11.6308	11.5077	11.5693	11.7267	11.6026	11.6647
10.5	11.1952	11.0547	11.1249	11.2874	11.1458	11.2166
11.0	10.7102	10.6015	10.6558	10.7985	10.6889	10.7437
12.0	9.7944	9.6162	9.7053	9.8752	9.6954	9.7853

Dry Exhaust Gas & Water Vapour as Function of Gas Flow Rate

Gas Flow Rate [l/min]	Dry Exhaust Gas [m3/m3]	Water Vapour [m3/m3]	Percentage Excess Air
8.0	12.2545	1.975	45.948
8.5	11.8393	1.971	41.269
9.0	11.5234	1.968	37.770
9.5	11.0577	1.965	32.714
10.0	10.6957	1.961	28.466
10.5	10.2459	1.958	23.532
11.0	9.7859	1.954	18.323
12.0	8.8159	1.946	7.768

APPENDIX M : Acoustic frequency theory

As stated in section 2.1.2 the most common formula used to predict the operating frequency of a Helmholtz-type pulse combustors is expressed as follows :

$$f = \frac{c}{2\pi}\left(\frac{A}{VL}\right)^{0.5}, \tag{1}$$

where f is resonant frequency,
c speed of sound,
A cross-sectional area of tailpipe,
V volume of combustion chamber
and L length of tailpipe.

Speed of sound can be obtained according to Kalcik [95] as :

$$c = (\gamma r T)^{0.5}, \tag{2}$$

where γ is ratio of specific heats,
r gas constant
and T absolute temperature.

Because $\gamma = c_p/c_v$ and $r = c_p - c_v$ equation 2 becomes :

$$c = \left(\frac{c_p}{c_v}(c_p - c_v)T\right)^{0.5}, \tag{3}$$

where c_p is the specific heat at constant pressure and c_v is the specific heat at constant volume.

After substituting equation 3 for the speed of sound in equation 1 and segregating variables from constants we obtain :

$$f = \left(\frac{c_p}{c_v}(c_p - c_v)T\right)^{0.5}\left(\frac{A}{4\pi^2 VL}\right)^{0.5}. \tag{4}$$

The second term in equation 4 is a constant and its value of $7.608 \cdot 10^{-2}$ was determined by substituting $0.5027 \cdot 10^{-4}$ m^2 for A (tailpipe diameter=8 mm), $110 \cdot 10^{-6}$ m^3 for V and 2.00 m for L.

Specific heats c_p and c_v in equation 4 are functions of the absolute temperature T which varies along the tailpipe. The latter temperature is usually estimated in the literature [45, 51] as a mean absolute temperature of exhaust gas in a combustor (T_{Mean}) and can be expressed for the investigated burner as :

$$T_{Mean} = \frac{t_{Ad}+t_{Exh2}}{2}+273 \ , \qquad (5)$$

where t_{Ad} is the adiabatic flame temperature and t_{Exh2} is the exhaust gas temperature at the tailpipe exit.

The adiabatic flame temperatures were assumed to be identical to those obtained for Test 1 (see Appendix F) and exhaust gas temperatures at tailpipe exit have been measured. Because the exhaust gas consists primarily of nitrogen the specific heat at constant pressure and constant volume for each T_{Mean} were determined from tables [97] as those of N_2. Finally, the predicted frequency was calculated from equation 4 and plotted in Figure 50.